

ONE-DIMENSIONAL SEISMIC SITE RESPONSE
ANALYSIS OF UNITED ARAB EMIRATES

by

Ahmed Mohamed Zaroug Eltayeb

A Thesis presented to the Faculty of the
American University of Sharjah
College of Engineering
In Partial Fulfillment
of the Requirements
for the Degree of

Master of Science in
Civil Engineering

Sharjah, United Arab Emirates
August 2021

Declaration of Authorship

I declare that this thesis is my own work and, to the best of my knowledge and belief, it does not contain material published or written by a third party, except where permission has been obtained and/or appropriately cited through full and accurate referencing.

Signed Ahmed Mohamed Zaroug Eltayeb

Date: 18th August 2021

The Author controls copyright for this report.

Material should not be reused without the consent of the author. Due acknowledgement should be made where appropriate.

© Year 2021

Ahmed Mohamed Zaroug Eltayeb

ALL RIGHTS RESERVE

Approval Signatures

We, the undersigned, approve the Master's Thesis of Ahmed Mohamed Zaroug Eltayeb

Thesis Title: One Dimensional Seismic Site Response Analysis of United Arab Emirates

Date of Defense: 18th Aug 2021

Name, Title and Affiliation

Signature

Dr. Magdi El-Emam
Associate Professor
Department of Civil Engineering
Thesis Advisor

Dr. Zahid Khan
Associate Professor
Department of Civil Engineering
Thesis Co-Advisor

Dr. Mousa Attom
Professor
Department of Civil Engineering
Thesis Committee Member

Dr. Samir Emam
Professor
Department of Mechanical Engineering
Thesis Committee Member

Dr. Irtishad Ahmed
Head
Department of Civil Engineering Program

Dr. Lotfi Romdhane
Associate Dean for Graduate Affairs and Research
College of Engineering

Dr. Sameer Al-Asheh
Interim Dean
College of Engineering

Dr. Mohamed El-Tarhuni
Vice Provost for Research and Graduate Studies
Office of Graduate Studies

Acknowledgement

Foremost thanks and praises are to Almighty who blessed me with the strength, capability, and knowledge to undertake and complete the research.

In the beginning, I would like to articulate my appreciation to the American University of Sharjah in general and to the Department of Civil Engineering in particular for providing me the graduate assistantship which gave me the honor to be part of this incredible society in addition to the chance to work with the best faculty members, and the best facilities possible in order to complete this research.

The ultimate credit of this study goes to my respected advisors Dr. Magdi El-Emam and Dr. Zahid Khan who have provided me with their infinite precious time, knowledge, guidance, support, and motivation throughout my research stages to assist me in accomplishing the objectives of this work. I am extremely grateful for their great supervision, worthy discussions, and suggestions.

Exceptional thanks to Dr. Mousa Attom for his extraordinary help in providing all the needed equipment and tools to complete this research.

Moreover, I would like to thank Dr. Muhammad Irfan for providing with the borehole logs of sites in Sharjah in addition to his great knowledge.

Special thanks to the professors of the Civil Engineering department who taught me the master level courses with great teaching methods and skills. I really appreciate their noble recommendations and motivation.

I would also like to extend my absolute appreciation for my colleagues Ahmed Mohsen Khalil, Hakem Al Khraisha, Mohammed Tarish, AbdulKareem Al Syouri and Shaziya Banu for their endless help and support during the entire period.

Last Of All, I would like to be thankful for the support of my family during this long and occasionally difficult journey. They were the backbone that pushed me and provided me with the ultimate motivation during the entire time.

Dedication

To my family:

My parents, Brothers, Sisters, Aunt, cousins, and friends.

Abstract

Seismic design of structures located in seismically active areas, like UAE, is primarily based on Seismic Site Response Analysis (SRA) of that area. SRA is the process of estimating the response of soil layers under earthquake excitation (i.e., bedrock motion) and the characterization of earthquake ground motion at the ground surface. This research aims to investigate the significance of shear wave velocity correlation and degradation models on the site response analysis. Three different shear wave velocity correlation equations and two different degradation models have been used in the analysis which reflects the adaptation of laboratory generated, field generated, and literature developed correlations. Moreover, the two different degradation setups replicate the computer programs built-in models and the laboratory generated models, respectively. The lab generated velocity correlation and degradation models were developed using dynamic triaxial machine, binder element test, However, the fields models were developed based on field geophysical instrumentations. A number of 38 boreholes were collected and classified into three categories based on their calculated V30; lowest V30 [$V30 \cong 250 (m/s)$], mean V30 [$V30 \cong 300 (m/s)$], and highest V30 [$V30 \cong 350 (m/s)$]. For each site, one dimensional site response analysis was performed using SHAKE2000. Results have shown that using site-specific shear wave velocity correlation can result in a totally different shear velocity distribution which can either result in different amplification factors or even change the site class of the soil in some cases. Moreover, the outcomes have depicted that the use of laboratory generated degradation models have led to an increase in the amplification factors values with respect to the outcomes obtained from using built-in degradation models. The amount of increase has ranged between 5% to 40%. These results justify the reason to generate site-specific shear wave correlations and degradation models, for seismic site response analysis.

Keywords: *Seismic Design; Site Response Analysis; Amplification Factors; Shear wave velocity correlation; Degradation Models.*

Table of Contents

Abstract.....	6
List of Figures	9
List of Tables	12
Chapter 1. Introduction	13
1.1. Overview	13
1.2. Problem Definition.....	15
1.3. Research Objectives and Contribution.....	16
1.4. Thesis Organization	16
Chapter 2. Background and Literature Review.....	18
2.1. Seismic Hazard Analysis	18
2.1.1. Identification of seismic sources.....	18
2.1.2. Recurrence parameters.....	18
2.1.3. Ground motion prediction equations (GMPEs).....	19
2.1.4. Results of PSHA.....	20
2.1.5. PSHA Deaggregation.....	22
2.2. Site Response Analysis and Local Site Effects.....	23
2.3. One-Dimensional Analysis	24
Chapter 3. Methodology	26
3.1. Seismic Hazard Analysis	26
3.2. Spectral Matching	27
3.3. Borehole logs	29
3.4. Site Response Analysis	31
3.4. Results of the Study	39
3.4.1. Site amplification factor profile.....	40
3.4.2. Site coefficients (Fa and Fv).....	41

Chapter 4. Results and Discussion.....	43
4.1. Preliminary Sensitivity Analysis.....	43
4.2. Effect of Initial Wave Velocity Correlation on Site Response Analysis ..	47
4.3. Effect of Degradation models on Site Response Analysis.....	60
4.4. Response Spectra	68
Chapter 5. Conclusion and Future Work	77
References.....	80
Appendix A.....	86
Appendix B	89
Vita.....	100

List of Figures

Figure 1: Seismic Hazard Curve of U.A.E. cities [10].	20
Figure 2: Seismic Map Developed for U.A.E Regions [10].	21
Figure 3: UHS Developed by Previous Researchers of proposed regions (Fig. 2) of UAE. (a) return period of 2,475 years and (b) 475 years [10].	21
Figure 4: Deaggregation of hazard for Abu Dhabi at a PGA and b spectral period of 1s (2,475 years return period) [10].	22
Figure 5: Input Motion Spectral Acceleration with Respect to Target Spectrum.	28
Figure 6: Relative error with respect to the target spectrum.	28
Figure 7: Generated Ground Motion.	29
Figure 8: SPT variation with depth on a real borehole	31
Figure 9: Triaxial Machine produced by VJ-Tech. [46].	34
Figure 10: Average Shear Modulus Reduction Curve for Sample C.	35
Figure 11: Lab Generated and Built-in Modulus Degradation Curves.	35
Figure 12: Lab Generated and Built-in Damping Degradation Curves.	36
Figure 13: Built-in BedRock Modulus Degradation curves Developed by Schnabel [47].	36
Figure 14: Built-in Bed Rock Damping Curves Developed by Schnabel [47].	37
Figure 15: Shear wave velocity profile.	39
Figure 16: Site amplification factor profile.	41
Figure 17: Typical Response Spectra plots to calculate site coefficients.	42
Figure 18: Fitted Response Spectra Curve.	42
Figure 19: Depth effect on site amplification factors.	43
Figure 20: Initial velocity effect on site amplification factors.	44
Figure 21: Effect of Lab Shear modulus Vs Built in Shear Modulus With the use of Built-in Damping Curve.	45
Figure 22: Effect of Lab Shear modulus Vs Built in Shear Modulus With the use of Lab Damping Curve.	46
Figure 23: Effect of Damping Reduction Curves.	46
Figure 24: Site Amplification Factors using PGA of Al Qasimya Borehole (Lowest V30).	51

Figure 25: Site Amplification Factors using RMS of Al Qasimya Borehole (Lowest V30).	51
Figure 26: Velocity distribution of the different integrated velocity correlations of Al Qasimya (Lowest V30).	52
Figure 27: Site Amplification Factors using PGA of Al Hemriyah Borehole (Lowest V30).	52
Figure 28: Site Amplification Factors using RMS of Al Hemriyah Borehole (Lowest V30).	53
Figure 29: Velocity distribution of the different integrated velocity correlations of AlHemriyah (Lowest V30).	53
Figure 30: Site Amplification Factors using PGA of Al Khan Borehole (Mean V30).	54
Figure 31: Site Amplification Factors using RMS of Al Khan Borehole (Mean V30).	54
Figure 32: Velocity distribution of the different integrated velocity correlations of Al Khan (Mean V30).	55
Figure 33: Site Amplification Factors using PGA of Al Braha-773 Borehole (Mean V30).	55
Figure 34: Site Amplification Factors using RMS of Al Braha-773 Borehole (Mean V30).	56
Figure 35: Velocity distribution of the different integrated velocity correlations of Al Braha-773 (Mean V30).	56
Figure 36: Site Amplification Factors using PGA of Al Butina Borehole (Highest V30).	57
Figure 37: Site Amplification Factors using RMS of Al Butina Borehole (Highest V30).	57
Figure 38: Velocity distribution of the different integrated velocity correlations of Al Butina (Highest V30).	58
Figure 39: Site Amplification Factors using PGA of Al Braha-11 Borehole (Highest V30).	58
Figure 40: Site Amplification Factors using RMS of Al Braha-11 Borehole (Highest V30).	59

Figure 41: Velocity distribution of the different integrated velocity correlations of Al Braha-11 (Highest V30).....	59
Figure 42: Effect of Degradation models on Al Qasimya Borehole (Lowest V30). ...	62
Figure 43: Velocity distribution of the velocity correlation of Al Qasimya (Lowest V30).	62
Figure 44: Effect of Degradation models on Al Hemriyah Borehole (Lowest V30)...	63
Figure 45: Velocity distribution of the velocity correlation of Al Hemriyah (Lowest V30).	63
Figure 46: Effect of Degradation models on Al Khan Borehole (Mean V30).....	64
Figure 47: Velocity distribution of the velocity correlation of Al Khan (MeanV30)..	64
Figure 48: Effect of Degradation models on Al Baraha-773 Borehole (Mean V30)...	65
Figure 49: Velocity distribution of the velocity correlation of Al Baraha-773 (MeanV30).....	65
Figure 50: Effect of Degradation models on Al Butina Borehole (Highest V30).	66
Figure 51: Velocity distribution of the velocity correlation of Al Butina (Highest V30).	66
Figure 52: Effect of Degradation models on Al Baraha-11 Borehole (Highest V30). ...	67
Figure 53: Velocity distribution of the velocity correlation of Al Baraha-11 (Highest V30).	67
Figure 54: Fitted Hazard Spectrum for Al Hemriyah Borehole (Lowest V30).	71
Figure 55: Fitted Hazard Spectrum for Al Soor Borehole (Lowest V30).....	71
Figure 56: Fitted Hazard Spectrum for Al Khan Borehole (Mean V30).	72
Figure 57: Fitted Hazard Spectrum for Al Baraha-773 Borehole (Mean V30).	72
Figure 58: Fitted Hazard Spectrum for Al Baraha-11 Borehole (Highest V30).....	73
Figure 59: Fitted Hazard Spectrum for Al Butina Borehole (Highest V30).....	73
Figure 60: Amplification factors (Fa & Fv) obtained using the lab generated degradation models and Khalil's velocity correlation.....	74
Figure 61: Amplification factors (Fa & Fv) obtained using the built-in degradation models and Khalil's velocity correlation.	75
Figure 62: Amplification factors (Fa & Fv) obtained using the built-in degradation models and Irfan's velocity correlation.	75
Figure 63: Amplification factors (Fa & Fv) obtained using the built-in degradation models and Niamatullah's velocity correlation.	76

List of Tables

Table 1: PGA and spectral accelerations for period 0.2 to 4.0 s for major cities for return period of 2,475 years [10].	27
Table 2: Criteria for selecting time histories.	27
Table 3: Typical Borehole log with SPT values [45].	30
Table 4: Description of Tested Soil [45].	33
Table 5: Unit weight values assigned to the soil sublayers.	39
Table 6: Amplification factors (F_a & F_v) obtained using the lab generated degradation models and Khalil's velocity correlation.....	74
Table 7: Amplification factors (F_a & F_v) obtained using the built-in degradation models and Khalil's velocity correlation.	74
Table 8: Amplification factors (F_a & F_v) obtained using the built-in degradation models and Irfan's velocity correlation.	75
Table 9: Amplification factors (F_a & F_v) obtained using the built-in degradation models and Niamatullah's velocity correlation	76

Chapter 1. Introduction

In this chapter, a general overview about the site response analysis and the dynamic soil parameter are being provided. Moreover, problem definition and objectives of this research are presented. Additionally, the available data and data collection stage would be introduced. Finally, general organization of the thesis is described.

1.1. Overview

Evaluation of seismic ground motion at a specific site is critical for computing the potential consequences of an earthquake including ground deformation and failure. Many infrastructures and superstructures have been damaged or destroyed due to the earthquakes that may occur. In the late 1920s American engineers have started recognizing the major factors that impact the dynamic response of structures [1, 2]. About the same period Huber (1930) had posted the first article that illustrated the effects of directionality on observed damage, contrasting the effects of the 1868 Hayward and 1906 San Francisco earthquakes on buildings. The 1933 Long Beach earthquake was observed, and it was the first to provide huge motion records, which resulted in significant insights on spectral accelerations and amplification [3]. Intensive motion records from the 1940 El Centro earthquake resulted in some initial signs about the importance of studying the local geology due to the major role it plays in amplifying the incoming seismic waves. Moreover, the effect of local geology on shaking force have been significantly recognized internationally after the 1985 Michoacán earthquake, which destroyed portions of Mexico City [4].

All these facts had made the integration of seismic effect together with the influence of local geology in the design a very significant factor, and this integration is known as site response analysis. To compensate for the local site effects, the 1994 version of NEHRP (National Earthquake Hazard Reduction Program) introduced some guidelines in the form of site amplification factors for the design of various structures [5]. Additionally, current building codes such as IBC06, UBC97 and CHBDC06 similarly provide guiding principles to estimate the response spectra for several structures depending on the site amplification factors at multiple natural periods. Yet, current studies recommend the development of amplification factors precisely to the

various tectonic areas instead of using the universal site amplification factors provided in NEHRP [6].

Soils can significantly impact and amplify seismic waves in terms of both amplitude and strain levels based on the dynamic properties of the existing soils [7]. This fact indicates the importance of developing site-specific amplification factors. To achieve that task, it is very important to conduct several tests to analyze the ground conditions and obtaining the dynamic properties of the ground soils. The dynamic parameters of the soils that highly influence the seismic response consist of; initial shear modulus (G) which is the parameter that represent the stiffness of the soil, shear wave velocity (V_s) which represent the speed of the shear waves traveling through the soil layer, and damping ratio (ζ) which indicates the reduction in wave energy due to the medium it travels through. Moreover, several factors such as shear strain (γ) that is imposed by the waves and the confinement rate (σ) can significantly influence the dynamic parameters, thus; it is not enough to obtain the dynamic properties at a specific shear strain or specific rate of confinement, yet, it is very important to analyze the dynamic properties as functions of both confinement rates and shear strain [8]. Dynamic properties could be estimated and obtained by conducting either field tests such as Seismic Reflection test, Seismic Refraction test, Cross-hole Seismic Surveys, etc. or by conducting laboratory tests for instance; Bender Element test (B.E.), Resonant Column test (R.C), or Cyclic Triaxial test (C.T) [9]. Both methods are generally considered efficient in terms of obtaining the dynamic properties, but each method has its own advantages and limitations. One of the major advantages of the field tests is that in addition to measure the dynamic properties efficiently, it can also develop a sub-surface image for the site. Yet. One major limitation of field methods is that they cannot be used to measure all dynamic properties unlike laboratory tests which could measure any desired dynamic soil property more accurately which is a major advantage. However, the high cost of the equipment setup and skilled technicians required are considered as major disadvantages. The previous facts indicate that the determination of the most suitable method of testing depends on two factors namely; purpose of the evaluation, and availability of equipment setup.

The purpose of this study is to evaluate the impact of using laboratory generated shear wave velocity correlation and degradation model on the seismic site response analysis, for selected sites on UAE.

1.2. Problem Definition

In the past two decades U.A.E. had experienced huge growth regarding its infrastructure. These developments included several mega projects such as Burj Khalifa. Even though UAE had not experienced any major earthquake in this period, yet the active seismicity in the nearby zones for instance Iran and Oman can put the infrastructure of the country under major threat. Current earthquakes of significant magnitudes in UAE and Oman have correspondingly increased the necessity for risk management plans for main cities of the country. Each Structure has a specific natural period, and the seismic waves approaching from long distances vibrate at multiple periods. If the natural periods of the buildings match the fundamental periods of the seismic waves' resonance will develop and the consequences will be catastrophic. Furthermore, the several layers of different soil types underlying the surface can amplify the seismic waves. This amplification could lead to a major change of the seismic waves when it approaches the ground surface. This indicates the fact that even if the buildings were designed to have different natural periods than the incoming seismic waves, the amplification that may result from the ground soil can still lead to catastrophic outcomes.

Several studies have been conducted to develop site amplification factors for UAE with the most recent study done by Khan et al. [10], which included major cities of UAE. Yet, some limitations were experienced which may affect the reliability of the results. The first limitation which is a common constrain for all the previous studies is the reliability of the dynamic properties adopted in the analysis. Most of the previous studies used correlations that were developed for other regions to estimate the dynamic properties of the regional soils. These correlations are developed with some factors to match the soil conditions in the region they specified for. This fact illustrates the importance of obtaining accurate dynamic properties of the local sites. Therefore, a major objective of the current study is to investigate the impact of using laboratory generated shear wave velocity correlation and degradation model on the site response analysis. Additionally, another major aspect of this research is to obtain the

amplification coefficients and compare the outcomes with the NEHRP design coefficients.

1.3. Research Objectives and Contribution

The objectives and contributions of this research work can be summarized as follows:

- Obtain a reliable dynamic soil properties and shear and damping degradation correlations for certain local sites in UAE using dynamic triaxial and binder element tests.
- Develop one-dimensional site response models for several sites in different cities of UAE. These models can adopt the effect of different shear velocity correlations.
- Use the 1-D site response models to establish detailed parametric study that shows the implication of adopting different degradation models (lab developed model, and built-in model).
- Obtain the amplification coefficients (F_a and F_v) and compare the results with the National Earthquake Hazard Reduction Program suggested design parameters to analyse the effect of laboratory generated velocity correlations and degradation models.

1.4. Thesis Organization

The following chapters of the thesis are organized as follows: Chapter 2 presents background and the available literature about the confinement and dynamic soil parameters and their impact on the site response analysis. Chapter 3 provides the methodology that was implemented to carry out the research. The two computer programs that were used and the corresponding results obtained from them are demonstrated as well. Additionally, the analysis of the outputs as well as the format and the presentation of the results is also shown. Chapter 4 presents the acquired results in the form of amplification factors and curves. Comparison of the different outputs will be done to obtain the effect of integrating the confinement level, site-specific degradation model, and site-specific shear wave velocity correlation in the numerical

modelling. Chapter 5 summarizes and provides conclusions in addition to some suggestions and recommendations for future work related to this field of research.

Chapter 2. Background and Literature Review

In this chapter, the definition, fundamentals, in addition to the previous work related to seismic hazard analysis and site response analysis are discussed. Afterwards, the methods used in conducting both analyses are presented.

2.1. Seismic Hazard Analysis

Seismic hazard analysis is the quantitative valuation of seismic hazards and their related uncertainty in terms of time, and space for a specific site as well as offering seismic hazard estimations for seismic risk assessment [10, 11]. Researchers have developed two methodologies to conduct a seismic hazard analysis, a deterministic approach (DSHA) and a probabilistic approach (PSHA). The determination of a suitable method relies on the nature of the study. For this research, a Probabilistic Seismic Hazard Analysis (PSHA) was preferred. PSHA studies the uncertainty incorporated in the location, duration of incidence, and size of future earthquakes. There are multiple stages for conducting the Probabilistic seismic hazard analysis [12, 13, 14]. Yet, the three most significant aspects out of those stages are illustrated in the following sections.

2.1.1. Identification of seismic sources. Analysis of geological, tectonic, in addition to seismological data form the basis of identifying seismic sources. In this section, a brief description of the classification process is presented. Based on the spatial allocation of the seismic ground motions, the seismicity among an area of consideration is distributed into various seismic sources. Faults, areas, and points represent the sources of seismic activity. Due to the lack of comprehensive knowledge related to both line and point sources, area sources are preferred. Uniform probability distribution among the sources is allocated to each seismic source as soon as all the close seismic sources to a site of interest are identified.

2.1.2. Recurrence parameters. One of the key differences between the DSHA and PSHA is the determination of recurrence factors. The recurrence relationship characterizes the uncertainty in size and duration of appearance of the future earthquakes allocated to each source. The mean/average rate at which an earthquake of a specific size would be exceeded is illustrated through this relationship. In 1944 Gutenberg et al. plotted the logarithm of annual exceedance against the

magnitude of an earthquake [15]. The plotted curve resulted in a linear relationship which was observed and reported by the researcher (Equation 1).

$$\text{Log } N = a - bM \quad (1)$$

where the magnitude of the earthquake is represented by the letter M. The number of earthquakes that have a magnitude that is greater than or equivalent to M is represented by the letter N. Moreover, a and b are coefficients, where a represents the number of earthquakes that are greater than magnitude zero, and it would be influenced by the number of events, the size of the source area and the number of years of seismic date. On the other hand, b represents the relative number of small magnitudes to large magnitude earthquakes [10, 16].

2.1.3. Ground motion prediction equations (GMPEs). The estimation of the ground motion generated by an earthquake at a specific distance from epicenter is done by using the Ground Motion Prediction Equations (GMPEs). Several parameters such as the distance from the epicenter, distance from the hypocenter, nature of fault rupture mechanism, damping of transmitting media, and properties of the region soil represent the characteristics that influence the GMPEs directly [17]. By utilizing the regression of accelerations documented at different distances, the GMPE's are developed. The standard deviation of the peak ground acceleration denotes the quantified unreliability in the regression. Most of the GMPE's represent the developed relationship between the peak ground acceleration to the magnitude of an earthquake (M), and the range from epicenter (R). Additional factors which represent the earthquake source, wave transmission and local site conditions are present in multiple attenuation equations. Equation 2 illustrates a typical form of the GMPEs.

$$\ln Y = C_1 + C_2M + C_3M^{C_4} + C_5 \ln[R + C_6 \exp(C_7M)] + C_8R + f(\text{source}) + f(\text{site}) \quad (2)$$

Based on the ground motion factor (Y) that is being predicted, the values of constants (C₁, C₂, C₃, etc.) fluctuate accordingly. By carrying out the regression analysis on a specific ground motion parameter, the magnitudes of the coefficients are determined. The correlation between the ground motion factor, spectral period, and the variable (magnitude or distance) is normally represented by these constants. Additionally, the utilization of the regression analysis can result in developing the

relationship between the ground motion parameter and the chosen variable [17]. GMPEs are then allocated to distinct seismic sources.

2.1.4. Results of PSHA. The seismic hazard curve is considered the main outcome of PSHA. Through this curve the relationship between the annual rate of exceedance (or return period) to any spectral acceleration is presented. Figure 1 depicts seismic hazard curve for Peak Ground Acceleration (PGA) developed for U.A.E. cities. It should be noted that PGA represents a spectral acceleration at spectral period of zero. Seismic hazard maps presented in Figure 2 are considered a major outcome of the PSHA. These maps simplify the process of selecting the ground motion for a specific return period since PGA and spectral accelerations for 0.2s and 1s are plotted on them. Furthermore, another form of representation of the results of PSHA is Uniform Hazard Spectrum (UHS). UHS depicts various spectral accelerations for multiple spectral periods at a mutual rate of exceedance. Figure 3 presents the results of previous UHS curves generated for the U.A.E.

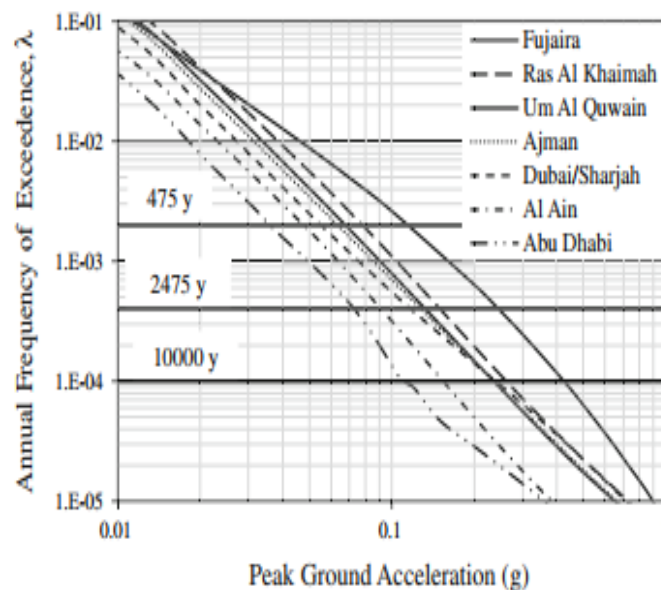


Figure 1: Seismic Hazard Curve of U.A.E. cities [10].

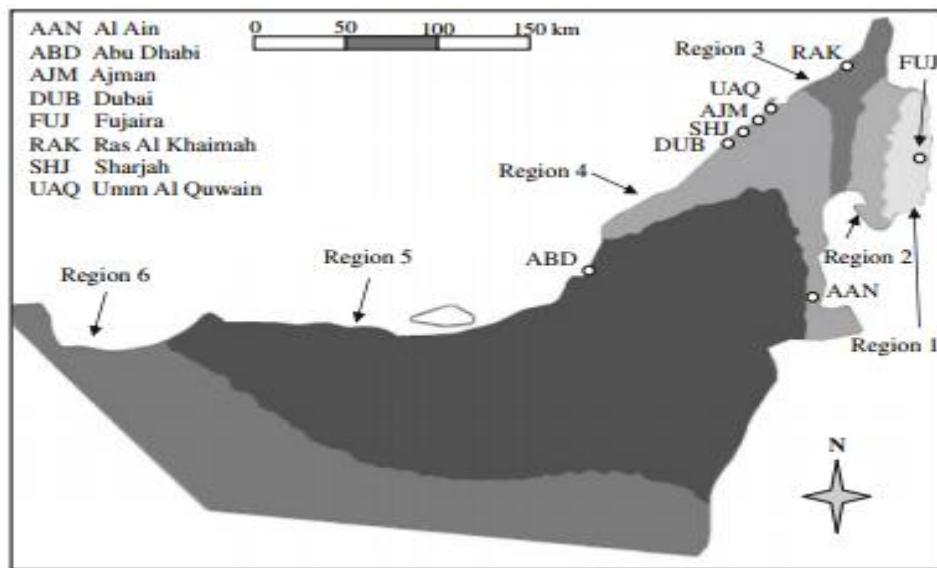


Figure 2: Seismic Map Developed for U.A.E Regions [10].

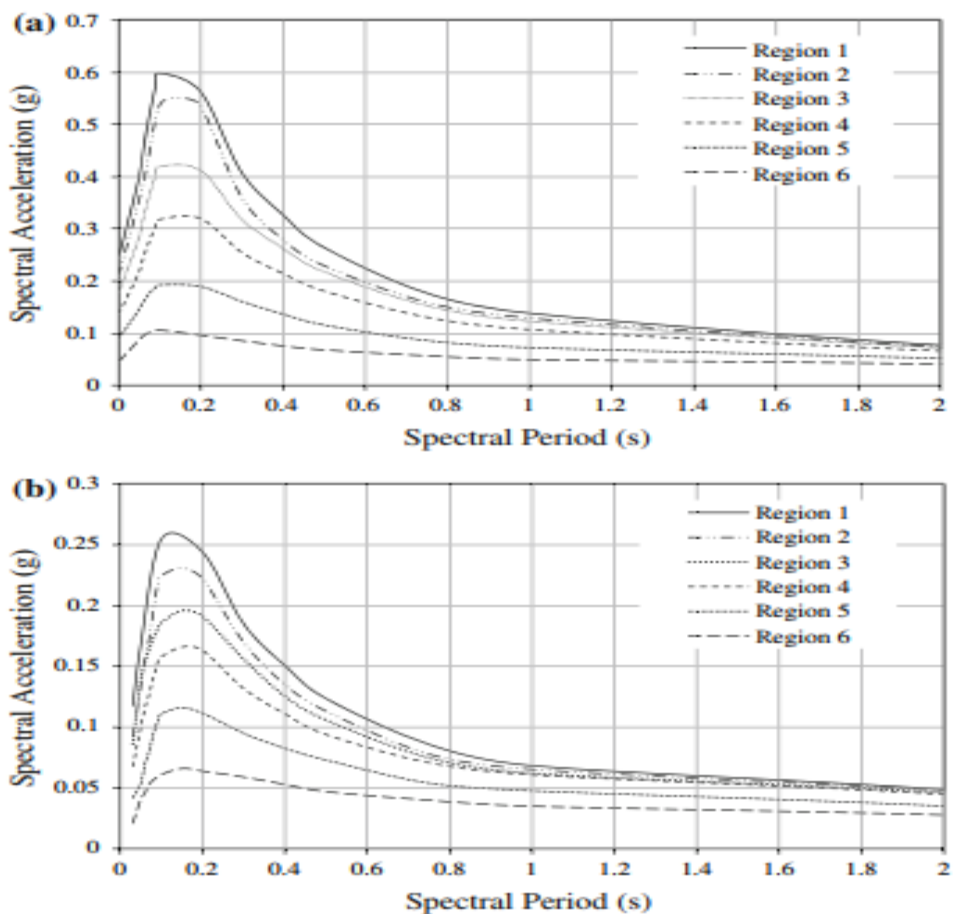


Figure 3: UHS Developed by Previous Researchers of proposed regions (Fig. 2) of UAE. (a) return period of 2,475 years and (b) 475 years [10].

2.1.5. PSHA Deaggregation. An earthquake acceleration time history that represents the local sites from the results of PSHA is required by the dynamic analysis of a structure. Determining the principal magnitude and distance from the results of PSHA is called Deaggregation. Several previous researchers have illustrated the methodology of performing deaggregation [18, 19, 20, 21]. Figure 4 represents a deaggregation plot developed for Abu Dhabi. The peaks of the histogram will vary based on the spectral accelerations and spectral periods related to the study. The selection of the representative earthquake is performed based on the magnitude and distance that corresponds to the peak value presented in the histogram.

Since deterministic approach integrates the influence of a single scenario seismic motion at a site, choosing a representative earthquake could be challenging. However, all potential combinations of ground motions magnitude and distances are considered in PSHA to obtain the dominant scenario which causes the greatest hazard level.

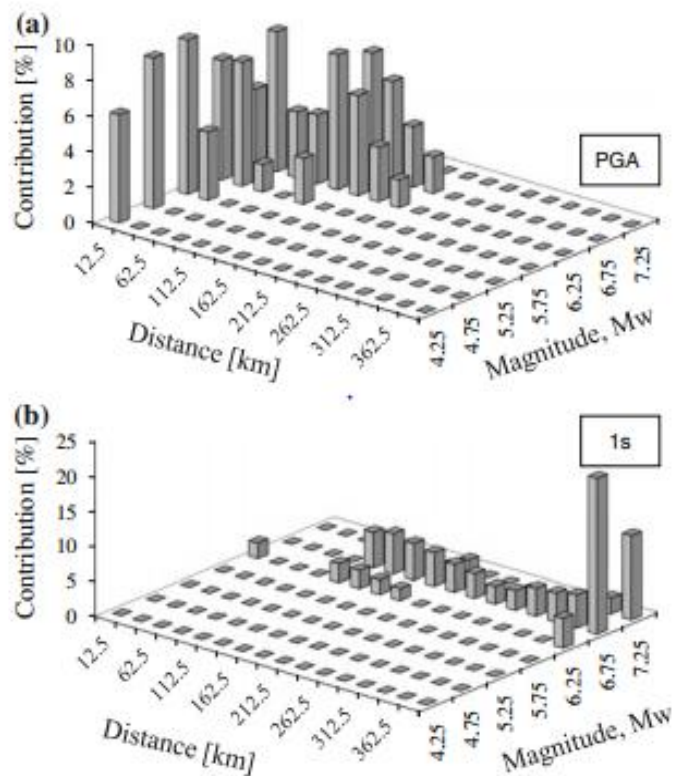


Figure 4: Deaggregation of hazard for Abu Dhabi at a PGA and b spectral period of 1s (2,475 years return period) [10].

2.2. Site Response Analysis and Local Site Effects

Site response analysis has been considered a significant subject in earthquake geotechnical engineering a long time ago. Following to the 1906 San Francisco seismic activity, the regional geology and soil conditions proved to have a major impact on the amount of damage experienced by structures. To examine the impact of local soil conditions on site response, Kanai and workers accomplished detailed studies including micro-tremors between 1930's and 1940' [22]. Additionally, in the 1950's the influence of geologic ground properties on seismic motions have been taken under consideration by Gutenberg [22]. Such studies have proved the significance of further research in this area. In the 1990's and with the arrival of computer programs, the attempt to extend and enlarge the understanding of site response has become greater than ever.

Several seismic hazards which occurred between 1980 and 1999 such as Loma Prieta (1989), Northridge (1994) Kobe (1995), and Chi-Chi earthquakes (1999) have validated the great effect that is imposed by the local site properties and geomorphologic conditions on the response of the sites [23]. Local site effect is a term which stands for the variations anticipated on the magnitude and the frequency of an earthquake motion after traveling through a soil deposit. The local geology of the site contains many parameters. However, the magnitude of the loading, number of cycles, soil type, shear strain and confining pressure are considered the main characteristics which defines the behavior of soil under seismic loading [24] [25] [23].

As concluded from the previous paragraph, it's very important to study the site conditions prior conducting site response analysis to obtain reliable results. To evaluate the response of any site there are several methods to be followed such as linear, equivalent linear and non-linear [26]. Strain-dependent dynamic properties are required by all the previous methodologies. These properties are incorporated into the analysis as inputs in terms of shear modulus and damping ratio degradation curves [26]. Several studies have been carried out to evaluate the influence of local site effects on the site response analysis for U.A.E. Maher et al. have reported that site response analysis is greatly impacted by the local soil parameters [27]. Moreover, El-Emam et al. have also reported that ground factors have huge capability of amplifying the incoming seismic motions [28]. Additionally, several studies have been conducted worldwide to evaluate this effect. Hashash et al. [29], Ordonez [30], Kumar et al. [31], and Basu et al. [32]

have all conducted ground response analysis targeting Indian cities and reported that there is a direct correlation between the local site conditions and amplification that occurs at the seismic motion. Most of the previous researchers have used 1-dimensional computer program such as SHAKE2000 to conduct their studies. Moreover, due to the lack of resources and time, the previous researchers utilized the built-in material models suggested by Seed and Idriss [33] to perform the work. However, integrating these built-in models could result in many uncertainties since they have been generated for soils of different regions and compositions. The uncertainty of using built-in models in the numerical analysis was highlighted by several researchers. Kumar et al [26] have reported that using site specific dynamic properties have exhibited 38% and 24% reduction in the peak ground accelerations and peak spectral accelerations respectively while comparing it with similar studies which have implemented built-in model. Field et al. [34] conducted a study on Turkey flat, California site to evaluate the linear elastic response of the under weak motions using Monte Carlo simulations. It was reported that the amplification predictions were significantly influenced by the uncertainties located in the shear-wave velocity profile and small strain damping ratio. Ellen et al [35] established a study to evaluate the influence of site property variabilities on ground motion site response analysis using Monte Carlo simulation. The study reported that the variability in soil properties highly impact the standard deviation of the amplification factors.

2.3. One-Dimensional Analysis

The simplest method to conduct a site response analysis is to use one dimensional (1-D) analysis. For any specified location, the analysis is performed on a perpendicular slice which represent an extracted borehole from the site. Therefore, the analyzed soil column is assumed to extend infinitely in all directions and be of constant depth. Due to the simplicity of the one-dimensional analysis, they are considered the oldest and initial method utilized for solving site response problems. However, nowadays, very complicated types of soil modeling could be involved in the analyses.

In 1950 Kanai has solved a case of viscoelastic material using the one-dimensional concept [36]. The case incorporated a uniform deposit of soil exposed to a harmonic shear wave and lie on top an elastic half-space. Kanai presented the outputs in terms of a curve that illustrated the ratios of displacement versus the period of the

input shear wave by solving the equations of motion. Around 1952 Kanai did improve this method to integrate two diverse material properties that form two uniform viscoelastic layers lying on an elastic half-space [37]. Moreover, the case of a uniform viscoelastic soil layer under a harmonic shear wave input was studied by Idriss and Seed in 1968 as well [38]. Both materials were examined using constant shear modulus and uniformly varying modulus as input variables. One of the cases that were investigated is determining the influence of uniformly changing the shear modulus with respect to the depth of the cube. The equations of motion were used to solve these cases directly. The lumped mass technique of solution was used to model irregular changing soil materials by Idriss and Seed. By utilizing a combination of dashpots and springs in series and parallel to generate a bi-linear illustration of the modeled material deposit, Idriss and Seed managed to extend the viscoelastic problem. Idriss and Seed made an effort to improve the viscoelastic case even further to model the nonlinear behavior of the materials by using an equivalent value to represent the shear modulus experienced in the nonlinear response. This development is known as the equivalent linear method. Laboratory tests such as cyclic triaxial or bender element could be used to obtain this value. Moreover, an iterative testing procedure could be used to obtain a relationship between the equivalent shear modulus values with respect to the average shear strain which is known as the degradation models. In 1972 Schnabel et al. utilized the concept of fast Fourier transforms to improve the efficiency of the analysis and developed a new methodology to solve the viscoelastic cases [39]. This work consists foundation of the software SHAKE which still one of the most common site response analysis tools used by researchers nowadays.

In 1978 Taylor et al. worked on improving the concept of a bi-linear one - dimensional analysis to analyze the soil nonlinearly [40]. An array of elastoplastic components was utilized to replicate the hysteretic nonlinear behavior of the modeled material instead of using a linear or bi-linear arrangement of springs joining the lumped masses. Laboratory results such as shear modulus versus shear strain curves could be used to acquire the characteristics of these components. Otherwise, they could be selected to fit a simple hyperbolic relationship.

Researchers managed to generate an adequate level of understanding of the one-dimensional site response impact on the input motion.

Chapter 3. Methodology

In this chapter, the steps needed, and the methodology followed to obtain the outcomes of the research are demonstrated. The chapter include a brief description about several aspects. The first aspect is the seismic hazard analysis. The outputs that were acquired and used in this thesis that are related to this subject are all mentioned. The second aspect is the spectral matching. The steps followed to match the obtained ground motion with the target spectrum are listed. The third aspect is the Borehole logs. The types, location, and source of obtaining the used borehole logs are stated below as well. The last aspect that was mentioned in this chapter is the site response analysis. Since this aspect represent the source of this study it was elaborated and explained in detail. The software used to conduct the analysis, the dynamic properties used, the methods of data analysis and sample of the end results are all listed and described.

3.1. Seismic Hazard Analysis

Online databases, catalogues, in addition to the available literature were the main sources to acquire seismic records related to the area of study [41, 42]. Some data included historic seismicity as additional information to the instrumental seismicity. However, only instrumental seismicity was used in this study. Repetition of any seismic occasions was avoided by cleaning up the collected seismic records. Additionally, Khan et al. have performed this study earlier in 2013 and it resulted in the peak ground accelerations, spectral accelerations and deaggregation of hazard for the major cities of U.A.E. which were used in this research [10].

Pacific Earthquake Engineering Research (PEER) database have been the source to obtain acceleration ground motion time histories. The selection of the ground motions has been done based on multiple factors such as magnitude, distance, or peak ground acceleration (PGA). These parameters were determined based on the results of the seismic hazard analysis conducted by khan et al [10]. Afterwards, 'RSP Match EDT' which is a commercial computer software was acquired and used to perform spectral matching on ground motion time histories with respect to a target spectrum that was developed based on khan's study.

3.2. Spectral Matching

Obtaining an accurate result of any site response analysis is directly related to the ground motion. This signifies the value of developing a representative time history based on a specified target spectrum. The outcomes of the deaggregation process will define the values assigned for these parameters. RSP Match EDT which is a commercial computer software was secured and utilized to match obtained time histories to a target spectrum that was developed based on Khan's research.

Two main parameters were required to perform the matching process. The first requirement is to obtain a target response spectrum. Target response spectrum is an outcome obtained by performing seismic hazard analysis. Since the time history is scaled to match its properties which will cover the pseudo acceleration of maximum earthquake events in database, it is called target. In this research the target response spectrum was developed based on the results of PSHA performed by Khan et al [10]. Table 1 represent the PGA and spectral accelerations resulted from Khan's study which were used to develop the target response spectrum.

The second requirement needed is a time history to be matched. One time history for Sharjah was selected based on the process illustrated by Boomer and Acevedo which relies on the spectral shape and similarity in magnitude and distance [43]. The data used for the selection is represented in Table 2. The selected time history was acquired using PEER and obtained in PEER format. Thus, a conversion process was done to convert the file into a compatible format. After obtaining the two main input parameters, RSP Match EDT was run.

Table 1: PGA and spectral accelerations for period 0.2 to 4.0 s for major cities for return period of 2,475 years [10].

City	PGA (g)	0.2s (g)	1s (g)	2s (g)	3s (g)	4s (g)
Sharjah	0.120	0.285	0.109	0.068	0.037	0.025

Table 2: Criteria for selecting time histories.

City	Fault Type	Magnitude	Distance (km)
Sharjah	Reverse	7	60

After running the RSP Match EDT, the input ground motion was generated and matched with respect to a target spectrum. The difference between the original, matched, and the target in terms of spectral accelerations and relative error are presented in Figure 5. Figure 6 The graphs clearly illustrate the accuracy of the matching process.

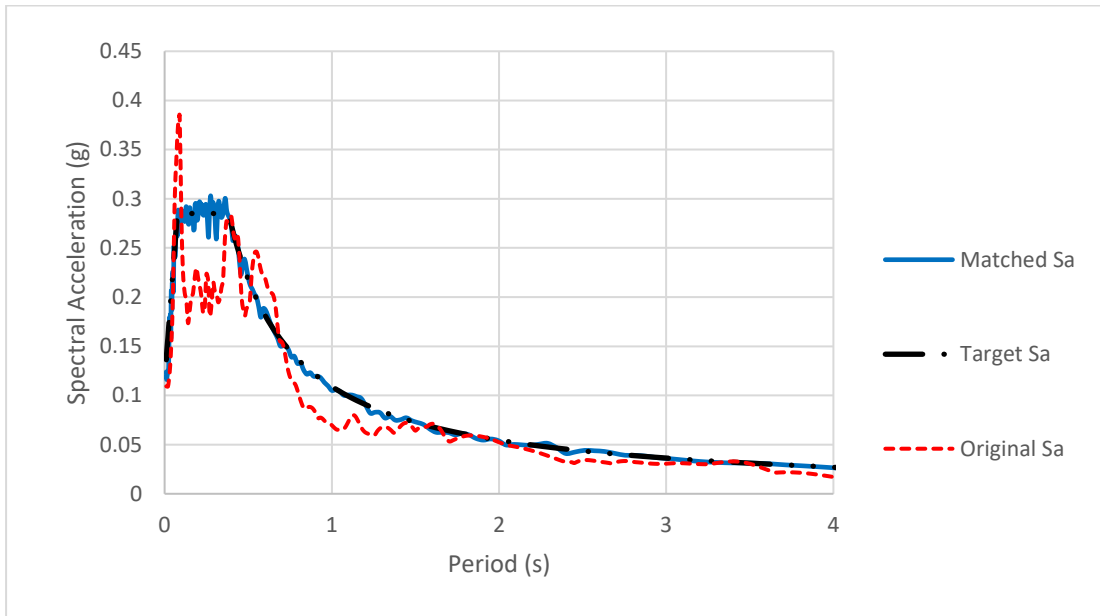


Figure 5: Input Motion Spectral Acceleration with Respect to Target Spectrum.

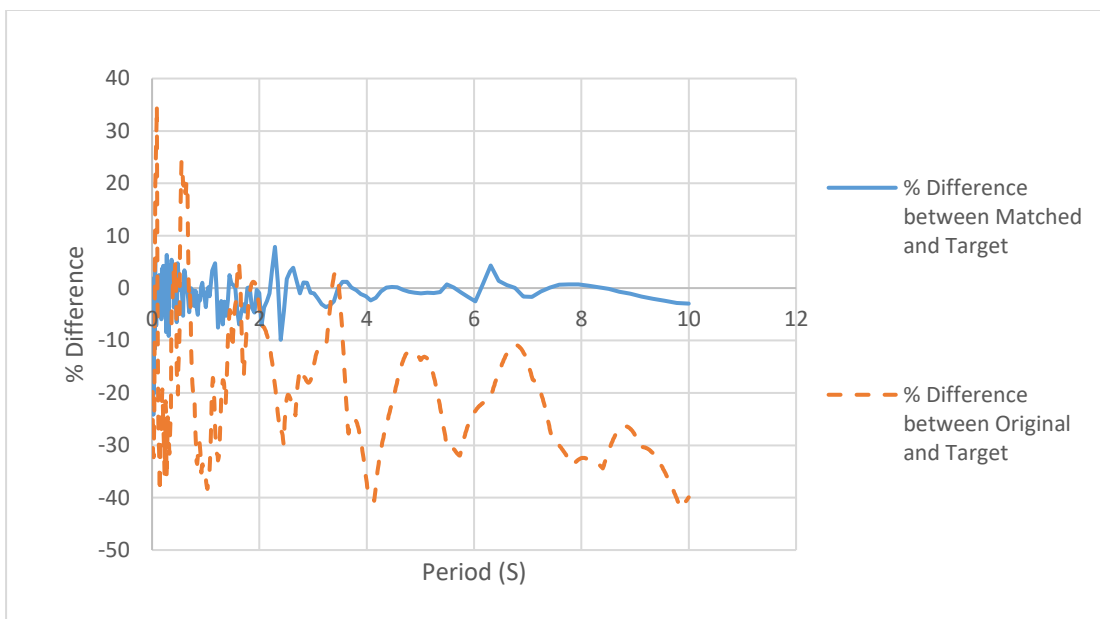


Figure 6: Relative error with respect to the target spectrum.

The First parameter required to execute the process and evaluate the effect resulted from exciting the soil layers under seismic loading was to assign the ground motion time history. The ground motion had to be assigned on top of a specific layer which is called the engineering bedrock or the half space. The engineering bedrock is typically located at the end of the borehole, and it replicates the role of the boundary to the soil column. The process of obtaining the ground motion is illustrated previously. Moreover, Figure 7 depicts the generated ground motion which was used in this research.

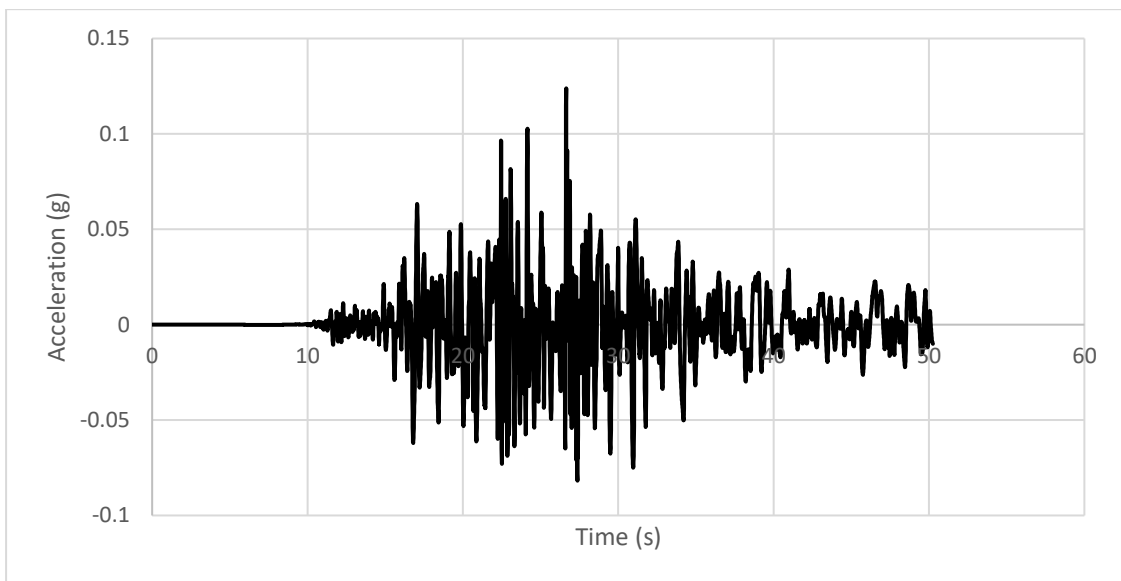
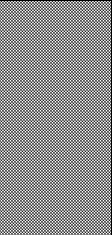
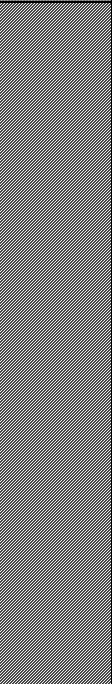
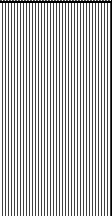


Figure 7: Generated Ground Motion.

3.3. Borehole logs

To obtain a representative dynamic property of the regional soils, different soil reports were required from various cities around the UAE. Such Boreholes were collected earlier by Muhammad Irfan [44] Some of these boreholes were used in this research to create 1-dimensional models. Most of the used boreholes were collected from Sharjah and the depth of the boreholes ranged from 15 to 45m in depth. Regarding to the site response analysis performed two computer programs were used to perform the numerical modeling. Table 3 demonstrates a typical borehole log. For detailed information regarding to the used borehole logs refer to Appendix B.

Table 3: Typical Borehole log with SPT values [45].

Depth Below Ground Level (m)	Soil description	Layer thickness	Legend	Soil classification	Sample Type	Depth	SPT N-Value
0.0 1.0	Fill Materials (0.01-1.5m). ▼	1.5m		SP-SM	DISTURBED UNDISTURBED SPT	1	N=20
2.0						2	N=24
3.0						3	N=26
4.0						4.5	N=24
5.0	SILTY-SAND (1.5-9.6) m	8.1m		SP-SM	UNDISTURBED SPT UNDISTURBED SPT	6	N=45
6.0						7.5	N=48
7.0						9	N=50/27
8.0							
9.0							
10.0 11.0 12.0.	MUDSTONE (9.6-50) m	BELOW 9.6m		SP-SM	UNDISTURBED SPT		



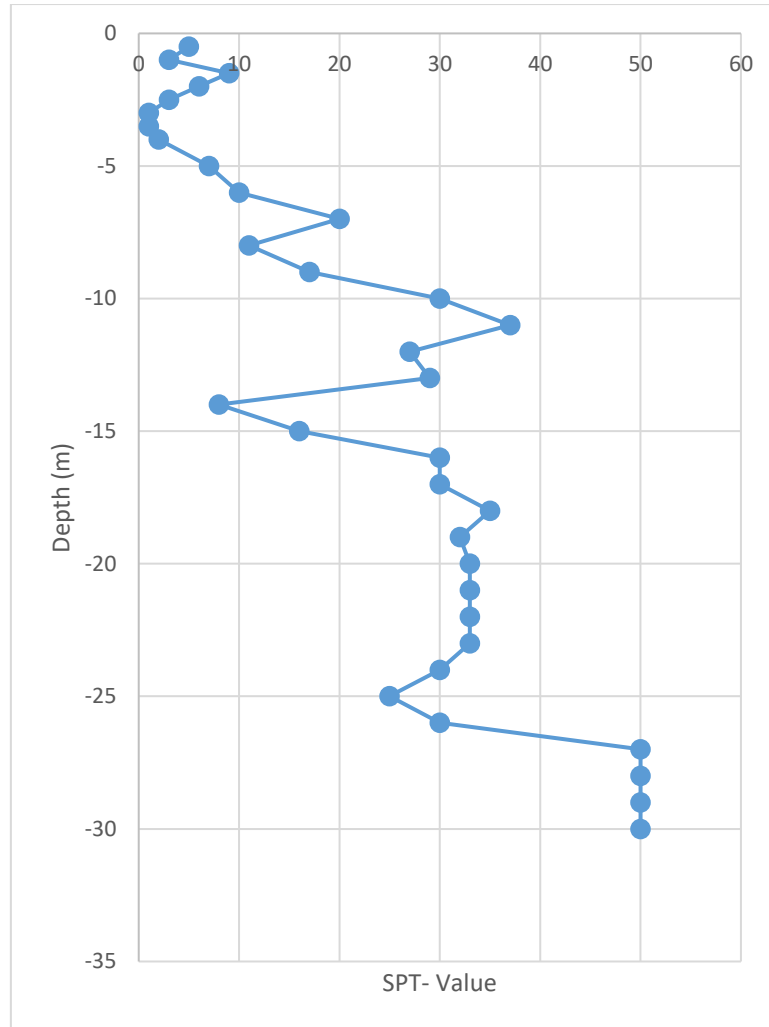


Figure 8: SPT variation with depth on a real borehole

3.4. Site Response Analysis

In this research, the obtained boreholes were used to perform the site response analysis. These boreholes were selected to represent the local soil. SHAKE 2000 which is a commercial computer software was used to execute 1D site response analysis on the boreholes.

SHAKE 2000 is considered one of the oldest computer programs used in geotechnical earthquake engineering. It was generated by Schnabel et al. [39] for mainframe environments. SHAKE 2000 is considered nowadays one of the most user-friendly programs due to the many changes that have been introduced into the software since it was developed.

Several inputs are needed to run SHAKE 2000. The first inputs are the thickness and material type for layers. These two inputs are attained from the borehole logs since

it depends on the local geology and underground soil composition. The first step was illustrated earlier which is to obtain the input motion.

The second inputs are the shear modulus and damping ratio curves. These curves are known as the degradation curves. Degradation curves are allocated to the generated layers based on the soil types in the borehole profile. Two categories of degradation models were used in the study. The first category is the degradation curves developed for U.A.E. soil in the laboratory. To develop the degradation curves, the cyclic triaxial test was performed using displacement control criteria on three different types of soil samples at three different confinement pressures (40kPa, 100kPa, and 140kPa). Figure 9 depicts the equipment used in the laboratory. Moreover, the displacement increment was increased gradually to obtain the impact of shear strain. Each run was recorded and saved based on a predefined labeling system. Afterwards, an Excel sheet was generated to obtain the values of shear modulus, damping ratio, with respect to the shear strain. For detailed calculation please refer to A.M. Khalil thesis [45]. A typical result of the degradation model is presented in Figure 10. However, since the difference between the different soil samples curves among the 3 different confinement levels was negligible, an average degradation curve was used to represent the different soil samples in addition to the confinement levels. Table 4 provide a description of the different soil samples used in the laboratory testing to obtain the dynamic properties of the local soil by A.M. Khalil. However, in this research sample A was not considered for developing the degradation curves since it has different composition than the other samples. The second category are the built-in degradation curves that are integrated in the software. Several researchers have presented degradation curves established for specific type of soils in the past such as Schnabel [46], Seed et al. [47], and Sun et al. [48]. Two broadly acknowledged degradation curves were used in the study, Seed et al. [33] for sandy soil, and Schnabel [46] for rocks since sandy soils represent majority of the soil composition in U.A.E. Each sand degradation model contained three different curves which are sand upper, sand average, and sand lower. Each sublayer was assigned one of these three degradation curves based on the classification of the layer. Sand lower curve was assigned to the layers with loose composition. Whereas sand average curve was allocated to medium dense layers. However, sand upper curve was designated to dense layers. Figure 11 and Figure 12 depicts and compares both the average degradation curves developed by in the lab with

the built-in degradation models. As can be noticed, the difference between the lab generated degradation model and the built-in degradation model varies with the change in shear strain. Regarding to the modulus degradation curves, the 4 used curves are almost identical while comparing them at a range of 0.0001% to 0.001% shear strain. However, while comparing at a range of 0.001% to 0.1% it can be seen that the difference between the lab curve and the upper curve, mean and lower curves ranges from 2% to 15.5%, 2% to 33%, and 2% up to 45.4% respectively. After that the variation is almost negligible. Nevertheless, regarding to the damping curves another variation could be noticed. While comparing the lab generated model to the other 3 curves at a range of 0.0001% to 0.001% shear strain, the difference is almost constant which is 74%. However, while comparing at a range of 0.001% to 0.1% it can be seen that the difference between the lab curve and the upper curve, mean and lower curves ranges from 0.5% to 60%, 2% to 58%, and 2% up to 15% respectively. Afterwards the difference remains constant. Figure 13 and Figure 14 represent the built-in degradation curves for the bedrock integrated in the analysis.

Table 4: Description of Tested Soil [45].

Sample Name	Borehole and Site Number	Material Description	Depth (m)
Sample A	BH1, Site 1	Weak, light brown to light grey mudstone with inclusions of crystalline gypsum	11-12
Sample B	BH1, Site 1	Medium dense to very dense, poorly graded sand with silt and trace fine to medium gravels	7-8
Sample C	BH1, Site 1	Medium dense to very dense, poorly graded sand with silt and trace fine to medium gravels	1.5-2
Sample D	BH2, Site 2	Medium dense, light grey to grey wet, non-plastic, silty sand, trace fine gravel, shell fragment, (SM)	4-5
Sample E	BH1, Site 3	Medium dense to very dense, light brown to light grey wet, non-plastic, silty sand, trace fine gravel, shell fragment, (SM)	5-6

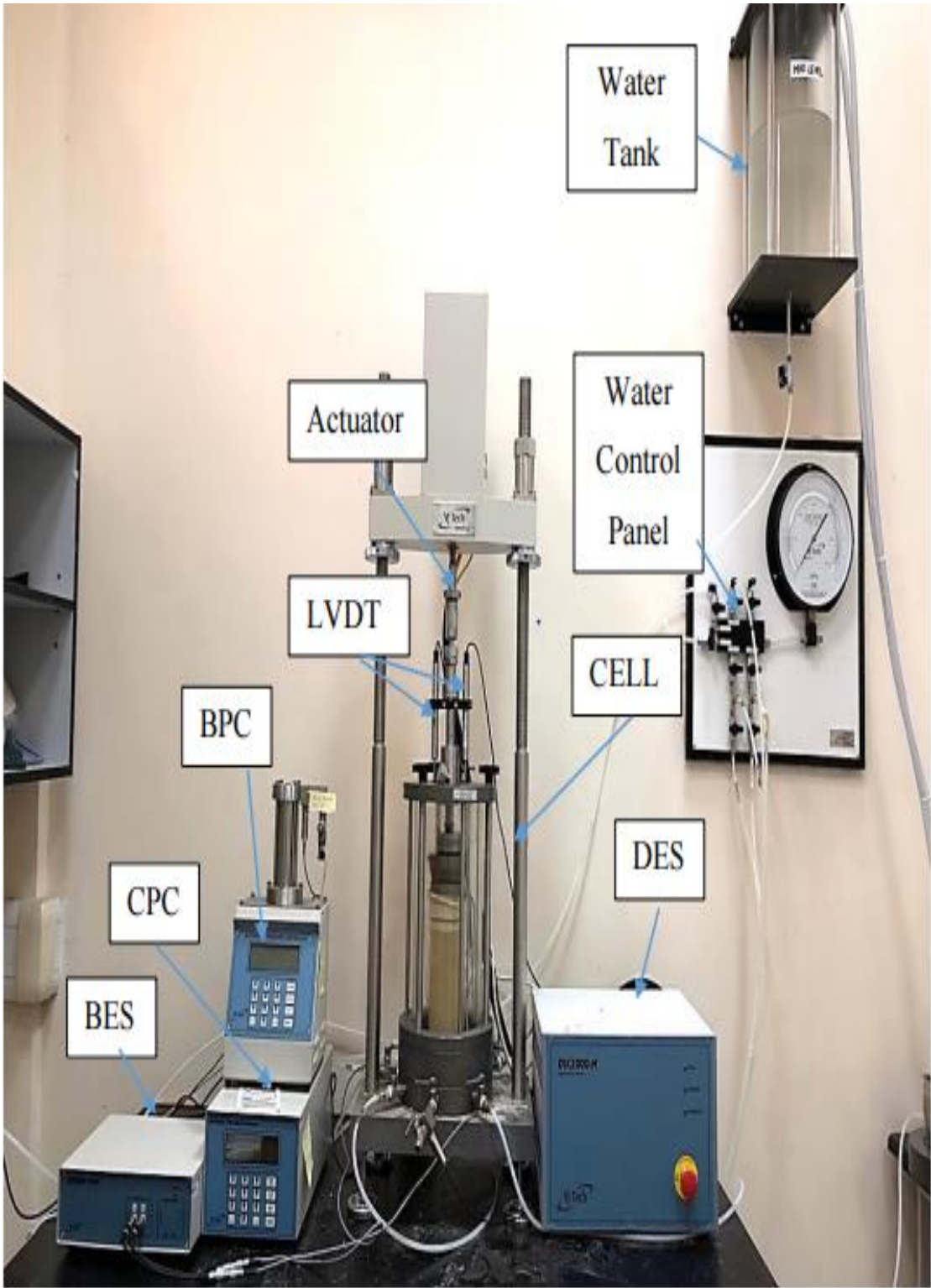


Figure 9: Triaxial Machine produced by VJ-Tech. [45].

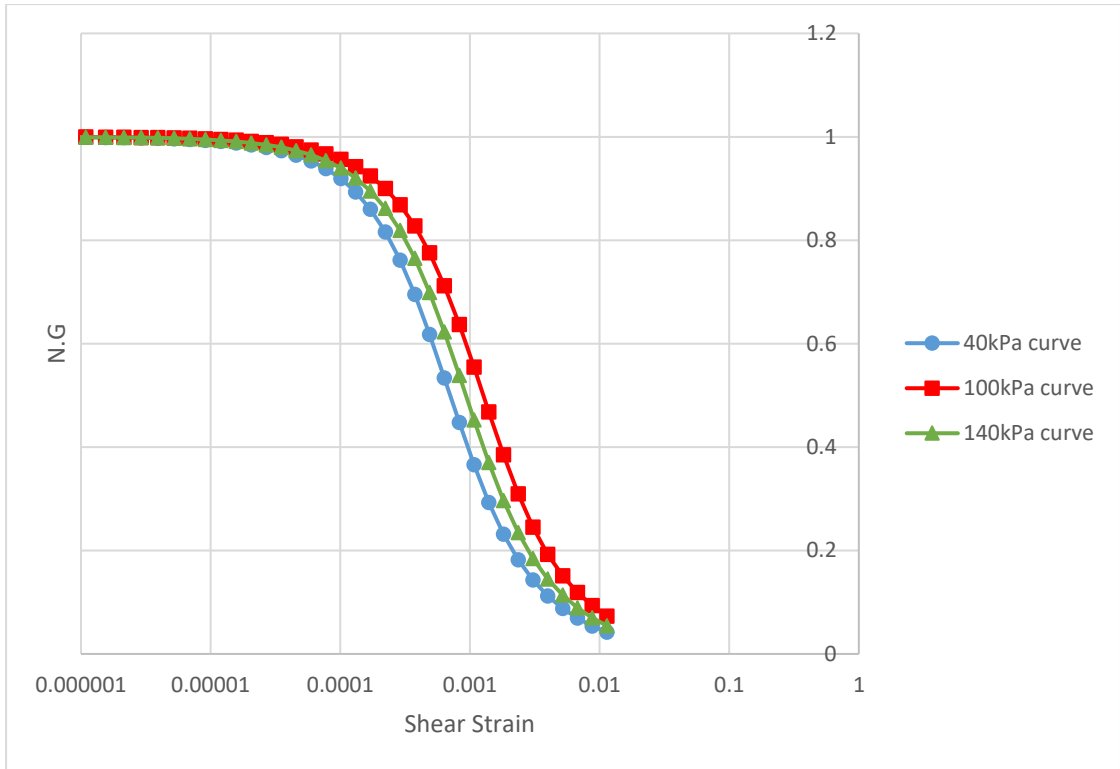


Figure 10: Average Shear Modulus Reduction Curve for Sample C.

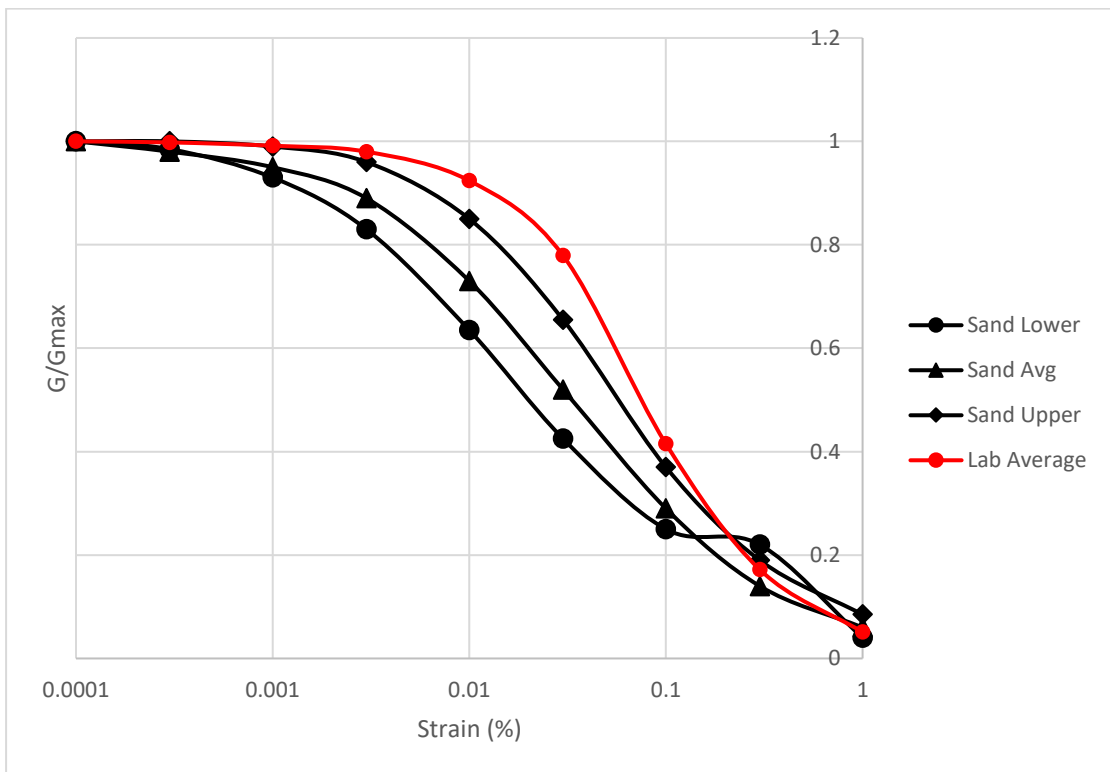


Figure 11: Lab Generated and Built-in Modulus Degradation Curves.

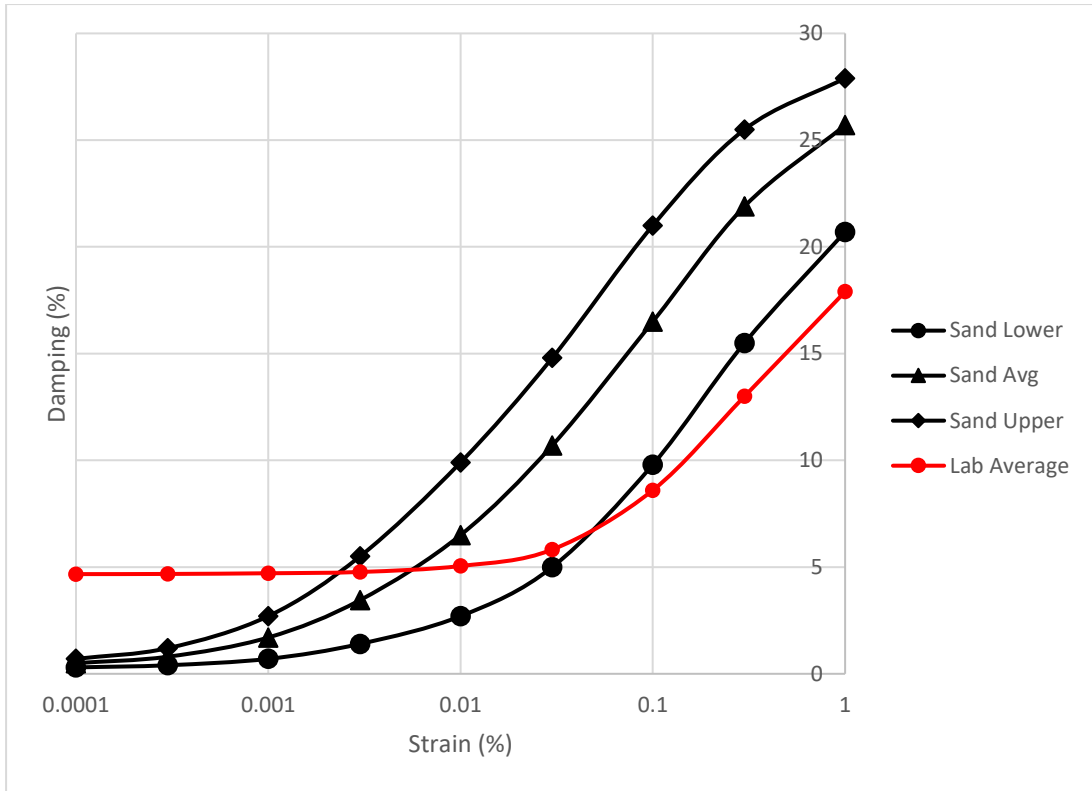


Figure 12: Lab Generated and Built-in Damping Degradation Curves.

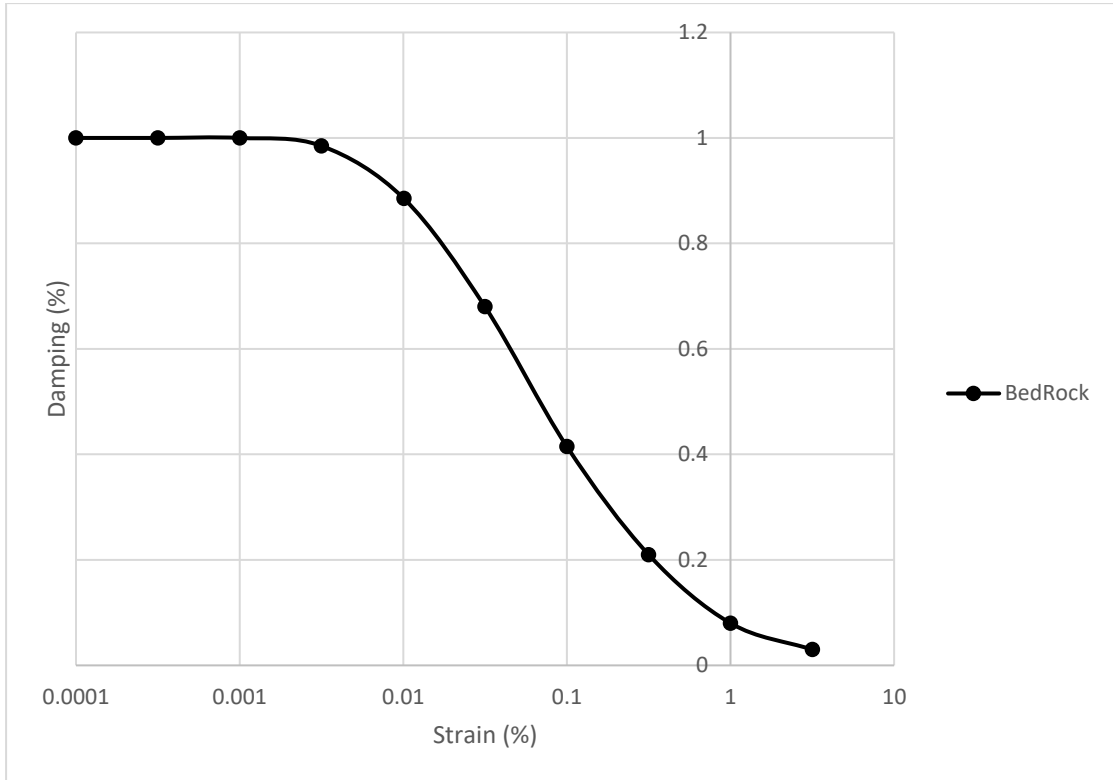


Figure 13: Built-in BedRock Modulus Degradation curves Developed by Schnabel [46].

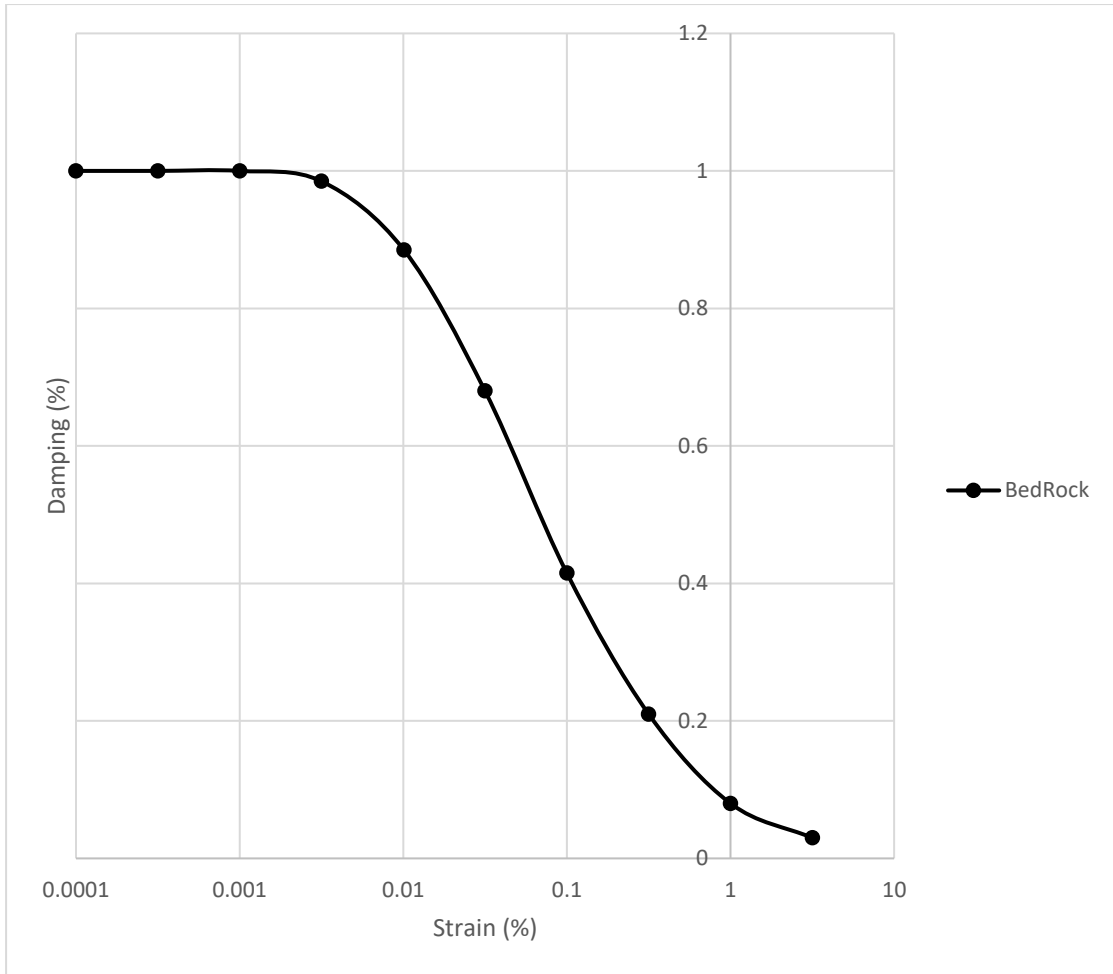


Figure 14: Built-in Bed Rock Damping Curves Developed by Schnabel [46].

The third input required by the software is the shear wave velocity. The average shear wave velocity was calculated for each sublayer of each borehole using three different correlations to evaluate the effect of shear wave velocity on the seismic response analysis. To obtain the shear velocity correlation Bender Element test was performed on the soil samples using two different sample sizes which are 7cm x 14cm and 10cmx 20cm. The pulse frequency was set to be 5kHz since and a time window 2mSec. To attain the highest amplitude and making the detection of first arrival more accurate, a 10 volts amplitude was used. Moreover, stacking of 10 signals was adapted in this study to improve the signal-to-noise ratio of the waves which increase the accuracy. The test was performed using different confining pressures of 20, 40, 60, 70, 80, 100, and 120 kPa. Afterwards, an Excel sheet was developed and used to obtain the shear wave velocity. Refer to A.M. Khalil for detailed calculation [45]. The different velocity correlations that were used in this study are as follows:

- a. Laboratory correlation derived by A.M. Khalil. (Equation 3) [45].
- b. Field correlation derived by Niamatullah Haji Bismillah. (Equation 4) [49]. This correlation was developed using field methods such as seismic reflection, seismic refraction, and cross-hole method.
- c. The average of the correlations proposed by Hasancebi et al. [50], Shibata [51], Seed and Idriss [52] and Athanasopoulos [53]. (Equations 5, 6, 7, and 8 respectively).

$$V_s = 115.000 \times N^{0.1719} \quad (3)$$

$$V_s = 94.655 \times N^{0.3512} \quad (4)$$

$$V_s = 90.820 \times N^{0.3190} \quad (5)$$

$$V_s = 31.700 \times N^{0.5400} \quad (6)$$

$$V_s = 61.400 \times N^{0.5000} \quad (7)$$

$$V_s = 107.600 \times N^{0.3600} \quad (8)$$

where V_s represent the shear wave velocity in (m/s) and N represents the Standard Penetration Test Number (SPT-N). Figure 15 presents a typical result of the generated velocity profile using the different shear velocity correlations. Moreover, to verify the site classification of the used boreholes based on the soil classification of NEHRP [54], the 30m average shear wave velocity (V_{30}) was obtained. To calculate the V_{30} the shear wave velocity of each sublayer was calculated using the correlations listed above. As illustrated earlier equation 3 reflects the adaptation of the laboratory site specific developed correlation, equation 4 reflects the field site specific developed correlation, and the average of equations 5,6,7, and 8 reflects the adaptation of the equations developed by literature. Afterwards the weighted average of the shear velocities over the entire depth of the boreholes was obtained which reflects the V_{30} . It should be noted that all the soil profiles used in this research were all of class D (V_s ranges between 180m/s to 360m/s).

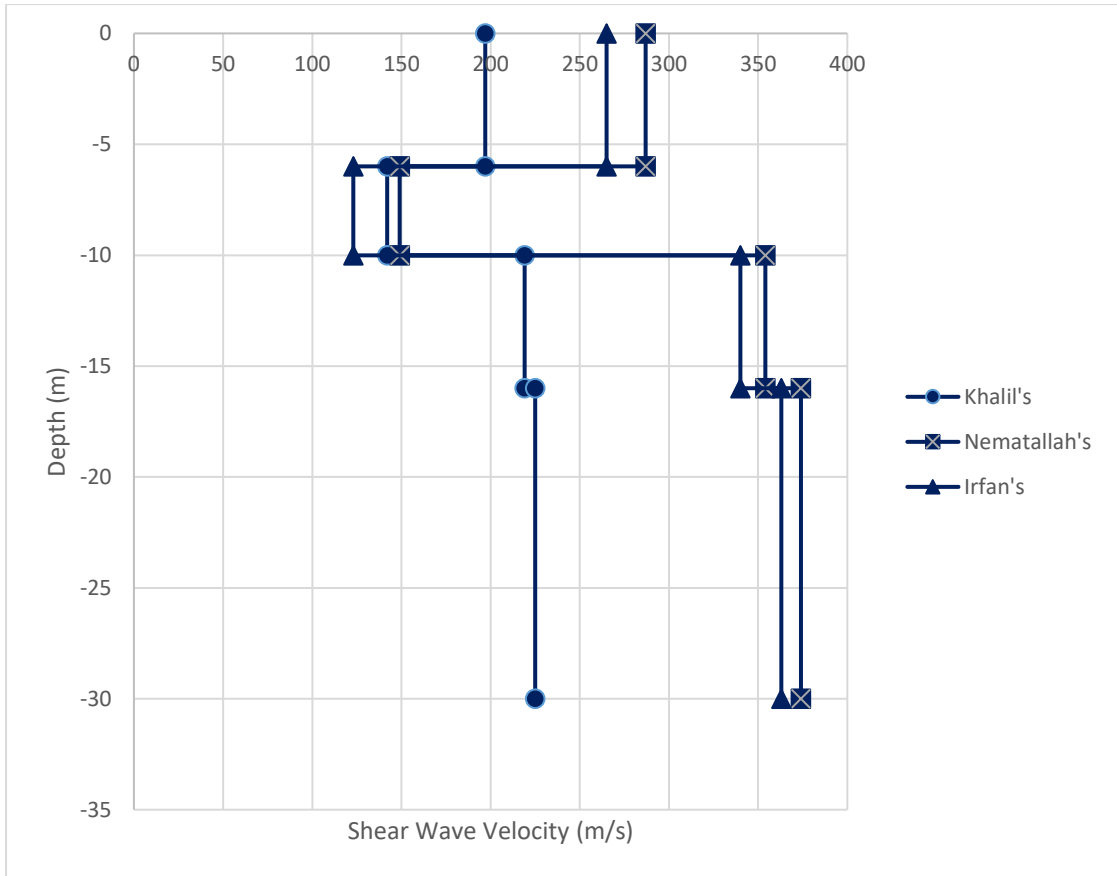


Figure 15: Shear wave velocity profile.

The fourth requirement needed to run the computer program is the unit weight. Estimated fixed values were assigned to the generated soil sublayers based on their type. Table 5 represent the unit weight values used in this research.

Table 5: Unit weight values assigned to the soil sublayers.

Layer Type	Loose Sand	Medium Dense Sand	Dense Sand	Rock
Unit Weight (kN/m ³)	15	16.5	18	22

3.4. Results of the Study

SHAKE 2000 was set to run and process the outcomes once all the input requirements were collected and inserted. The software generates several outcomes such as the acceleration velocity displacement time histories, calculated results with depths, the response spectra, the shear strain & shear stress time histories, ... etc. The user can select and customise the options of the output results based on his need. In this research, the software was customised to generate the four outputs mentioned earlier,

yet the analysis only required the acceleration velocity displacement time histories, calculated results with depths, and the response spectra files. The results were analysed to obtain two major results which are the site amplification factor profile and the site coefficients (Fa and Fv).

Among the several boreholes that were analysed in this research, six different boreholes were used to represent the outcomes of the study. The selected boreholes were chosen to present the variation in the V30 between the soil profiles. Determination of the average V30 have demonstrated that the lowest V30 obtained was 250m/s and the highest was found to be 350m/s. Thus, the two boreholes were selected to present the effect on the lower bound of the V30 (250m/s), another two boreholes were selected to present influence resulted on the mean V30 (300m/s), and the last two boreholes were selected to present the impact resulted on the highest V30 (350m/s).

3.4.1. Site amplification factor profile. Using the generated acceleration velocity displacement time histories and the calculated results with depths, the site amplification factor profile was generated. Different methods were used to estimate the amplification factors of the models which are The Peak Ground Acceleration (PGA) and Root Mean Square (RMS). The PGA is a simple method which depends on estimating the ratio between the maximum obtained acceleration value at each mid-sublayer over the maximum acceleration value from the input motion to obtain the amplification factor. This means that the PGA method considers evaluating the amplification factor at one specific time step. The RMS is a comprehensive method which depends on estimating the RMS value of the outputs at each mid-sublayer using the whole generated acceleration time history which will be divided over the calculated RMS of the input motion. Equation 9 depicts the equation used to obtain the RMS values.

$$RMS = \left[\frac{1}{T} \int_0^T a(t)^2 dt \right]^{\frac{1}{2}} \quad (9)$$

After obtaining the amplification factors of each sublayer using both methods, those values have been used to generate site amplification factor profile which is a graph that describes the variation of the amplification factor through the soil column

with respect to the depth. Figure 16 presents a typical output of the generated relationship.

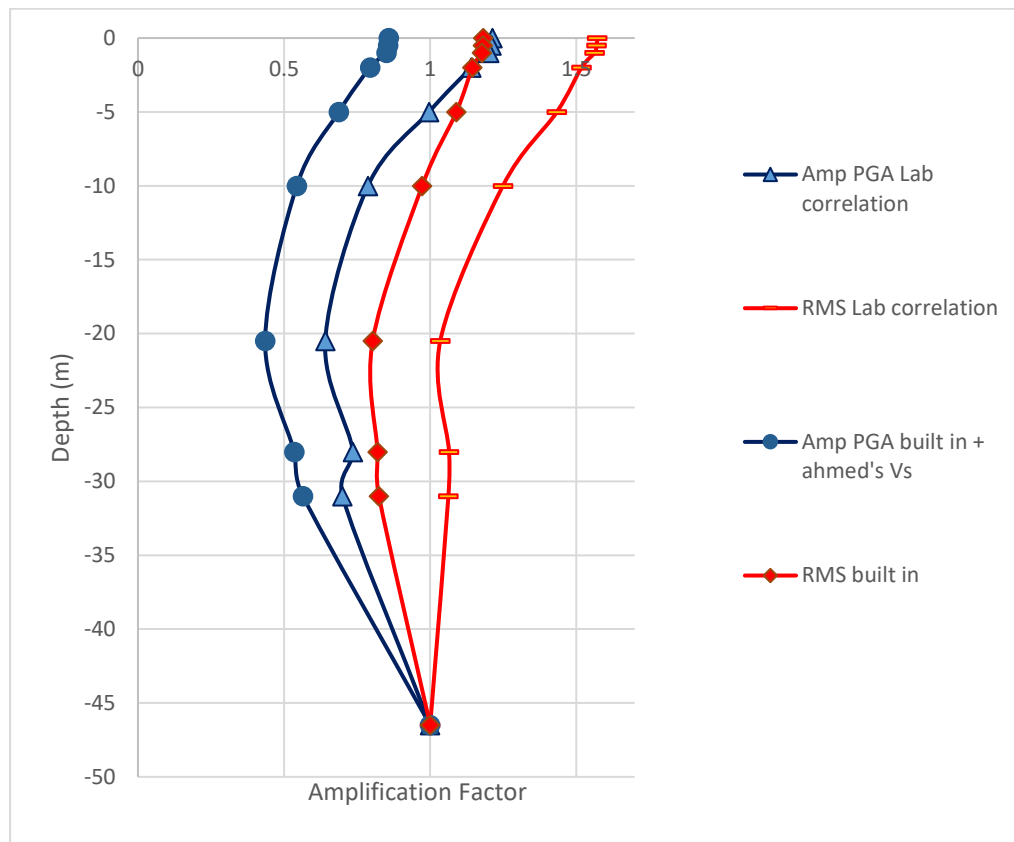


Figure 16: Site amplification factor profile.

3.4.2. Site coefficients (Fa and Fv). Using the generated response spectra, site coefficients were computed at short (0.2s) and long periods (1s). To evaluate the response throughout the entire soil column, the response spectra was customized to be produced at the surface layer and the engineering bedrock. Figure 17 illustrates an example to the process. Surface layer response spectra is represented by the blue color and the half space layer is represented by the red color. Fa was calculated by dividing the value that correspond to 0.2s at surface layer over the value that correspond to 0.2s at the engineering bedrock. Fv was calculated by dividing the value that correspond to 1s at surface layer over the value that correspond to 1s at the engineering bedrock. Yet, since the response spectra curves seems to have some noise which can affect the accuracy of the results, an excel sheet was developed to develop a smooth curve fitted response spectra and calculate the coefficient factors that correspond to least standard

error. Figure 18 shows the outcome of fitting the response spectra. Moreover, based on NEHRP guidelines [54], design spectra were generated for the various boreholes.

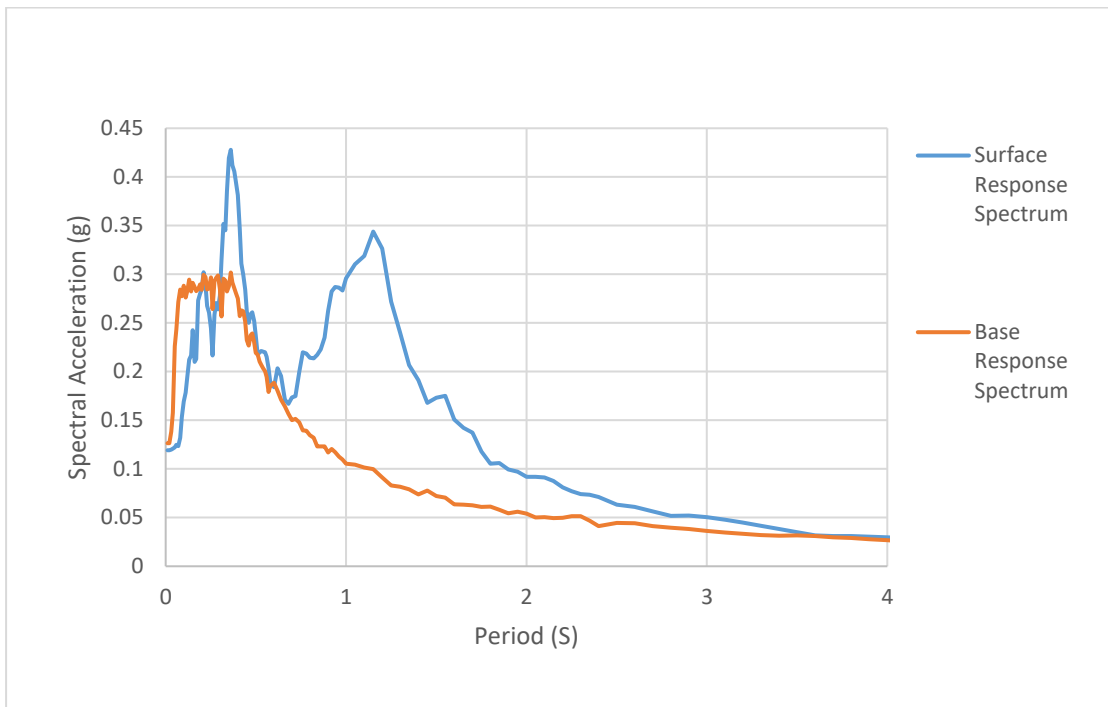


Figure 17: Typical Response Spectra plots to calculate site coefficients.

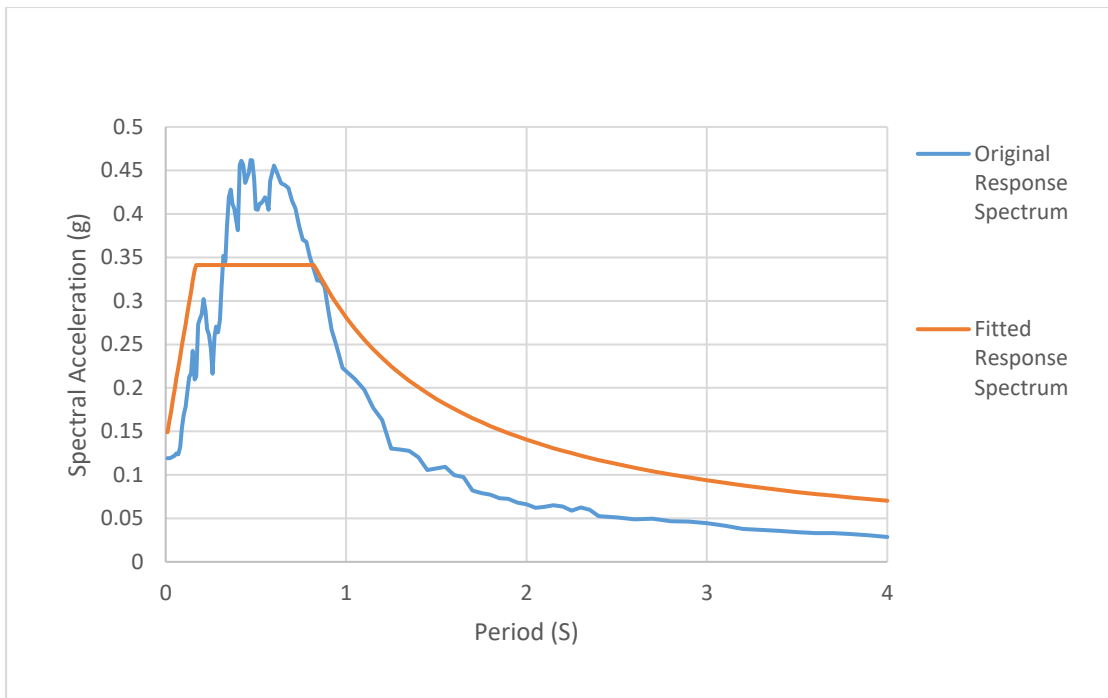


Figure 18: Fitted Response Spectra Curve.

Chapter 4. Results and Discussion

In this chapter, we present the simulation results achieved for the one-dimensional site response analysis. Moreover, the effect of the velocity correlations and degradation models on the site amplification factors are evaluated and discussed.

4.1. Preliminary Sensitivity Analysis

As the used boreholes depicted a variation in the SPT number of the layers and the depths, a single layer model was generated to study the influence of the depth and the effect of the initial velocity to fully comprehend the behaviour of the two parameters prior the in-depth analysis of the complex generated models. Figure 19 and Figure 20 present the results of the depth and velocity effect. The results showed that as the depth increases the site amplification rate decreases. The reason behind this trend is related to the distance travelled by the wave, because as the waves travel more, they tend to lose energy and thus less amplification will occur. Same effect was found for the shear wave velocity as the initial velocity decreases the site amplification rate increases and vice-versa. This outcome is logical since less velocity reflects less shear modulus and hence less rigidity which leads to higher amplification.

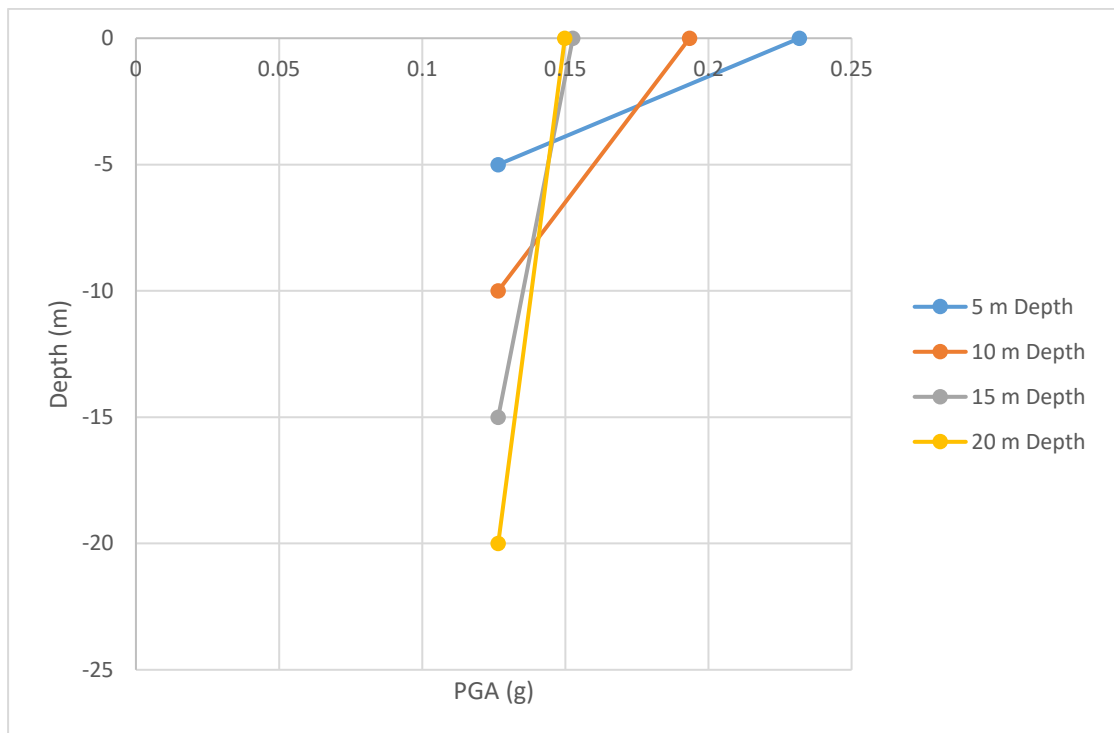


Figure 19: Depth effect on site amplification factors.

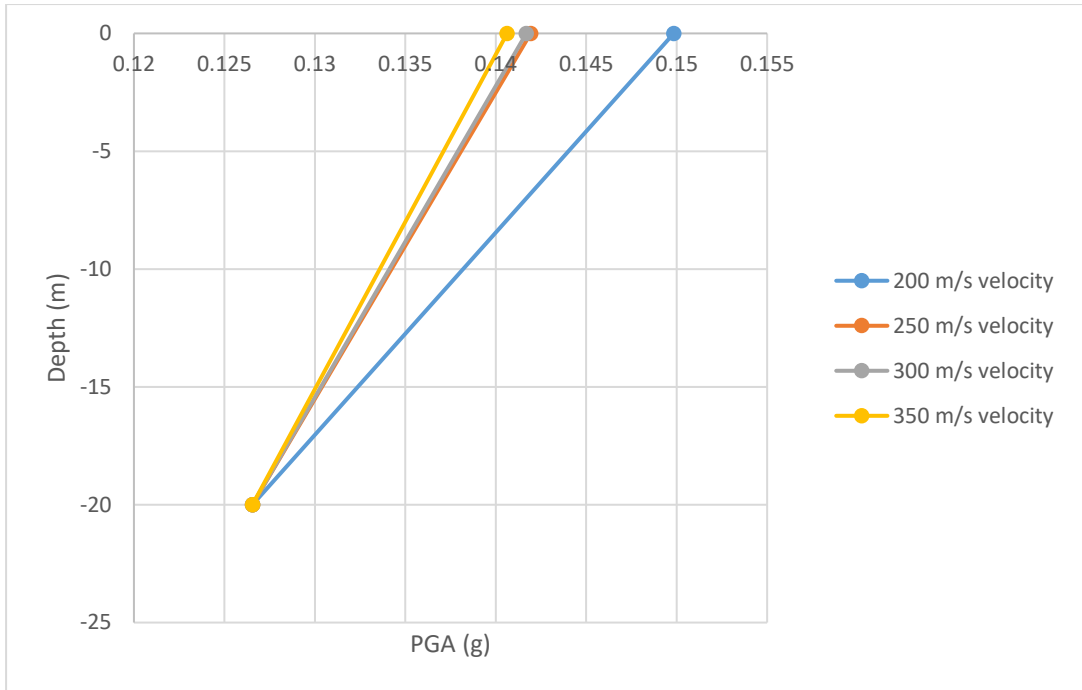


Figure 20: Initial velocity effect on site amplification factors.

Figure 21 reflects the results of modelling two single layer models with both constant initial velocity and built-in damping curve. The difference between the two models relies in the use of the shear modulus degradation curve. Built-in shear degradation model has been used with the first model and lab generated shear degradation model have been used with the second model. The use of built-in shear modulus curve resulted in an amplification rate that equals to 5.7% which is higher than the use of lab generated shear modulus curve which resulted in 2.5%. This is logical since the built-in shear curve falls under the lab shear curve which reflects less rigidity as shown in Figure 11.

Figure 22 reflects the results of modelling two single layer models with both constant initial velocity and lab damping curve. The difference between the two models relies in the use of the shear modulus degradation curve. Built-in shear degradation model has been used with the first model and lab generated shear degradation model have been used with the second model. The use of lab damping curve has resulted in increasing the surface amplification factor for both models with respect to the outcomes obtained with the use of the built-in damping curve. The use of lab degradation curve

resulted in 36.9% amplification which is higher than the use of built-in generated shear modulus curve which resulted in 36.5% amplification rate.

Figure 23 compare the effect of using the lab damping curve and the built-in damping curve. As can be seen the use of the lab generated damping curve leads to a higher surface amplification rate than the surface amplification obtained by using the built-in damping curve. Moreover, this curve illustrated that the highest surface amplification is expected when the lab degradation model is used with the lab generated shear degradation model. This is because the variation in the lab damping reduction curve values was higher in terms of percentage and range than the shear modulus degradation curve values when compared to the built-in damping and shear modulus degradation curves. Refer to section 3.4. for more information. The conclusion that could be obtained from these curves is that the lab-generated degradation curve is the main factor in obtaining the highest surface amplification factors.

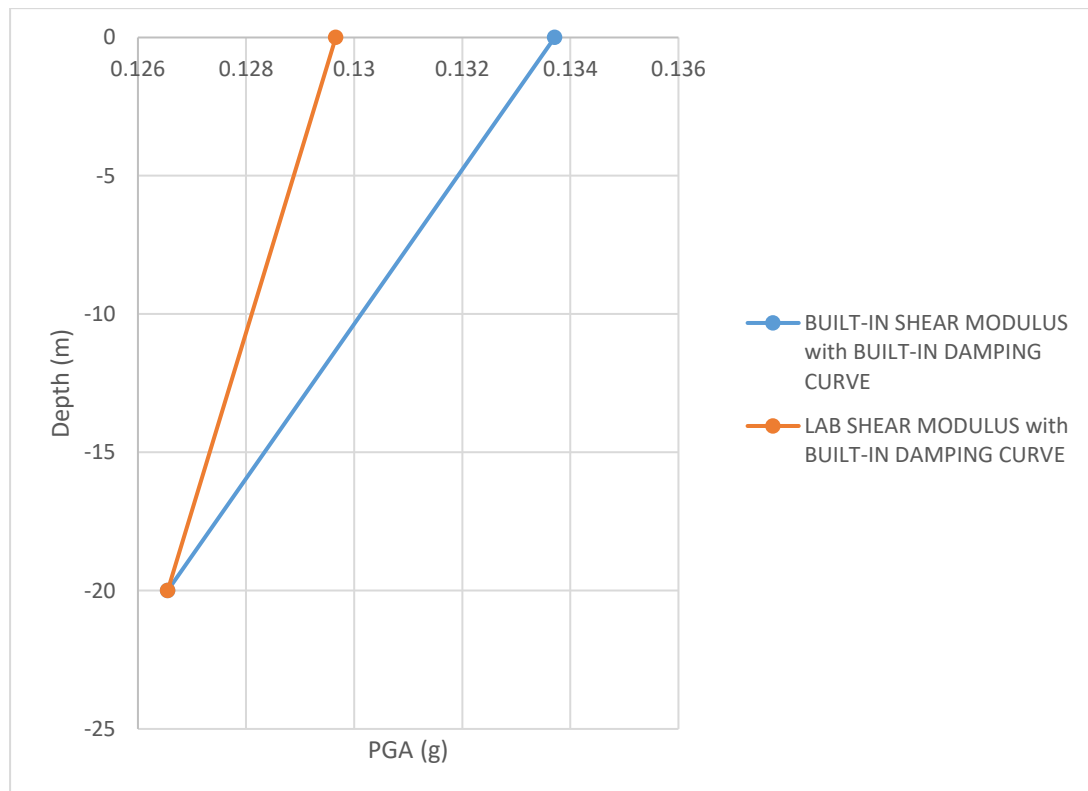


Figure 21: Effect of Lab Shear modulus Vs Built in Shear Modulus With the use of Built-in Damping Curve.

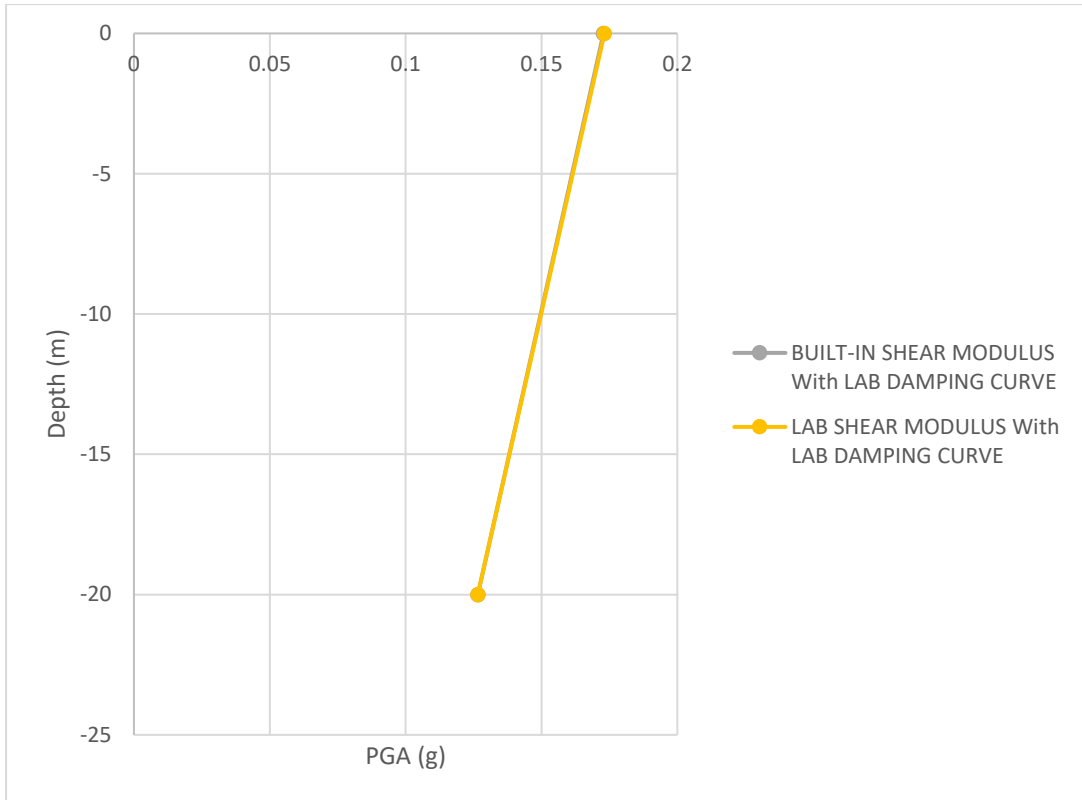


Figure 22: Effect of Lab Shear modulus Vs Built in Shear Modulus With the use of Lab Damping Curve.

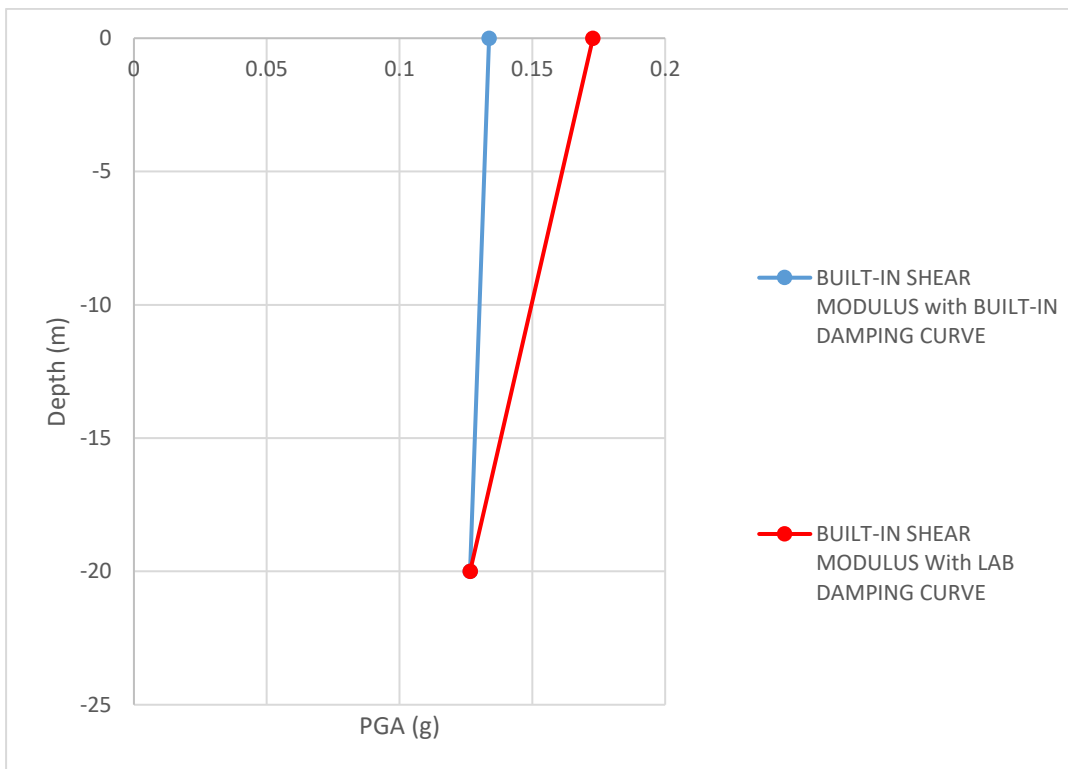


Figure 23: Effect of Damping Reduction Curves.

4.2. Effect of Initial Wave Velocity Correlation on Site Response Analysis

As illustrated in the previous chapter, to study the effect of the shear wave velocity 3 different velocity correlations were implemented in this research which are Irfan's correlation, Niamatullah's correlation, and A.M. Khalil's correlation. These correlations reflect the adaptation of general correlations developed by previous researchers, the site-specific developed velocity correlations using field methods, and the site-specific velocity correlations developed by laboratory methods, respectively. It should be also noted that built-in degradation models (Damping and Shear Modulus) were fixed in this analysis. Moreover, to show the outcomes of the analysis, six different boreholes which depicts the variation in the V30 were used (Low V30, Mean V30, and High V30).

Collectively, Figure 24 to Figure 41 shows the results of the response of the ground soil to the input ground motion with respect to the depth in addition the distribution of the used velocity correlations integrated in the analysis.

The graphs below show a general trend which denotes that as the shear wave velocity of the soil increase the amplification factor tends to decrease as illustrated by the effect of initial velocity explained earlier in section 4.1. The reason behind this effect is attributed to the increase in the shear wave velocity which implies that the soil tends to be stronger as the shear modulus is increasing. This trend could be clearly noticed while comparing the results of using a low V30 borehole with the result of integrating mean V30 and the outputs of employing a high V30 borehole. Figure 25-Figure 31-Figure 37 illustrates the results obtained from RMS analysis for a low, mean, and high V30 boreholes correspondingly. It should be noted that PGA graphs may not be suitable to compare between boreholes that have different V30 values since the method only takes the single PGA values into consideration which could be misleading. As a result, RMS graphs were used to compare between the different V30 boreholes since the method takes the whole-time history response into consideration.

The response of each two boreholes that have similar overall V30 values have been analysed. Starting with the lowest V30 boreholes, by analysing Figure 24 and Figure 27 together in addition to analyse of Figure 25 and Figure 28 together it could be noticed that same trend has been recognized between the two boreholes. The two boreholes have suffered a slight de-amplification at low depths and then an

amplification occurred near the surface when PGA graphs are considered (Figure 24 and Figure 27). This slight de-amplification could be attributed to the different soil mediums that took place through the soil column. However, considering the RMS graphs, it can be noticed that both boreholes have experienced an amplification and it's considered the maximum amplification among the whole runs. This is logical since these two boreholes depicts the lowest V30 values and as illustrated earlier the amplification increase with the decrease in the shear wave velocity as shown in Figure 20. Yet, there is a noticeable difference in the response values of the two boreholes at the ground surface and this difference is due to the variation in the distribution of the shear wave velocity. Figure 26 shows that Al Qasimyah borehole has a shear wave velocity that ranges from 130 m/s to 170 m/s near the surface based on the shear wave velocity correlation that is been considered while Figure 29 depicts that Al Hemriyah borehole has a shear wave velocity that ranges from 200 m/s to 280 m/s near the surface based on the velocity correlation that is been considered. This variation in the shear wave velocity at the surface led to the variation in the resulted amplification factor. This could lead to the conclusion that the individual sub-layer velocity has more effect than the average V30 of the borehole log.

The adopted initial velocity correlation model caused a noticeable difference on the resulted surface amplification factor. As shown in Figure 25 the laboratory correlation developed by A.M. Khalil have resulted in 39% reduction in the surface amplification factor with respect to the correlation developed by literature and field (Irfan's and Niamatullah's correlations). Moreover, as presented in Figure 28 the laboratory correlation has resulted in 7% reduction in amplification factor with respect to the correlation developed by literature and field.

Regarding the two boreholes that have almost mean V30, while comparing the PGA graphs of Al Khan borehole and Al Braha-773 borehole (Figure 30 and Figure 33 respectively) it could be noticed that both boreholes have suffered both a massive de-amplification and a slight amplification throughout the soil column. The de-amplification resulted from the PGA graph does not necessarily means that a de-amplification took place, yet it indicates the percentage of the maximum PGA obtained at each sublayer with respect to the maximum PGA value obtained from the input motion. This means that although the graph shows that most of the sublayers are having

PGA values less than one, still an amplification could take place since the two values that are being used are most likely out of phase. This could be proved by comparing the RMS graphs together (Figure 31 and Figure 34) which shows that an amplification took place in both boreholes however, the percentage of the amplification resulted in Al Khan and Al Braha-773 boreholes is less than the percentage resulted in Al Qasimyah and Al Hemriyah boreholes and this is due to the increase in the shear wave velocity values in Al Khan and Al Braha-773 boreholes which leads to increase the rigidity of the soil and thus reducing the amplification effect.

The implemented initial velocity correlation model produced a noticeable difference on the resulted surface amplification factor. As shown in Figure 31 the laboratory correlation developed by A.M. Khalil have resulted in 31% reduction in the surface amplification factor with respect to the correlation developed by literature and field. Furthermore, as shown in Figure 34 the laboratory correlation has resulted in 9% reduction in amplification factor with respect to the correlation developed by literature and field correlation.

Al Butina borehole and Al Braha-11 borehole represent the last two boreholes used in the analysis and they correspond to the boreholes with the highest V30 values. By comparing the PGA graphs of Al Butina borehole and Al Braha-11 boreholes together (Figure 36 and Figure 39 respectively) it could be noted that almost the same trend could be noticed. Both boreholes suffered mostly from a de-amplification throughout the soil column. Yet, the main difference between the two graphs is that Al Baraha borehole suffered a huge amplification at the surface with respect to Al Butina borehole. This difference is mainly due the huge variation in the shear wave velocity distribution between the two boreholes near the surface. As can be seen in the shear velocity distribution of Al Butina borehole which is presented in Figure 38 the shear wave values near the surface are ranging from 200 m/s to 300 m/s depending on the velocity correlation that is been considered. However, Al Baraha-11 borehole has a shear wave velocity distribution that ranges between 170 m/s to 200 m/s near the surface. This variation in the shear wave velocity at the surface led to the variation in the resulted amplification factor since the increase in the decrease in the shear wave velocity values leads to decrease the shear modulus of the soil which will reflect in decreasing the rigidity of the soil and thus increasing the amplification effect. However,

as mentioned in the previous graphs the de-amplification which is present in the PGA graphs does not necessarily mean that a de-amplification took place, yet it reflects the fact that the highest PGA at each corresponding sublayer is less than the maximum PGA value of the input motion which is present at a single time step of the total motion. As a result, while comparing the RMS graphs of Al Butina borehole and Al Baraha-11 borehole (Figure 37 and Figure 40 respectively) it could be noted that both boreholes have almost undergone amplification, nevertheless, the values are close to one which is logical since both soils have high V30 values which reflects that both soils are considered to be stiff and rigid which will reduce the amplification effect.

The applied initial velocity correlation model developed a visible variation on the resulted surface amplification factor. As shown in Figure 37 the laboratory correlation produced by A.M. Khalil have resulted in 43% reduction in the surface amplification factor with respect to the correlation developed by literature and field. Furthermore, as shown in Figure 40 the laboratory correlation has resulted in 25% reduction in amplification factor with respect to the correlation developed by literature and field.

These results demonstrate that using site-specific velocity correlation can result in a totally different velocity distribution over the soil profile depth, which leads to either a variation in the values of the amplification factors or change the site class of the soil in some cases. These two aspects are very significant things during the seismic design, and they could lead to the use of different site class design parameters. This result is in agreement with the findings of Kumar et al [26] who reported that adopting site-specific dynamic properties led to a decrease in the peak ground acceleration values when compared to the studies that adopted general soil dynamic properties. Moreover, it should be noted that the use of lab developed velocity which generates the least velocity values among the different correlations with the built-in degradation models have led to obtain a less amplification factors. The reason could be denoted to the weak interaction between the velocity values obtained from the lab correlation with the built-in degradation models since the degradation models were generated based on a specific range of shear velocities. Thus, developing a site-specific initial velocity correlation is considered very essential towards a reliable and sustainable design.

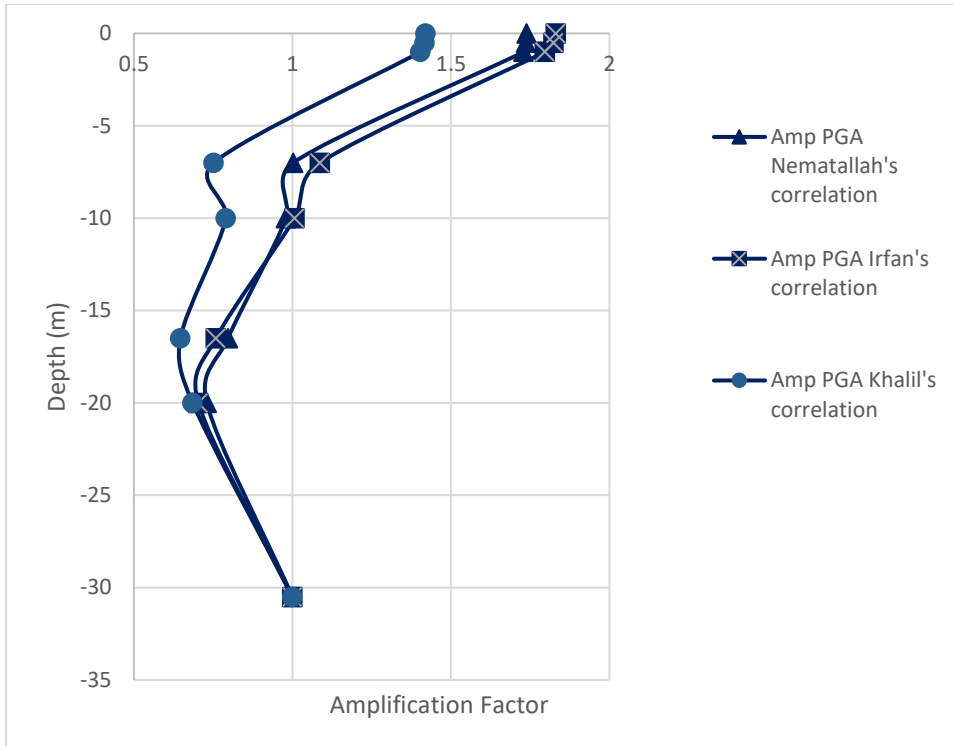


Figure 24: Site Amplification Factors using PGA of Al Qasimya Borehole (Lowest V30).

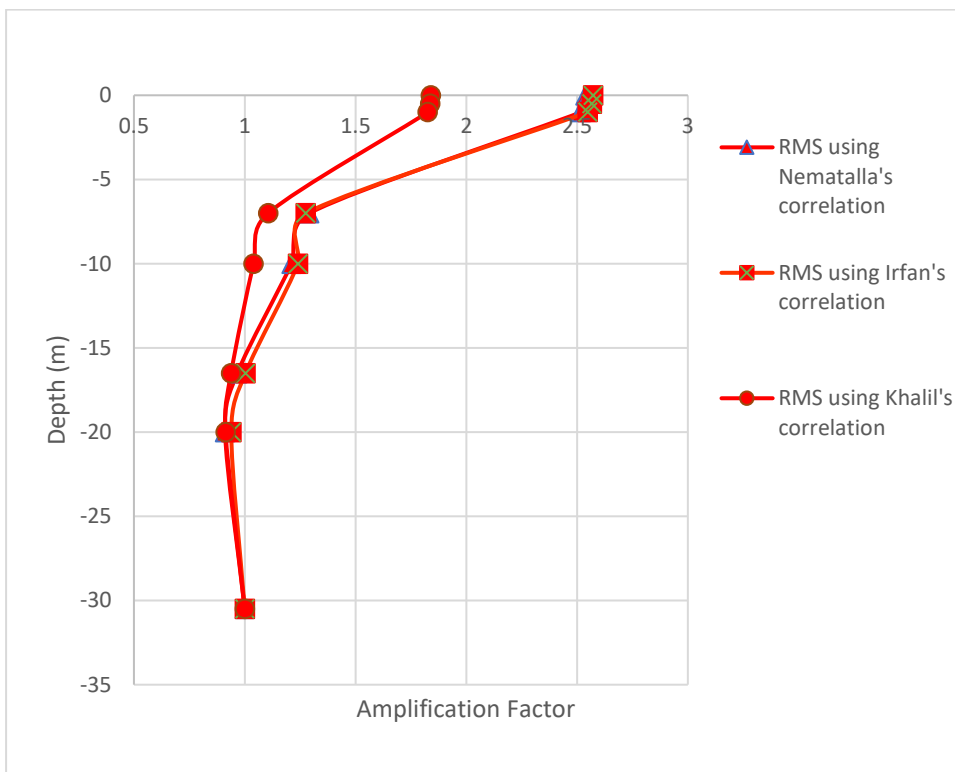


Figure 25: Site Amplification Factors using RMS of Al Qasimya Borehole (Lowest V30).

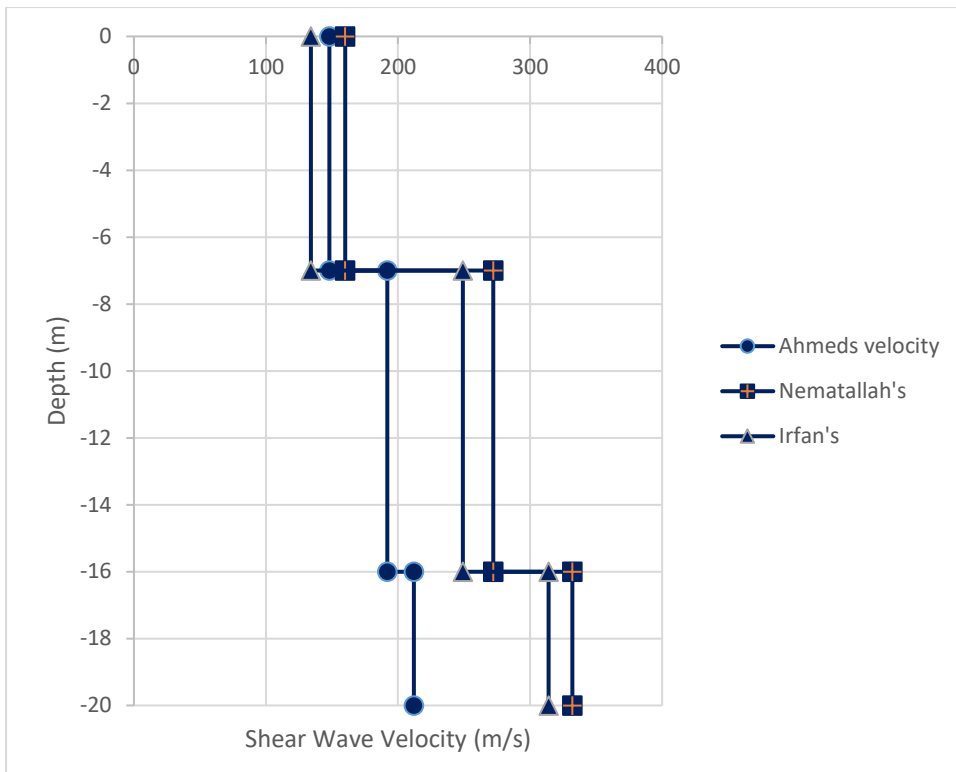


Figure 26: Velocity distribution of the different integrated velocity correlations of Al Qasimya (Lowest V30).

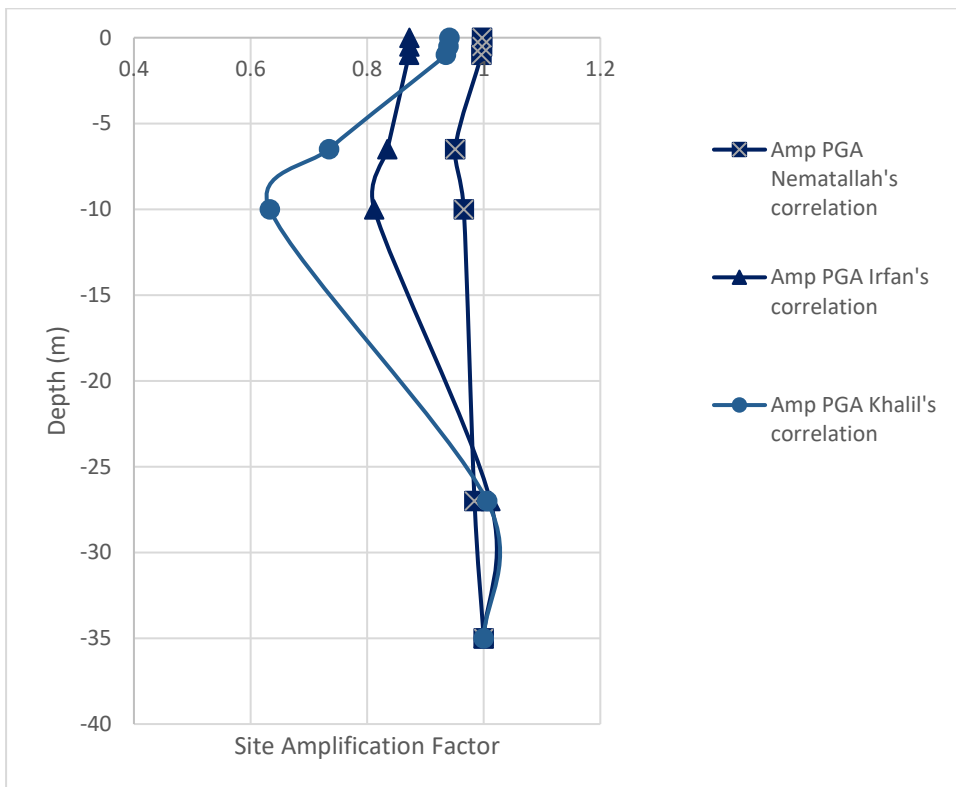


Figure 27: Site Amplification Factors using PGA of Al Hemriyah Borehole (Lowest V30).

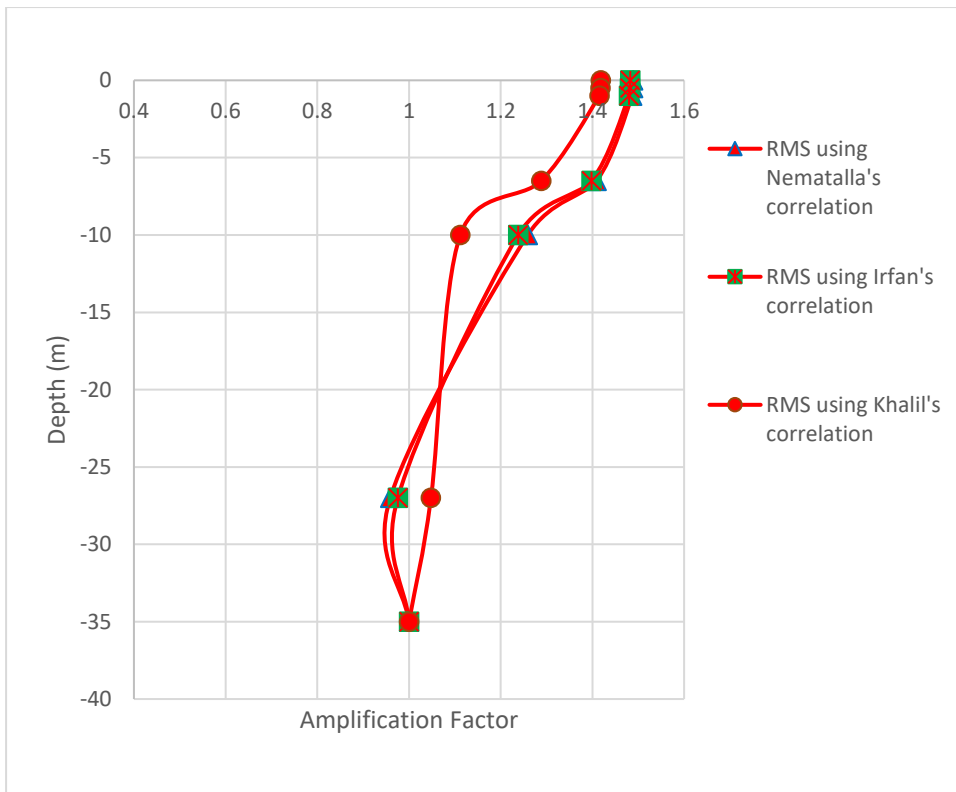


Figure 28: Site Amplification Factors using RMS of Al Hemriyah Borehole (Lowest V30).

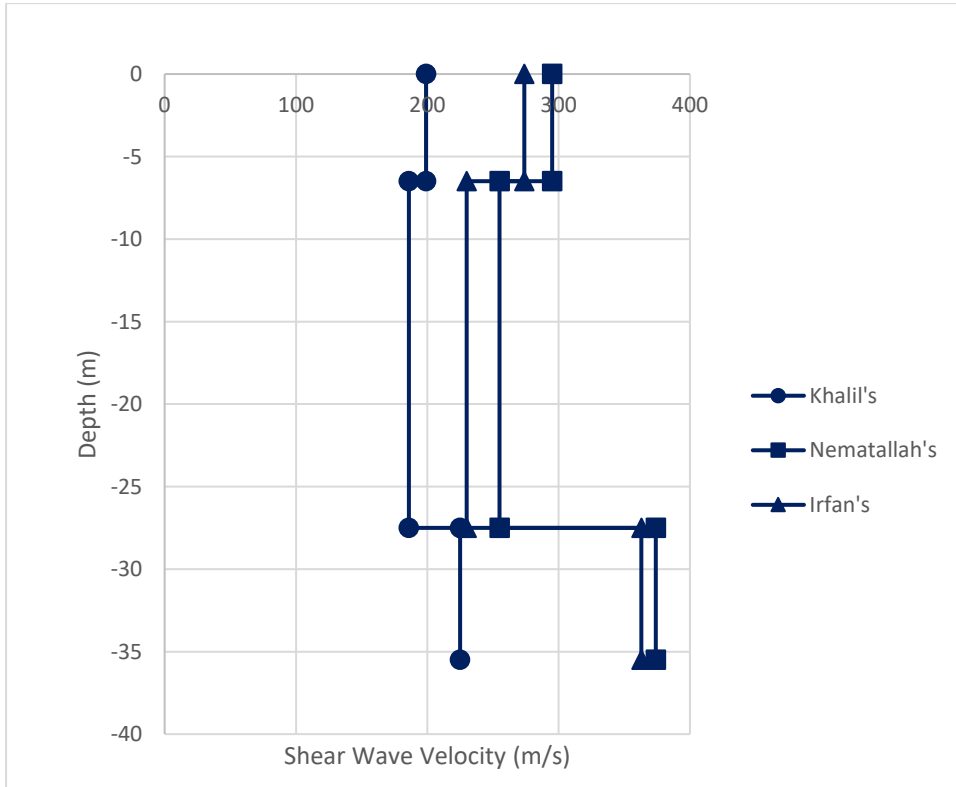


Figure 29: Velocity distribution of the different integrated velocity correlations of Al Hemriyah (Lowest V30).

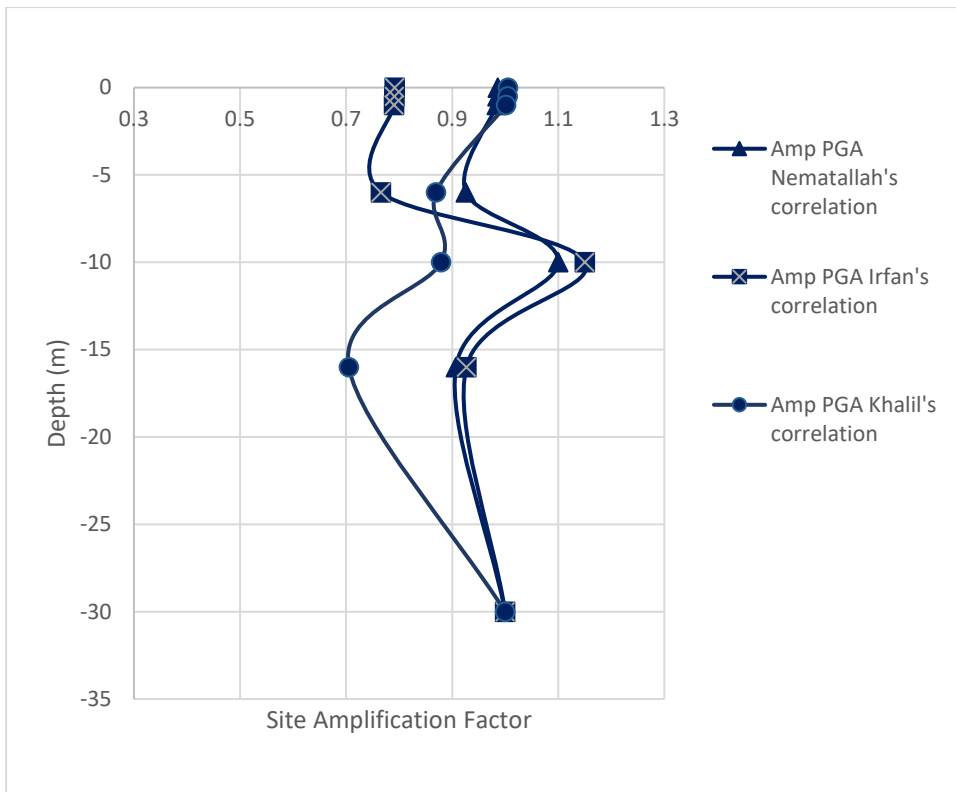


Figure 30: Site Amplification Factors using PGA of Al Khan Borehole (Mean V30).

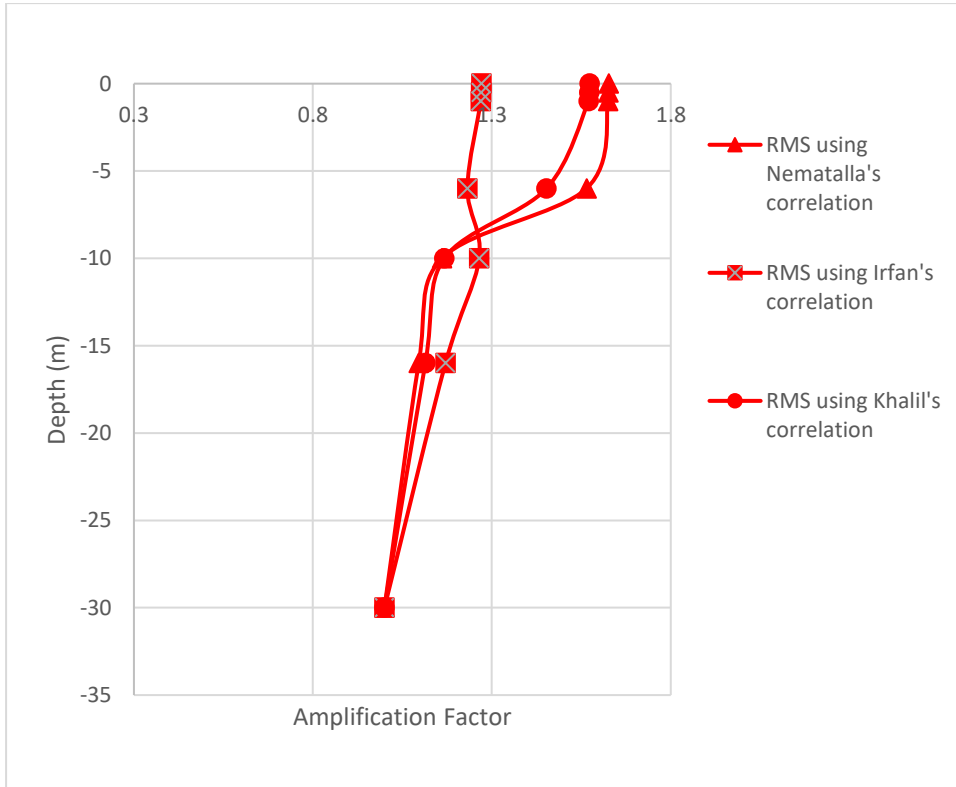


Figure 31: Site Amplification Factors using RMS of Al Khan Borehole (Mean V30).

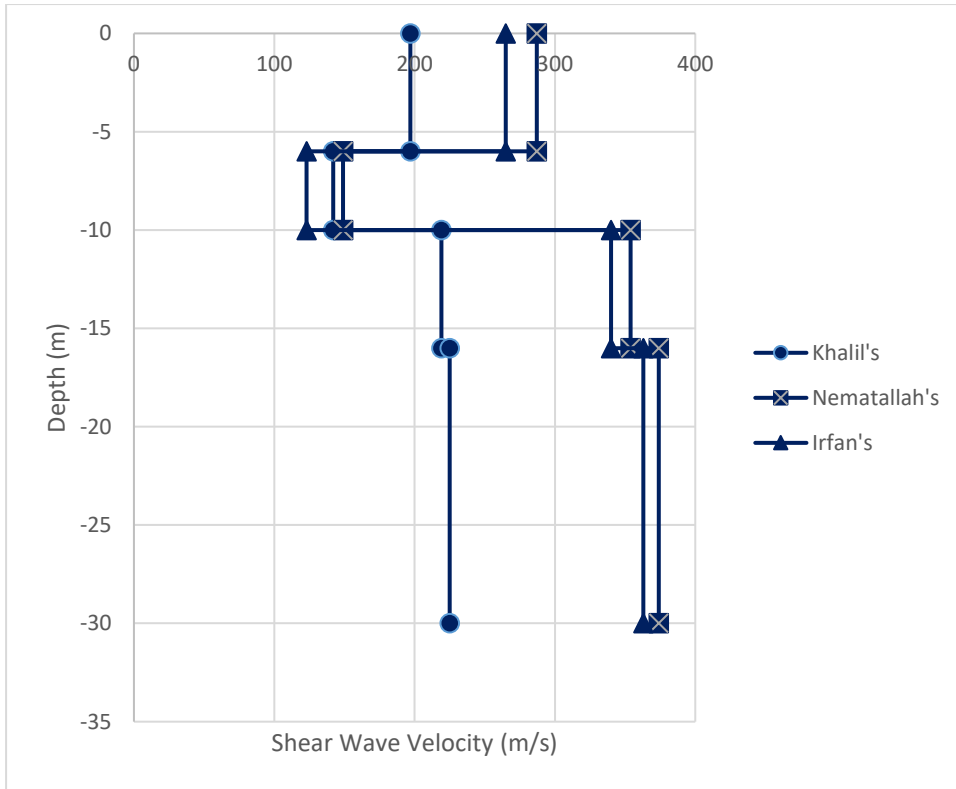


Figure 32: Velocity distribution of the different integrated velocity correlations of Al Khan (Mean V30).

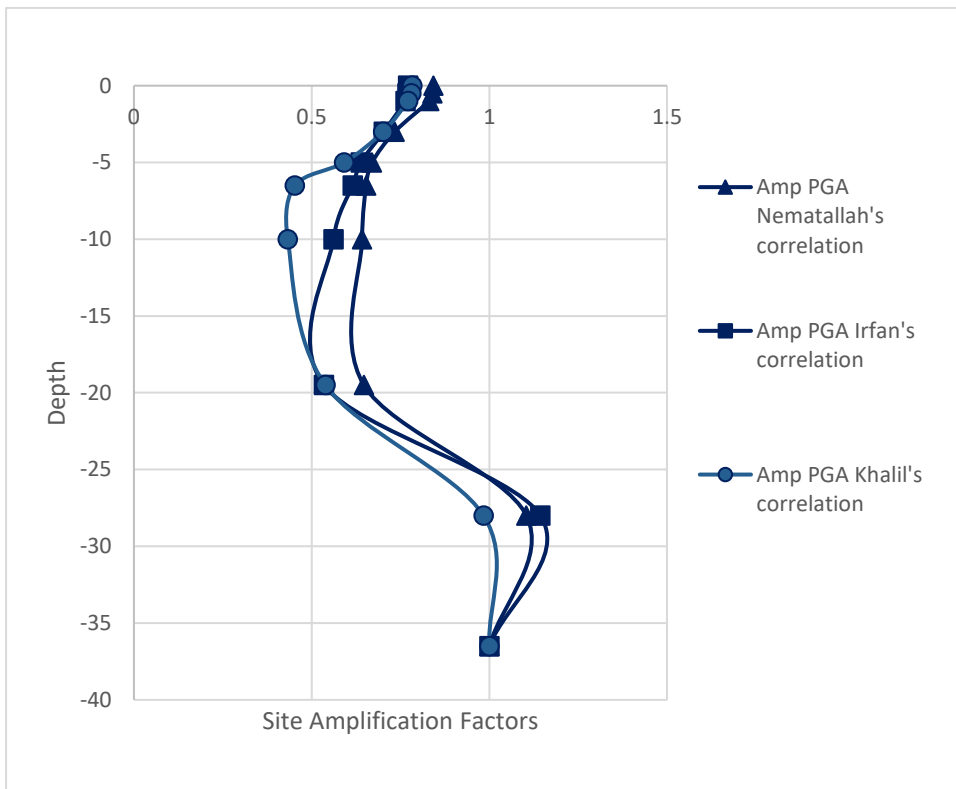


Figure 33: Site Amplification Factors using PGA of Al Braha-773 Borehole (Mean V30).

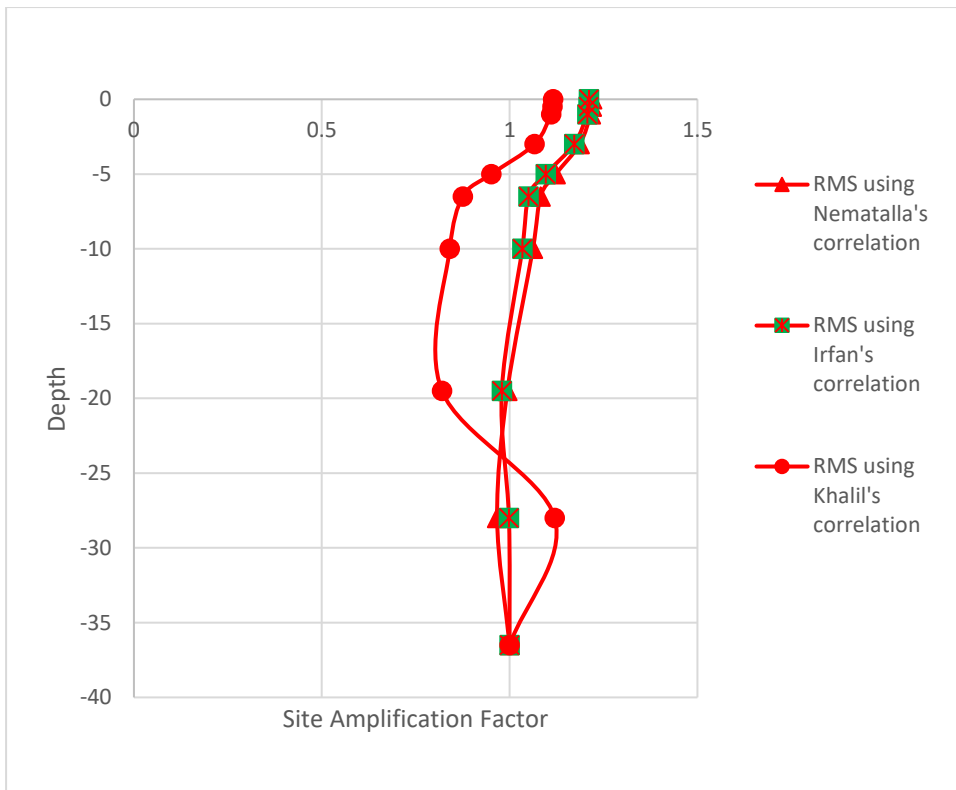


Figure 34: Site Amplification Factors using RMS of Al Braha-773 Borehole (Mean V30).

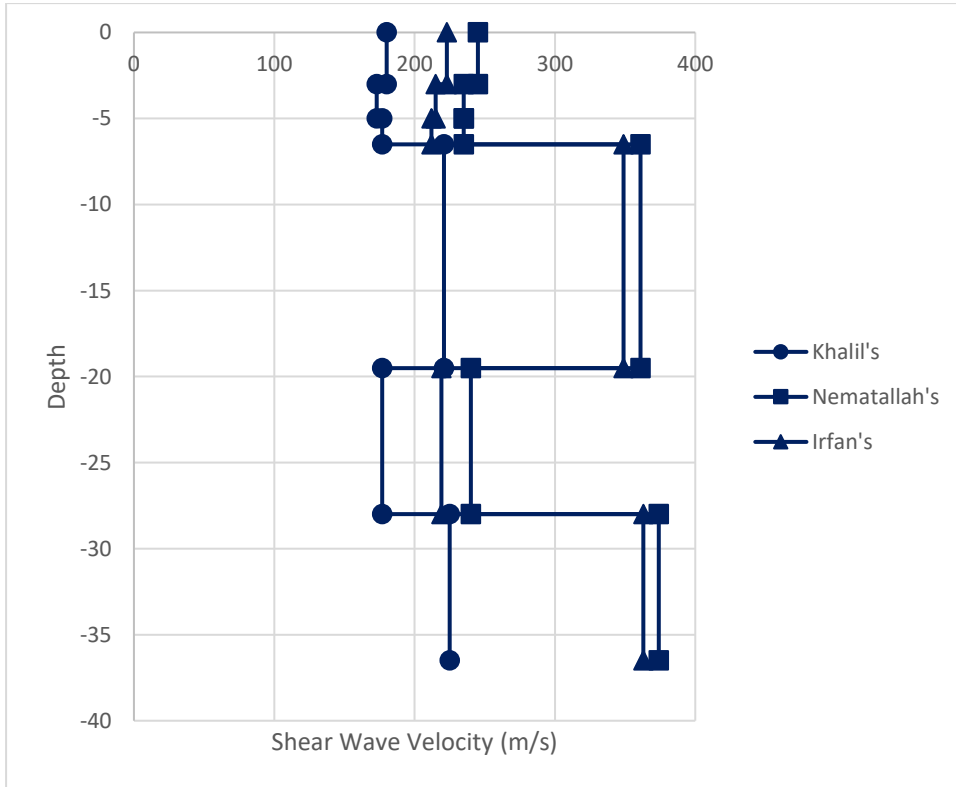


Figure 35: Velocity distribution of the different integrated velocity correlations of Al Braha-773 (Mean V30).

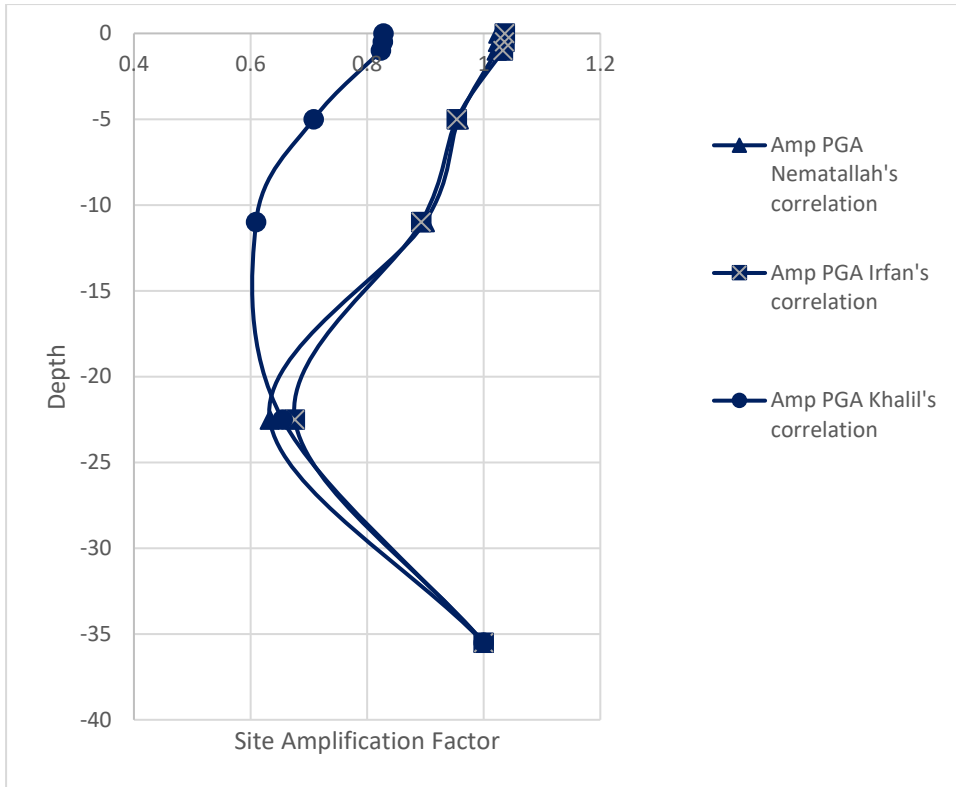


Figure 36: Site Amplification Factors using PGA of Al Butina Borehole (Highest V30).

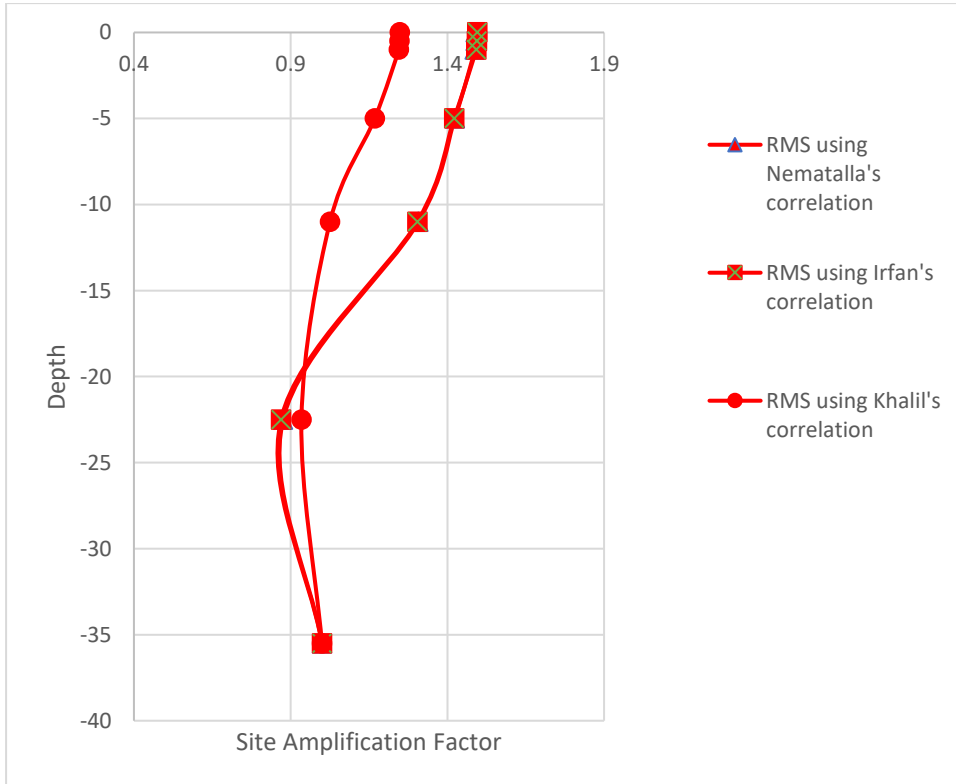


Figure 37: Site Amplification Factors using RMS of Al Butina Borehole (Highest V30).

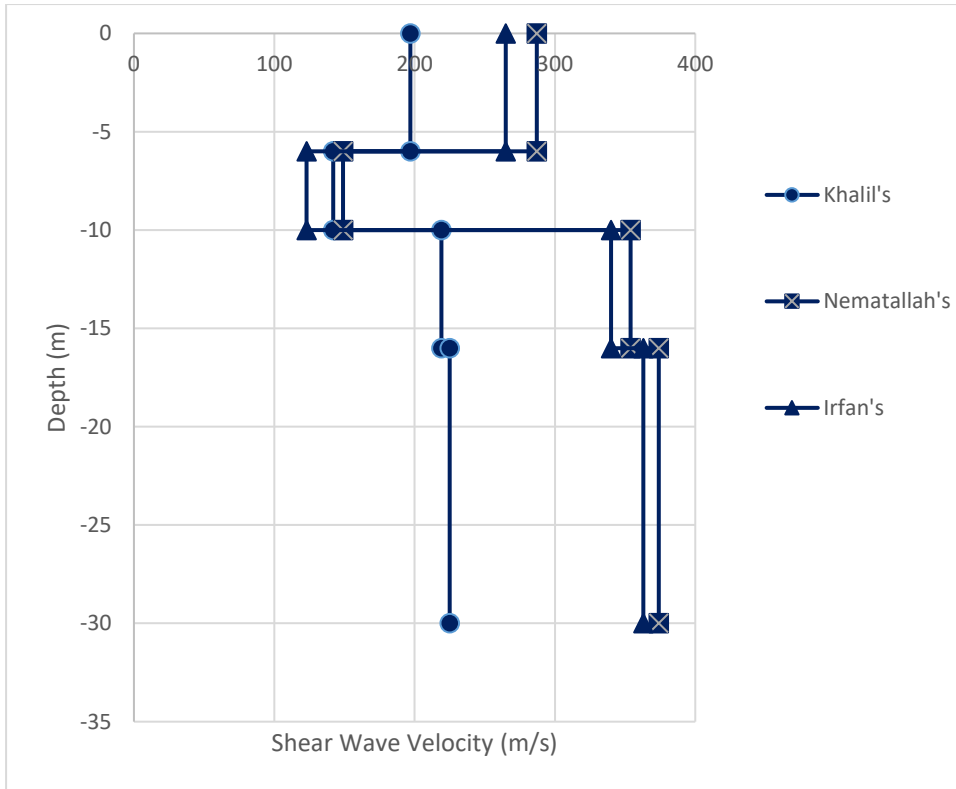


Figure 38: Velocity distribution of the different integrated velocity correlations of Al Butina (Highest V30).

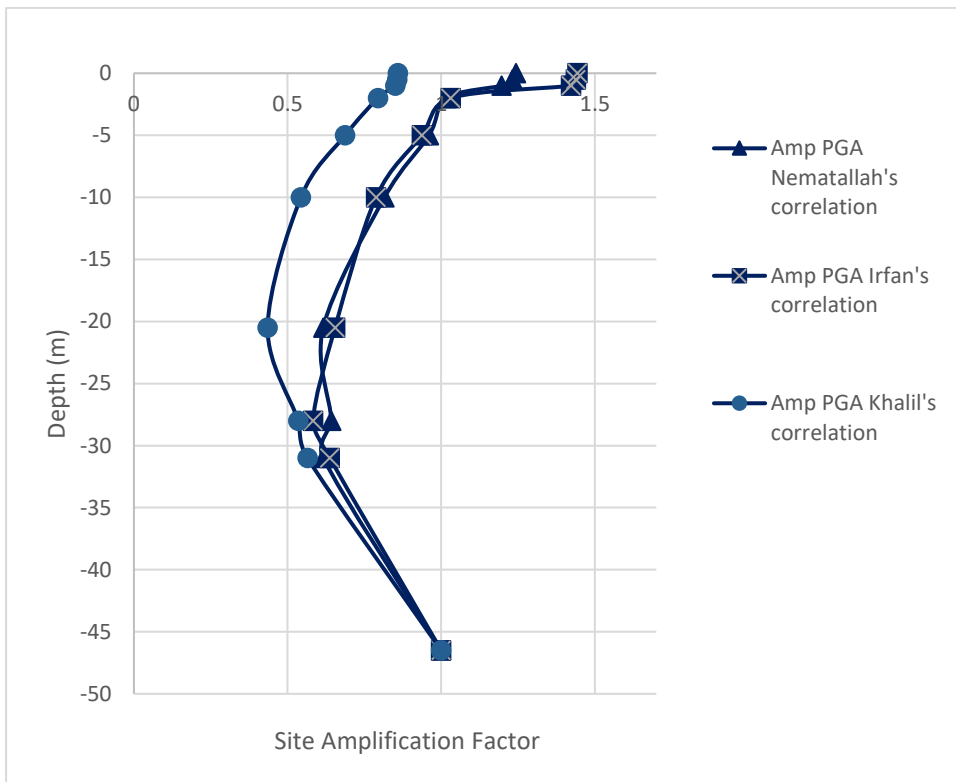


Figure 39: Site Amplification Factors using PGA of Al Braha-11 Borehole (Highest V30).

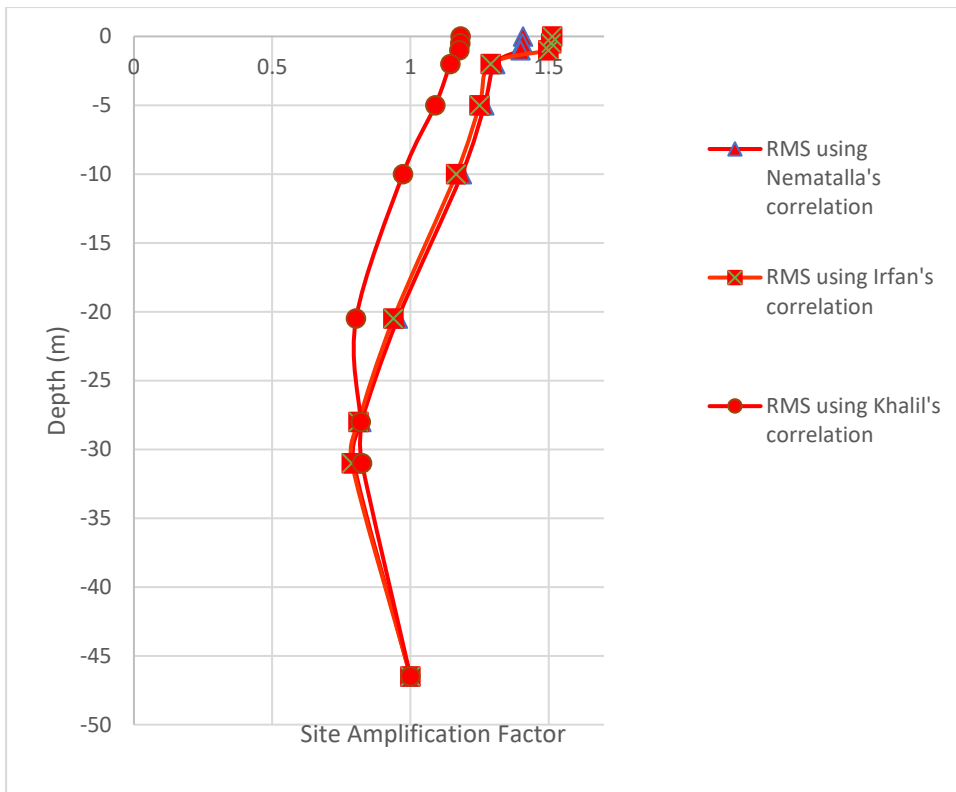


Figure 40: Site Amplification Factors using RMS of Al Braha-11 Borehole (Highest V30).

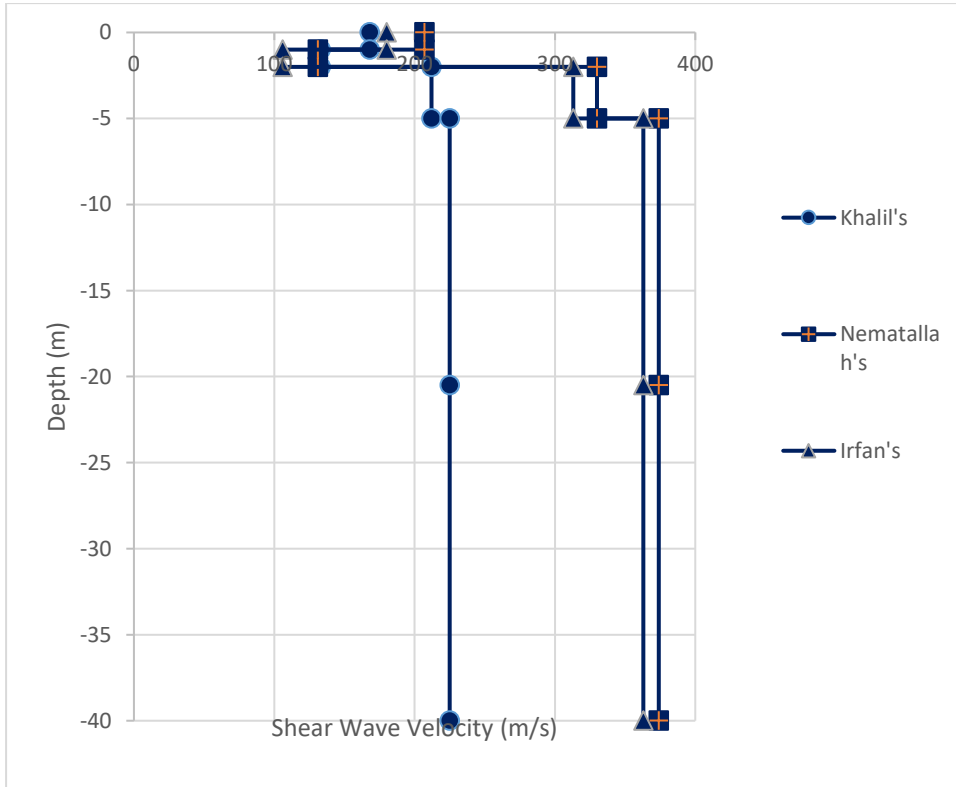


Figure 41: Velocity distribution of the different integrated velocity correlations of Al Braha-11 (Highest V30).

4.3. Effect of Degradation models on Site Response Analysis

As demonstrated in the previous chapter, to evaluate the effect of the degradation model two different sets of degradation models were adopted in this research which are the SHAKE2000 built-in degradation models developed by Seed et al [33]. and laboratory degradation models generated by A.M. Khalil [45]. The comparison between Seed et al [33] and A.M. Khalil [45] degradation models are presented in Figure 11 and Figure 12. It should be also noted that the lab generated initial velocity correlation developed by A.M. Khalil [45] was used with both built-in and lab generated degradation models. Moreover, to show the outcomes of the analysis, the same six different boreholes which describes the variation in the V30 were used. (Low V30, Mean V30, and High V30).

All Figures between Figure 42 and Figure 53 depicts the response of the ground soil to the input ground motion with respect to the used degradation model, depth, in addition the distribution of the used initial velocity correlations integrated in the analysis.

All the outcomes of the runs have demonstrated similar general trend in which implementing a generated lab degradation leads to increase the values of the surface amplification factors. The amount of growth have varied from 5% up to 40% through all the runs. Starting from Figure 42 and Figure 44 which both represent the lowest V30 values (Al Qasimeya borehole and Al Hemriyah borehole respectively). It could be noticed that in each of the two graphs the results of using lab models have resulted in higher surface amplification factor in both PGA or RMS graphs which is logical, since the developed degradation models in the lab contain different shear modulus and damping ratio values than SHAKE2000 built-in degradation models. The difference in the degradation models is directly reflected on the response of the soil column to the applied seismic motion.

Addressing each borehole individually, Figure 42 shows that the laboratory degradation model have resulted in 6% increase in the surface amplification factor with respect to the SHAKE2000 built-in degradation model. However, as presented in Figure 44 the laboratory degradation model have resulted in 14% increase in the surface amplification factor with respect to the SHAKE2000 built-in degradation model.

Although Figures Figure 42Figure 44 show a slight difference in the results, yet the degradation models can result in a huge difference in some cases such as the other boreholes that were tested. Figure 46 and Figure 48 illustrates the obtained resulted for Al Khan, Al Baraha-773 which correspond to the mean V30 values. The difference is clear for both PGA and RMS values. The results showed that the use of lab generated models resulted in higher surface amplification factor with respect to the use of the built-in degradation model. Specifically, Figure 46 shows that the laboratory degradation model has resulted in 33% increase in the surface amplification factor with respect to the SHAKE2000 built-in degradation model. This outcome is approximately close to the other borehole presented in Figure 48. For the second borehole the laboratory degradation model resulted in 37% growth in the surface amplification factor with respect to the SHAKE2000 built-in degradation model.

Figure 50 and Figure 52 signify the boreholes that correspond to the highest V30 values (Al Butina, and Al Baraha-11), respectively. As can be noted from the two figures the change in the degradation model led to a significant change in the surface amplification factor. The developed lab models resulted in higher surface amplification factor with respect to the used built-in degradation model. As shown in Figure 50 the laboratory degradation model resulted in 20% increase in the surface amplification factor with respect to the SHAKE2000 built-in degradation model. Likewise, as presented in Figure 52 the laboratory degradation model resulted in 25% growth in the surface amplification factor with respect to the SHAKE2000 built-in degradation model.

As discussed earlier, the use of the laboratory generated degradation models instead of built-in degradation models leads to a significant variation in the obtained surface amplification factor. In this study, the variation of the results of the surface amplification factors have ranged from 6% to 40%. The different soil composition of the tested soil which is considered the main reason in this huge variation. This validate the significance of developing soil-specific degradation models instead of relying on the built-in degradation models that is developed for a group of soil that may not be representative the soil located in the site of interest.

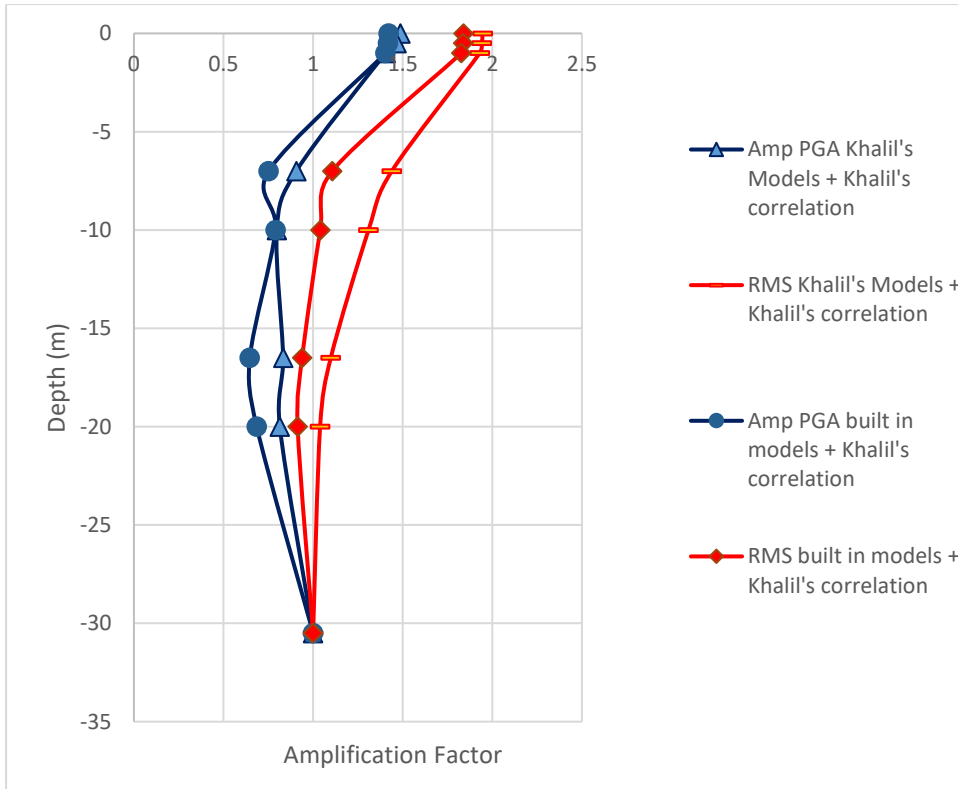


Figure 42: Effect of Degradation models on Al Qasimya Borehole (Lowest V30).

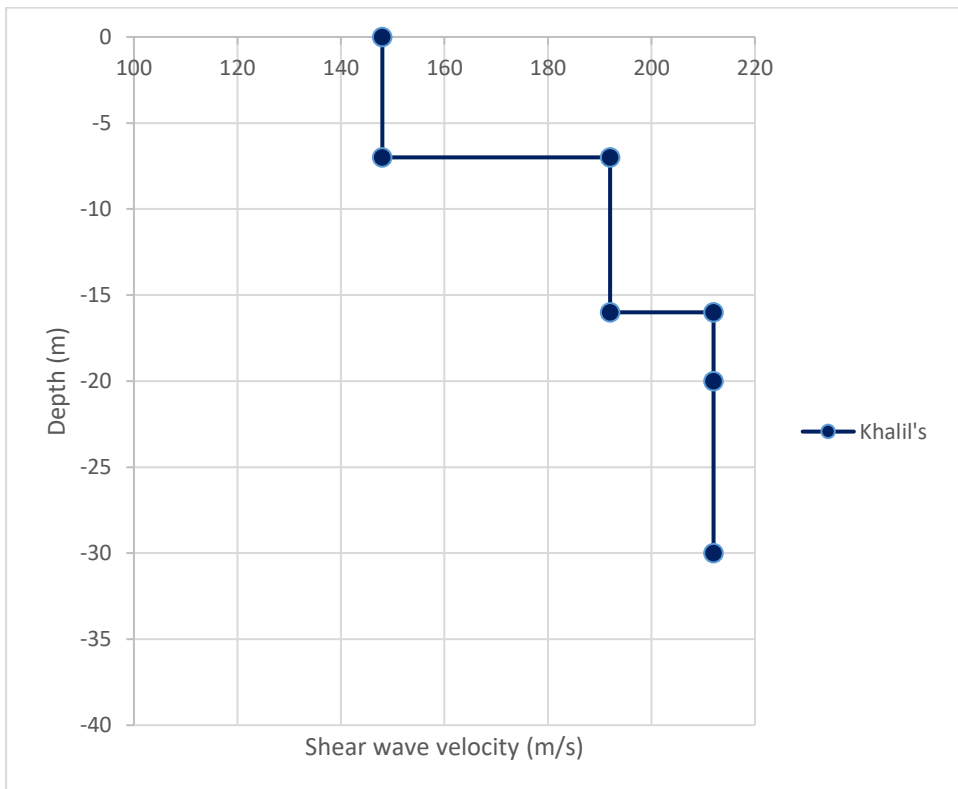


Figure 43: Velocity distribution of the velocity correlation of Al Qasimya (Lowest V30).

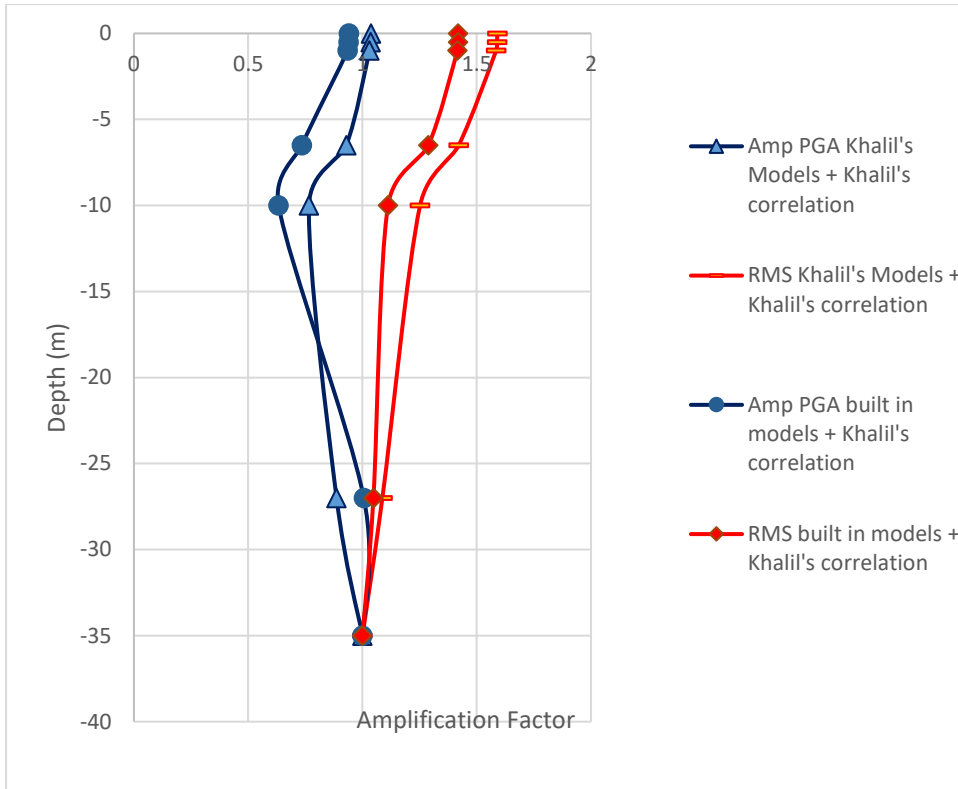


Figure 44: Effect of Degradation models on Al Hemriyah Borehole (Lowest V30).

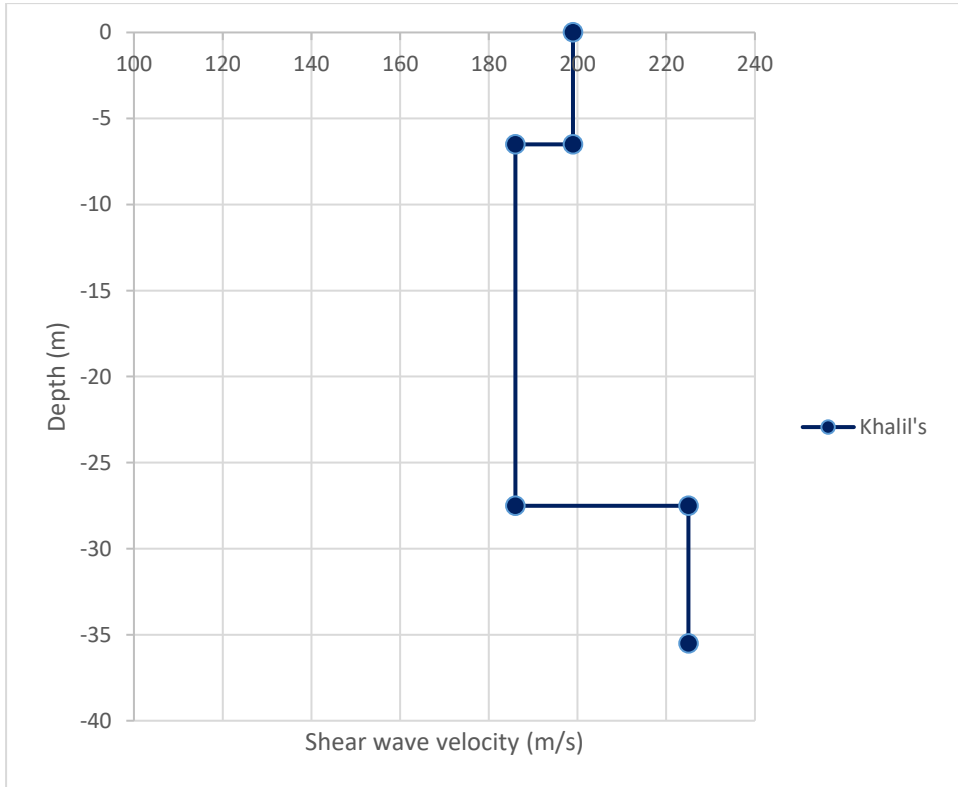


Figure 45: Velocity distribution of the velocity correlation of Al Hemriyah (Lowest V30).

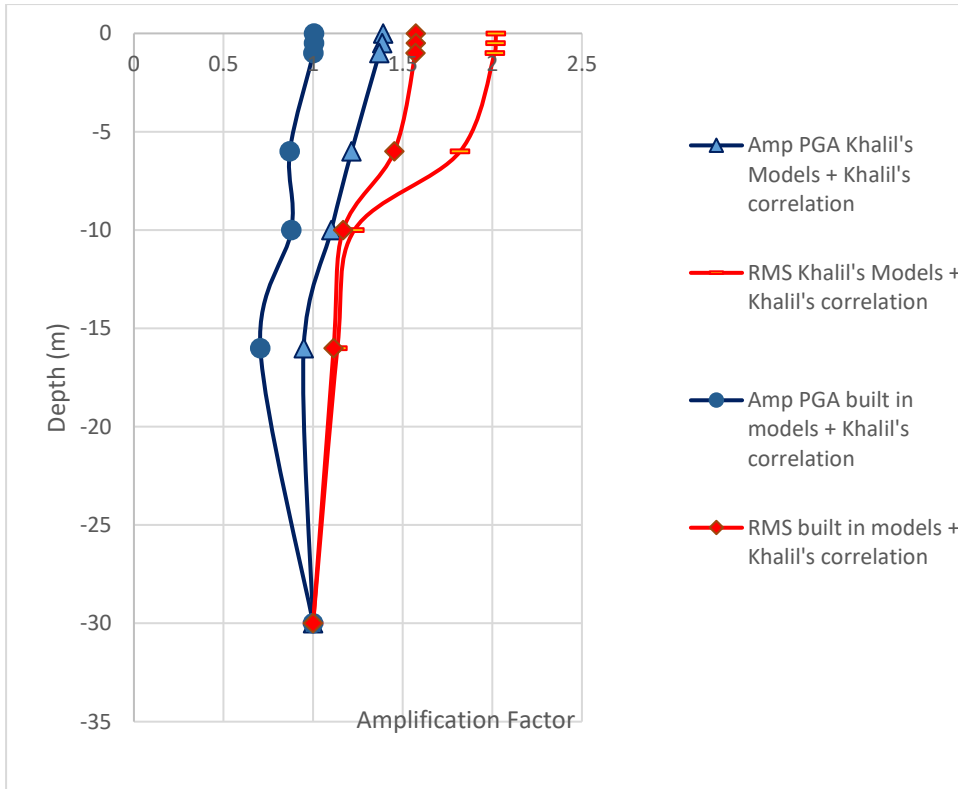


Figure 46: Effect of Degradation models on Al Khan Borehole (Mean V30).

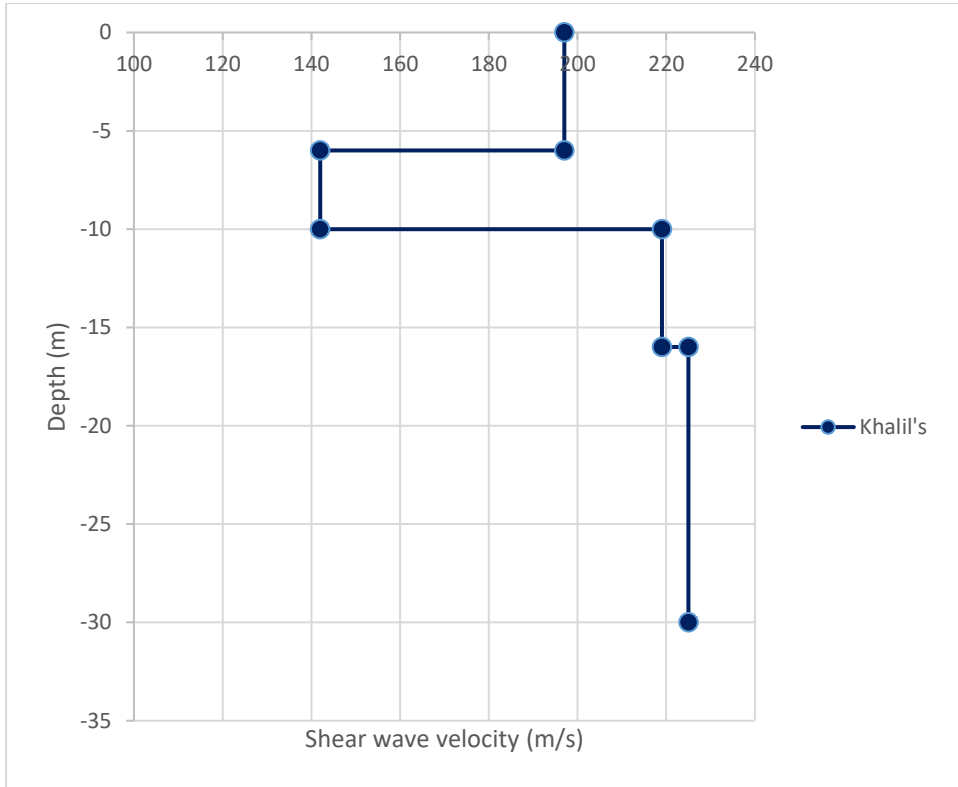


Figure 47: Velocity distribution of the velocity correlation of Al Khan (MeanV30).

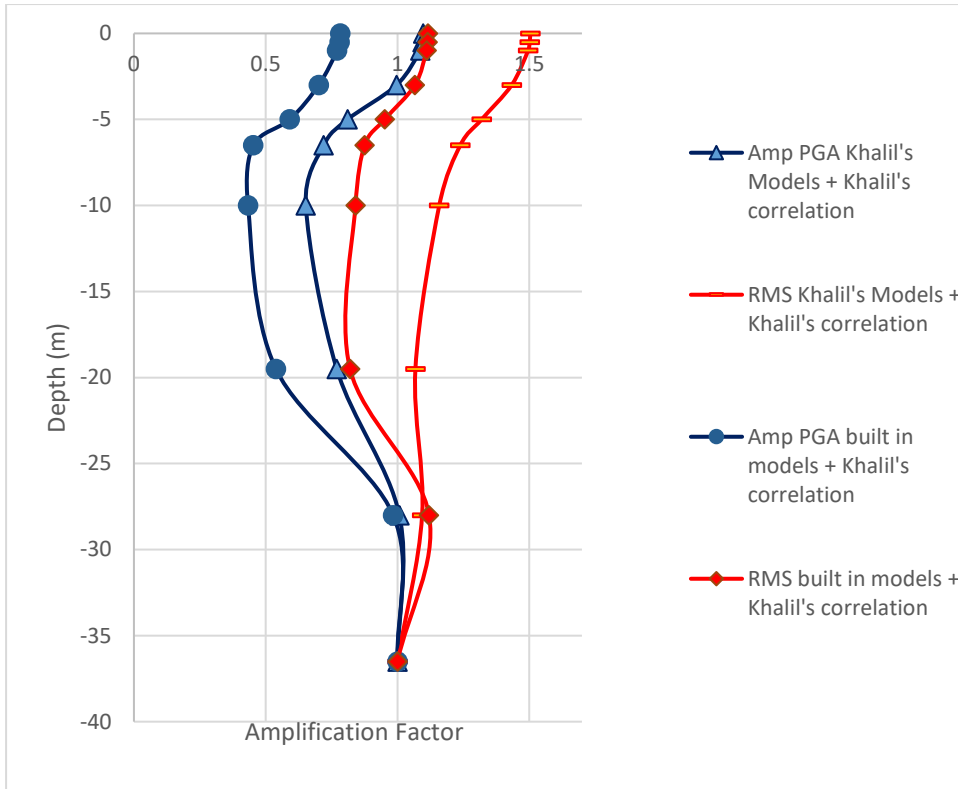


Figure 48: Effect of Degradation models on Al Baraha-773 Borehole (Mean V30).

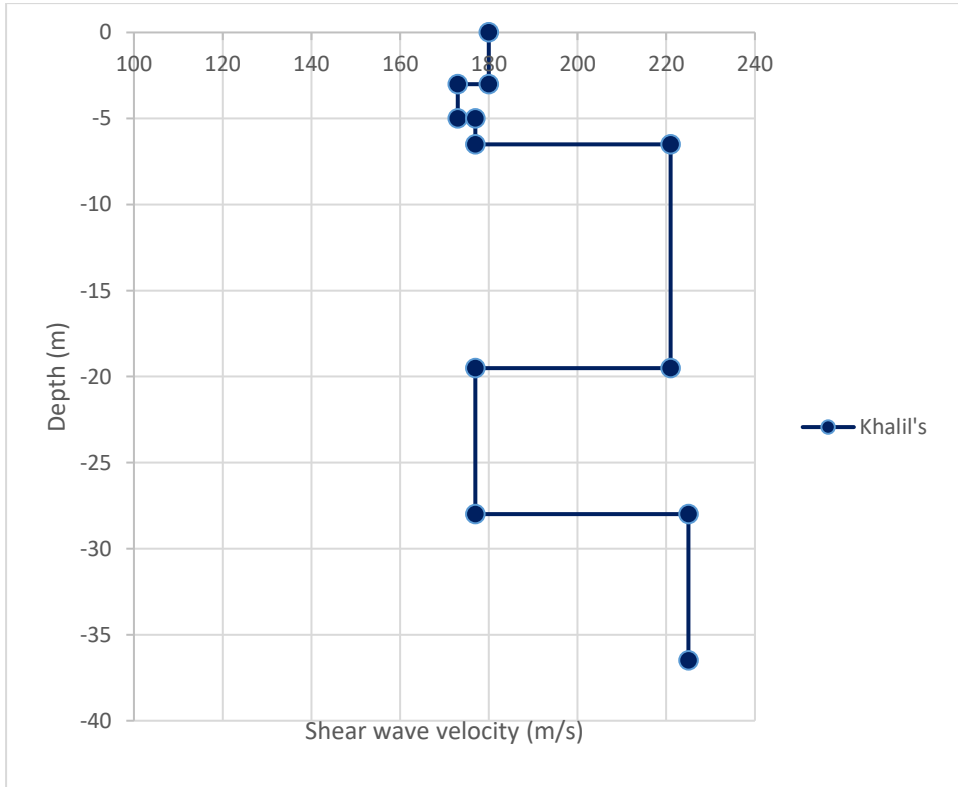


Figure 49: Velocity distribution of the velocity correlation of Al Baraha-773 (MeanV30).

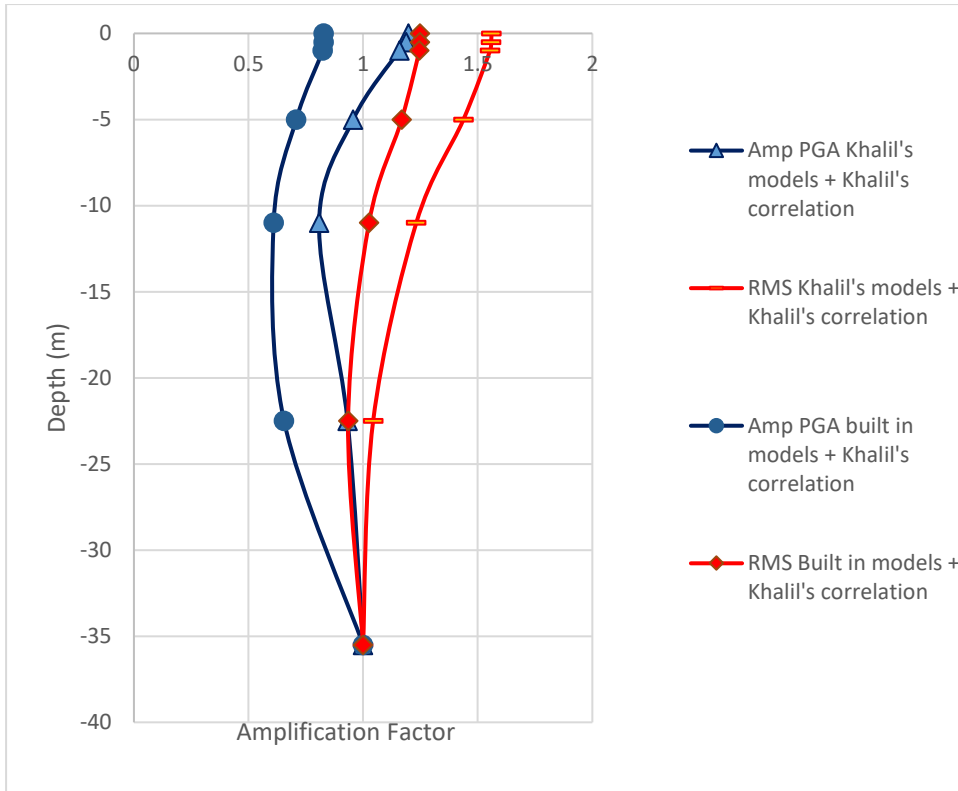


Figure 50: Effect of Degradation models on Al Butina Borehole (Highest V30).

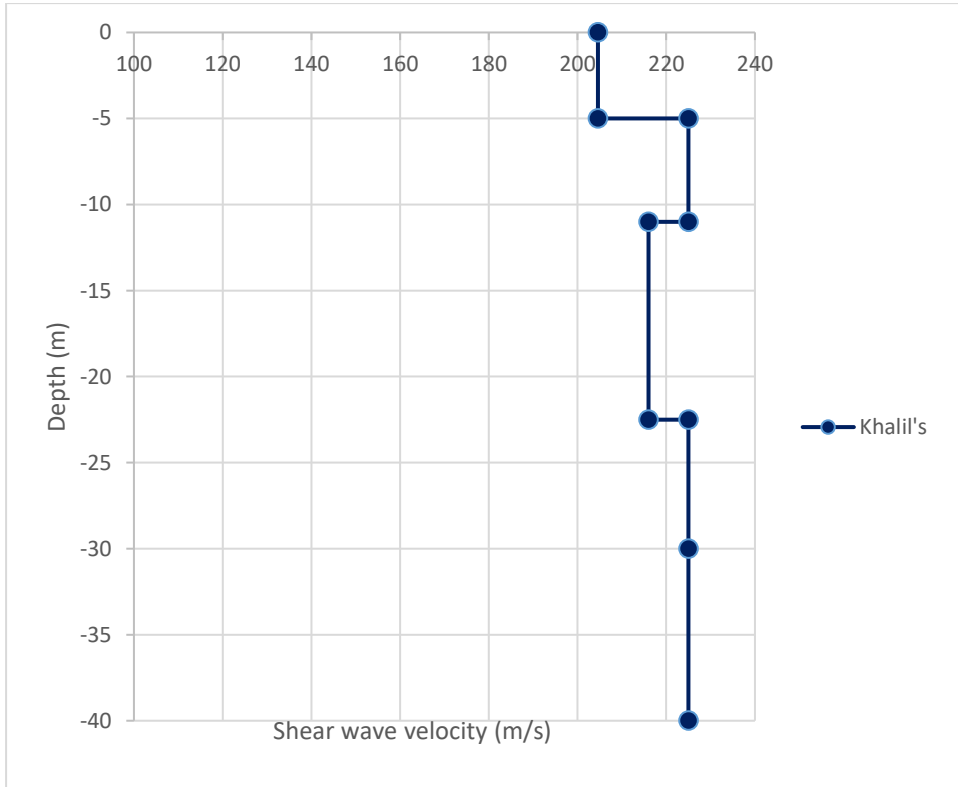


Figure 51: Velocity distribution of the velocity correlation of Al Butina (Highest V30).

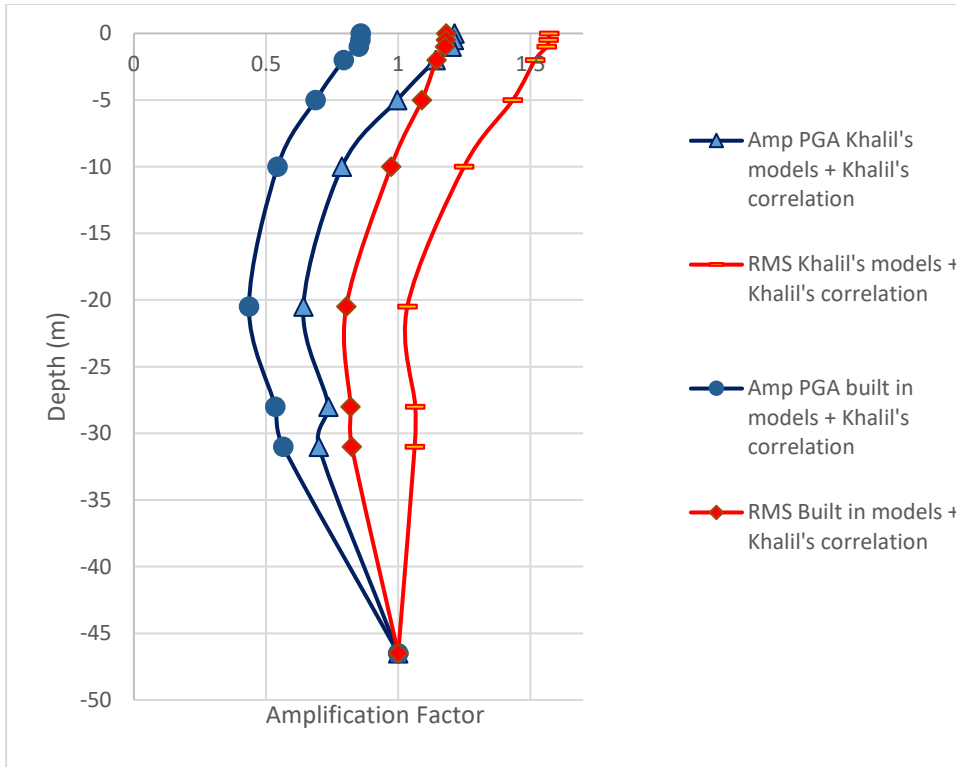


Figure 52: Effect of Degradation models on Al Baraha-11 Borehole (Highest V30).

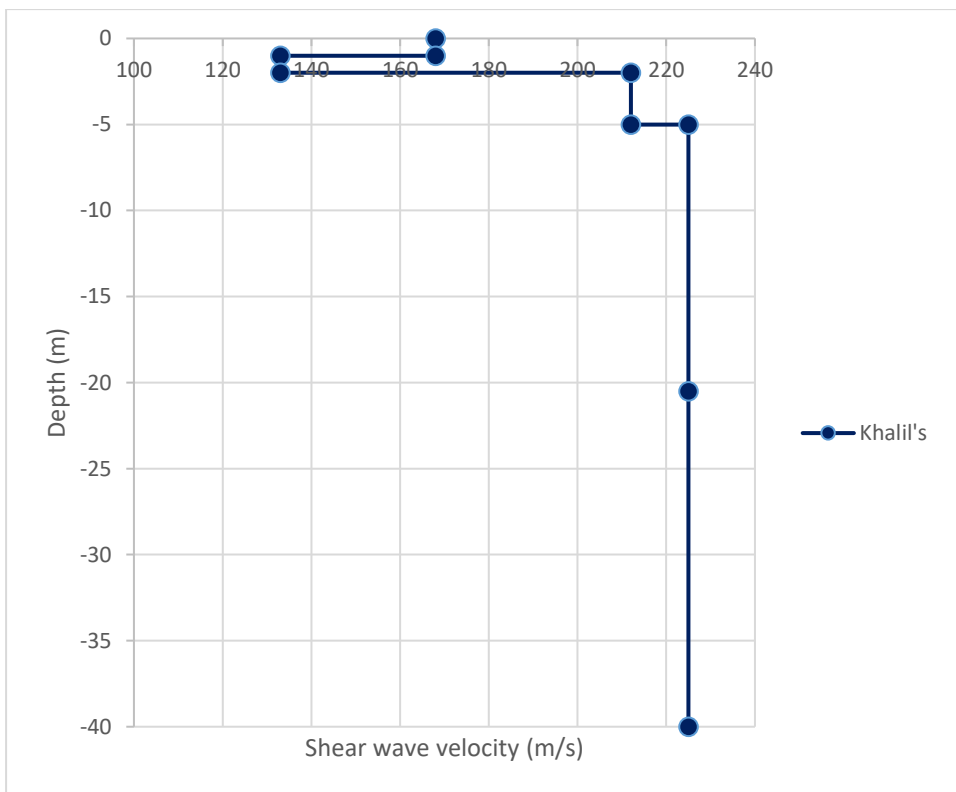


Figure 53: Velocity distribution of the velocity correlation of Al Baraha-11 (Highest V30).

4.4. Response Spectra

As illustrated in the previous chapter, by utilizing the produced spectral accelerations, site coefficients were computed at short (0.2s) and long periods (1s) after generating and fitting the uniform hazard spectra.

All the Figures in this section illustrate the results of the fitted hazard spectrums for the different tested boreholes as well as for the hazard spectrum of the used input motion. Six different graphs were generated. Each graph corresponds to the results obtained for one borehole from the same six boreholes used in the analysis. Moreover, every graph contains five different hazard spectrums. Three of the hazard spectrums represent the outcomes of modeling separately each of the three different velocity correlations integrated in this analysis (Khalil's, Niamatullah's, and Irfan's) combined with the built-in degradation model. The fourth hazard spectrum depicts the outcomes of using the lab generated degradation model with Khalil's velocity correlation (lab correlation), whereas the last hazard spectrum stands for the used input motion. The site coefficients (F_a & F_v) were summarized in Table 6 to Table 9 for each borehole.

All Figures listed between Figure 54 until Figure 61 illustrate that there is a consistent trend occurring through the different outputs. It can be noticed that all the boreholes have undergone through an amplification process due to the applied input motion. The amount of amplification has differed based on the type of soil conditions (borehole composition), degradation model used, and the applied velocity correlation during the simulation. Yet, by comparing the different hazard spectrums to each other in each graph, it could be concluded that always the highest amplification is linked with the use of Khalil's velocity correlation. This is because the lab velocity correlation always renders the smallest initial velocity among all the other correlations. A general conclusion could be stated that highest amplification would occur on the locations that correspond to the lowest velocity correlation. This is logical since the decrease in the velocity directly reflects the decrease in the rigidity of the soil and thus the resistant of the soil to changes would become less effective.

Additionally, it could be observed that the highest amplification has been also corresponded with the use of the lab degradation models. This is because the damping curve tend to have more dominant effect than the shear modulus degradation curve as the highest difference between the lab generated shear modulus and the built-in shear

modulus curves is equal to be 45% which took place at a narrow band of shear strain. However, the difference between the built-in damping curve and the lab generated damping curve have reached to a maximum of 60% and this value have taken place over large range of shear strain. Refer to section 3.4. for more explanation. It could be worth noticed that the above explanation is valid for short period and long period up to 1.5 s. For periods above 2.0 sec the trend might change a little bit due to the effect of the degradation models. For instance, by referring to Figure 56 it can be seen that after the 2.0 sec period that the built-in degradation model combined with the lab generated velocity correlation has become the highest curve which reflects that it would generate the highest surface amplification factor. This performance could be related to the comparison between the soil column natural frequency and input motion frequency content.

Nevertheless, by comparing the obtained site amplification factors shown in Table 6 to Table 9 with the NEHRP 2009 amplification factors, it could be seen that there is a noticeable difference between the values. For example, as shown in Table 6 which reflects the results of adopting the lab degradation models and the lab velocity correlation, the results shows that most of the obtained F_a values are less than the provided F_a value by the code. The difference ranged between 14.5% up to 40%. Similar trend was obtained for the F_v estimated values as they tend to be less than the provided value by the code. The difference has ranged between 4% up to 18%.

All Figures ranging between Figure 60 and Figure 63 illustrate the site coefficients for each borehole as column chart to facilitate the comparison with the values provided by the code. Figure 60 reflects the results of modelling the combination of lab degradation models and the lab velocity correlation. It can be observed that AlSoor borehole has resulted in F_a value which is higher than the code value by 40%. Similarly, AlBaraha-11 borehole has resulted in F_a value which is also higher than the code value by 6.3%. The is because both of these boreholes have very weak layers at the surface (SPT ranges from 3-11) which leads to increase the surface F_a significantly. The rest of the boreholes resulted in lower F_a values compared to the code. The reduction that has been observed ranged between 9.4% up to 14.5%. However, all the estimated F_v values have fallen under the suggested value by the code. The lab correlations led to a reduction that have ranged between 4.0% up to 13.3%.

Figure 61 denotes the outcomes of using the combination of built-in degradation models with the lab generated velocity correlation. Similar to the previous combination, it was observed that AlSoor and AlBaraha-11 boreholes resulted in Fa value that is higher than the code value by 20% and 1.5% respectively. The remaining boreholes resulted in a lower Fa values compared to the code. The reduction that has been detected varied between 12% up to 25%. Nevertheless, all the obtained Fv values have been decreased when compared to value set by the code. The reduction ranged between 12% up to 24%.

Figure 62 represents the results of combining the built-in degradation models with the velocity correlation obtained from literature. The results revealed that only AlSoor borehole resulted in Fa value that is higher than the code. The value has increased by an amount of 17%. The remaining boreholes resulted in lower Fa values compared to the code. The reduction that has been detected varied between 9% up to 30%. On the other hand, all the obtained Fv values have been decreased when compared to value set by the code. The reduction ranged between 4% up to 30%.

Figure 63 signifies the outcomes of running the built-in degradation along with the velocity correlation developed by field tests. The results displayed that the only increase in Fa occurred at AlSoor borehole. The obtained Fa value was higher than the code by a total of 15% while the remaining boreholes suffered from a reduction that varied between 13% up to 28.8%. Yet, the obtained Fv values have fallen under the code value. The reduction varied between 2.5% up to 27.7%.

To summarize, site amplification factors that were obtained from the study are noticed to have lower values from the NEHRP 2009 amplification factors. In some cases, having an SPT-values which are considered very low (3-11) can result in Fa value which is higher than the suggest value by the NEHRP. These result shows the significance of generating site specific degradation models which can improve the anticipation of the response of the local site to the seismic activity which can improve the design and make it more economical since an accurate anticipation would reduce the percentage of the safety factors.

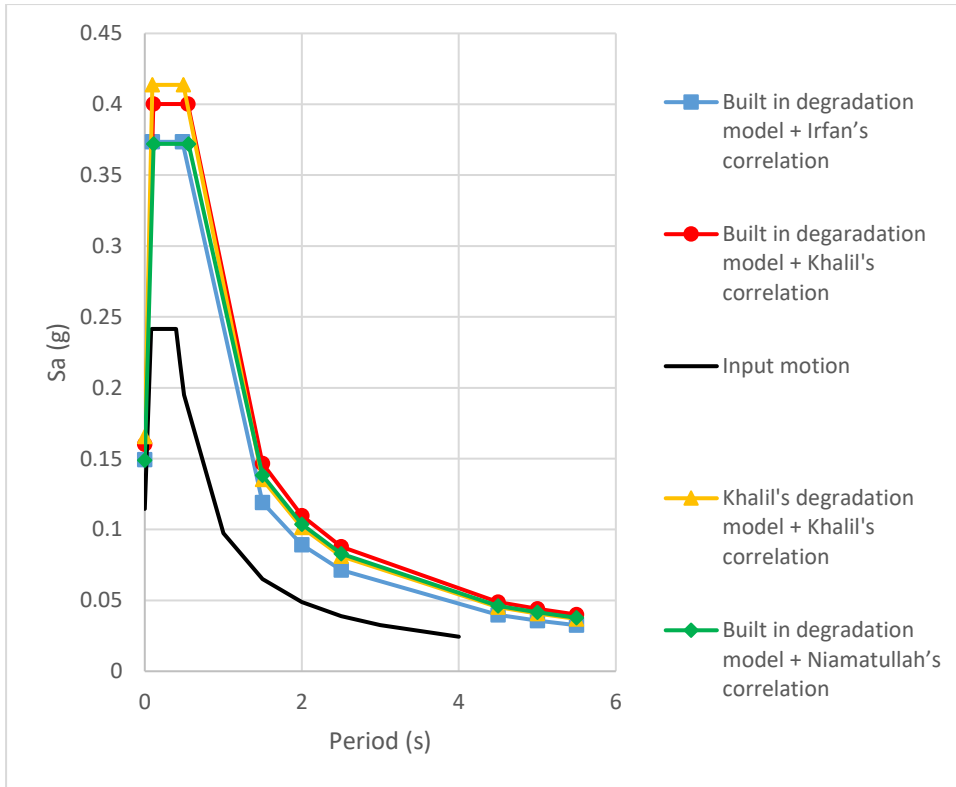


Figure 54: Fitted Hazard Spectrum for Al Hemriyah Borehole (Lowest V30).

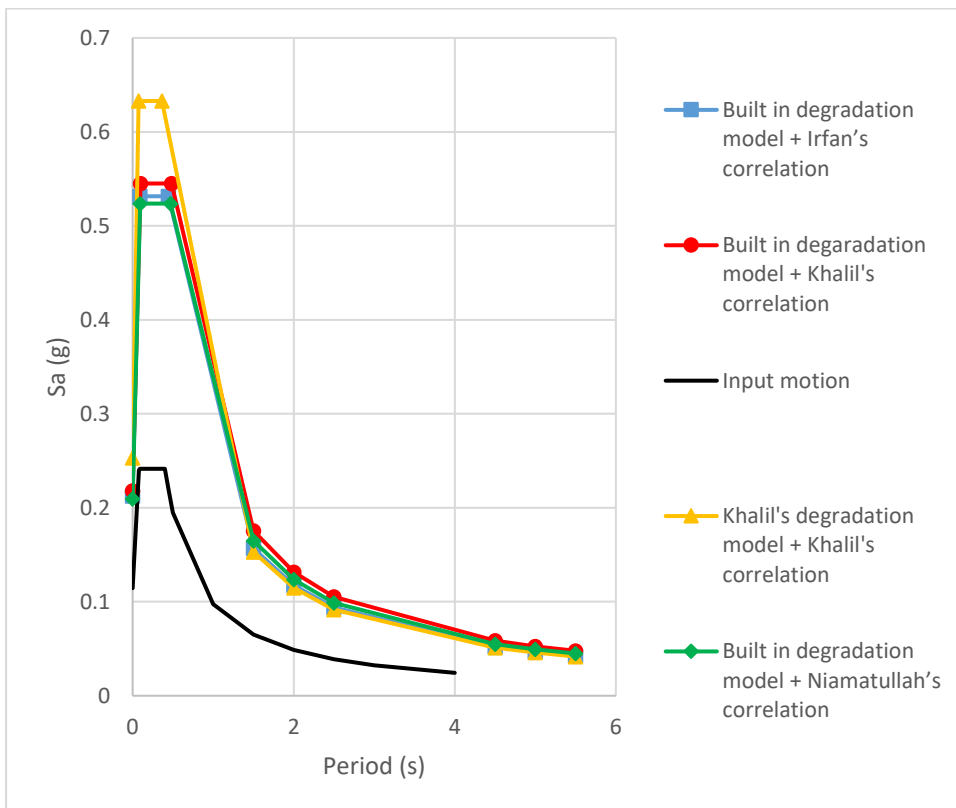


Figure 55: Fitted Hazard Spectrum for Al Soor Borehole (Lowest V30).

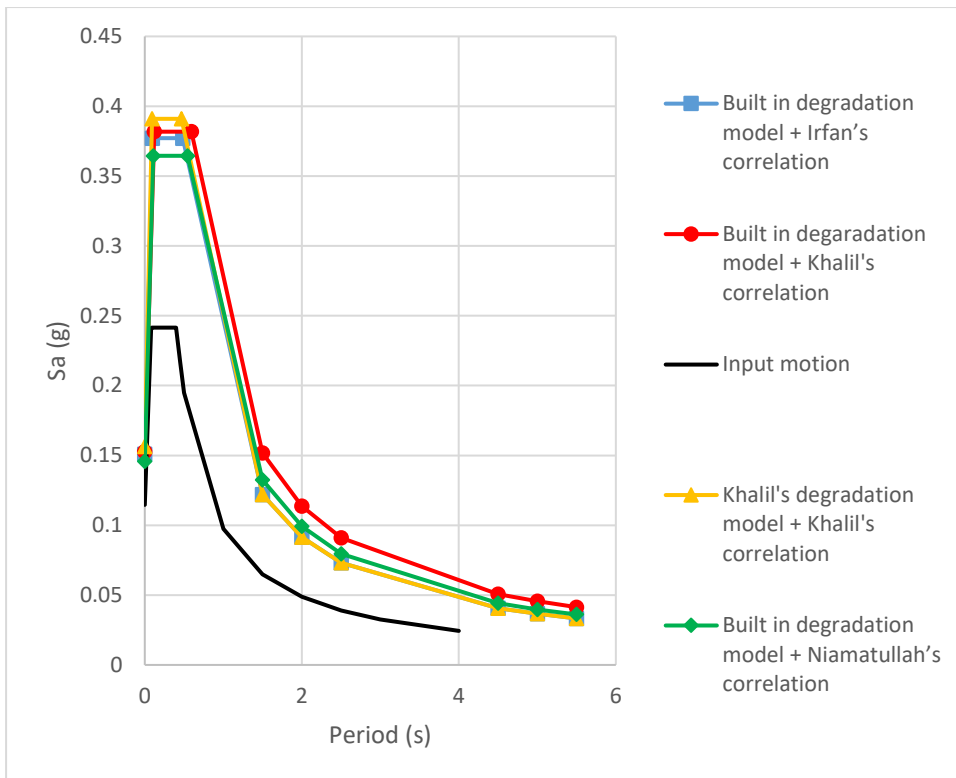


Figure 56: Fitted Hazard Spectrum for Al Khan Borehole (Mean V30).

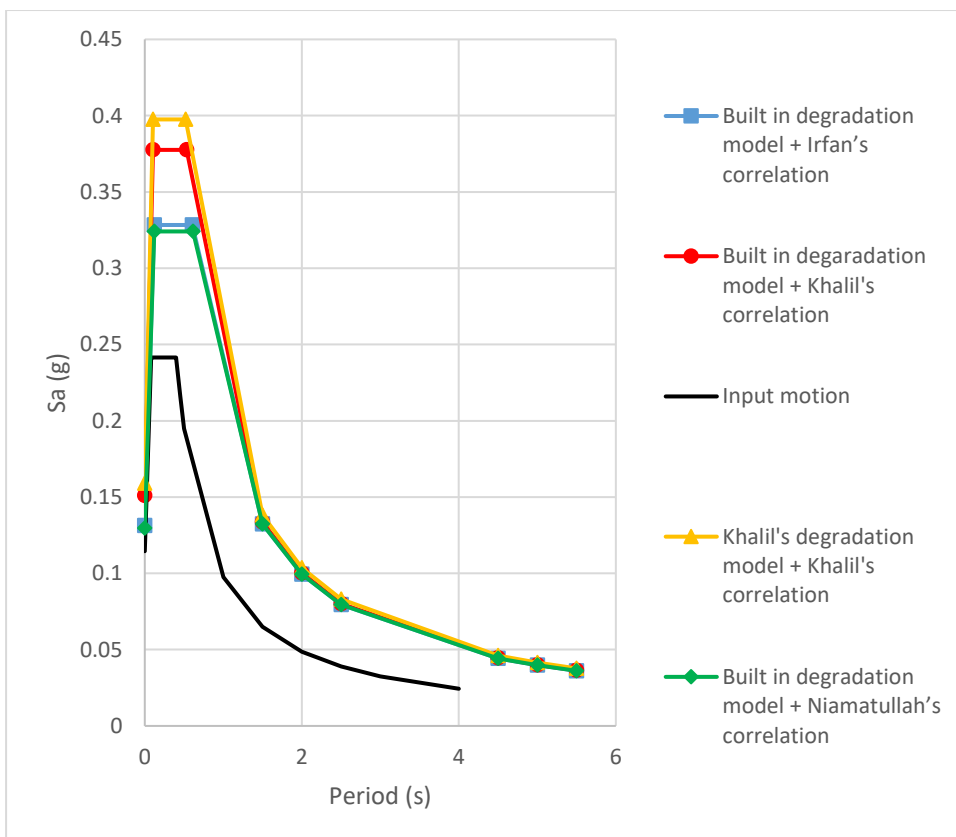


Figure 57: Fitted Hazard Spectrum for Al Baraha-773 Borehole (Mean V30).

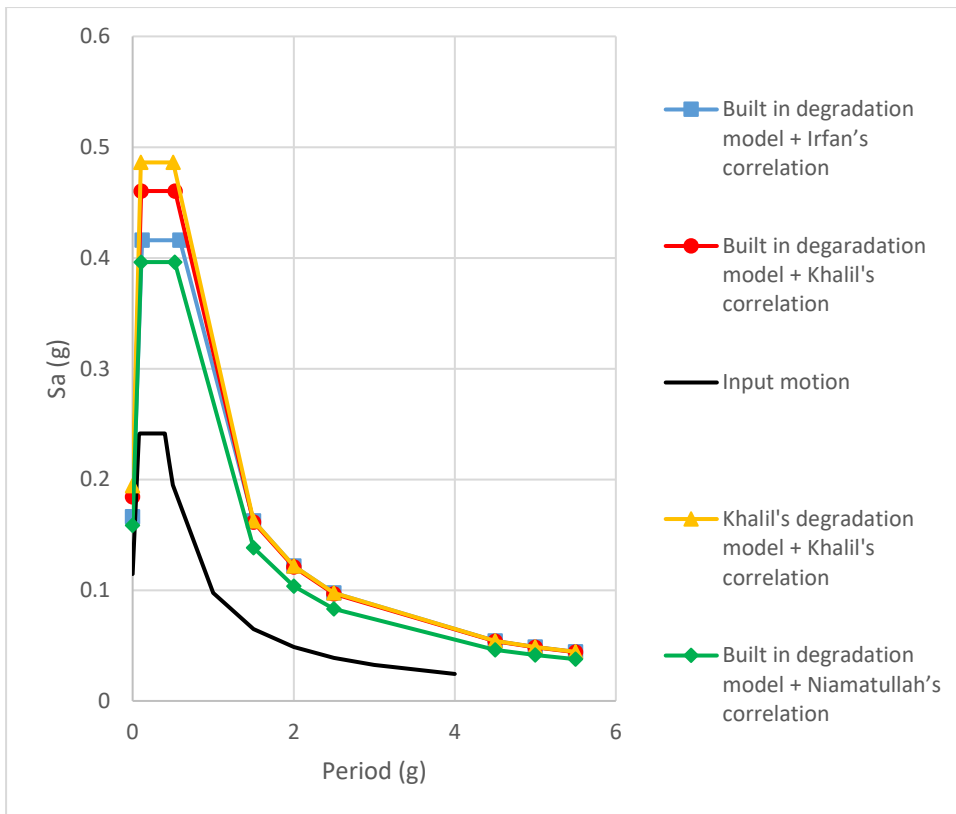


Figure 58: Fitted Hazard Spectrum for Al Baraha-11 Borehole (Highest V30).

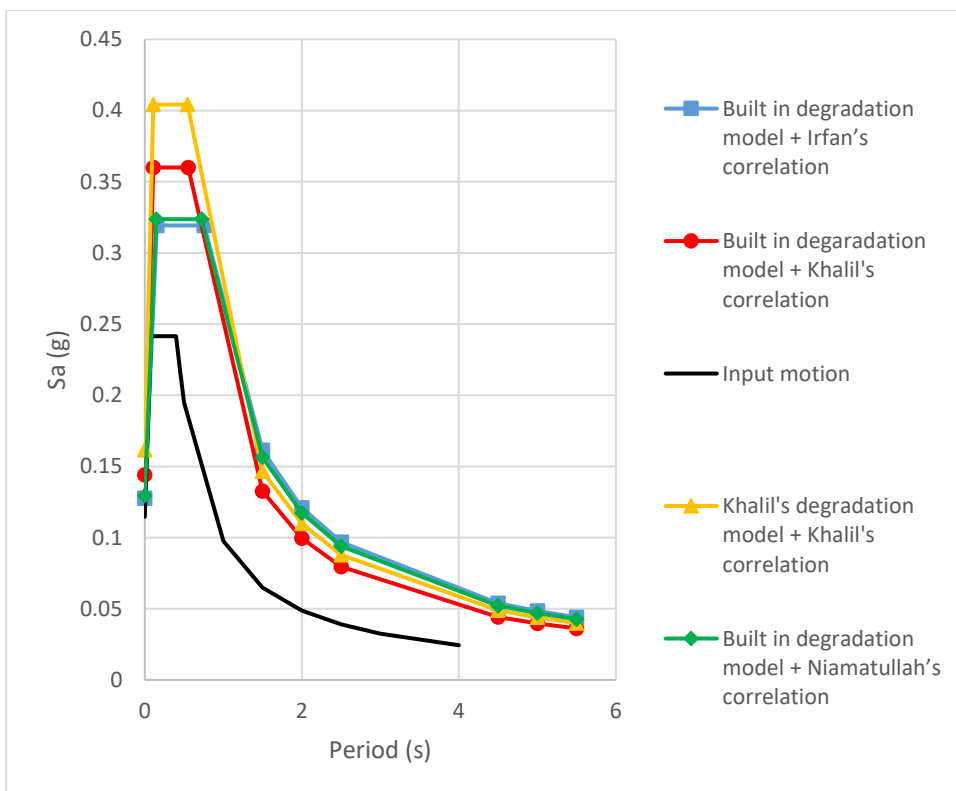


Figure 59: Fitted Hazard Spectrum for Al Butina Borehole (Highest V30).

Table 6: Amplification factors (Fa & Fv) obtained using the lab generated degradation models and Khalil's velocity correlation.

Borehole/ Site Class D	Fa (at 0.2 s)		Fv (at 1.0 s)	
	Current Study	Code	Current Study	Code
Al Hemriyah	1.45	1.6	2.08	2.4
Al Soor	2.23	1.6	2.17	2.4
Al Khan	1.37	1.6	2.16	2.4
Al Braha-773	1.4	1.6	1.97	2.4
Al Braha-11	1.7	1.6	2.31	2.4
Al Butina	1.42	1.6	2.08	2.4

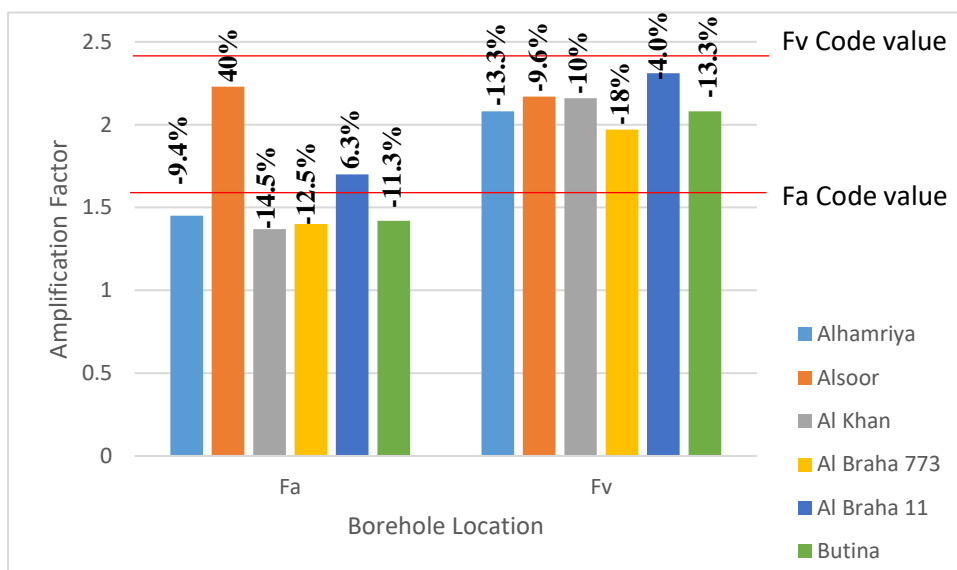


Figure 60: Amplification factors (Fa & Fv) obtained using the lab generated degradation models and Khalil's velocity correlation.

Table 7: Amplification factors (Fa & Fv) obtained using the built-in degradation models and Khalil's velocity correlation.

Borehole/ Site Class D	Fa (at 0.2 s)		Fv (at 1.0 s)	
	Current Study	Code	Current Study	Code
Al Hemriyah	1.41	1.6	2	2.4
Al Soor	1.92	1.6	2.02	2.4
Al Khan	1.35	1.6	2	2.4
Al Braha-773	1.33	1.6	1.83	2.4
Al Braha-11	1.62	1.6	2.12	2.4
Al Butina	1.20	1.6	2.1	2.4

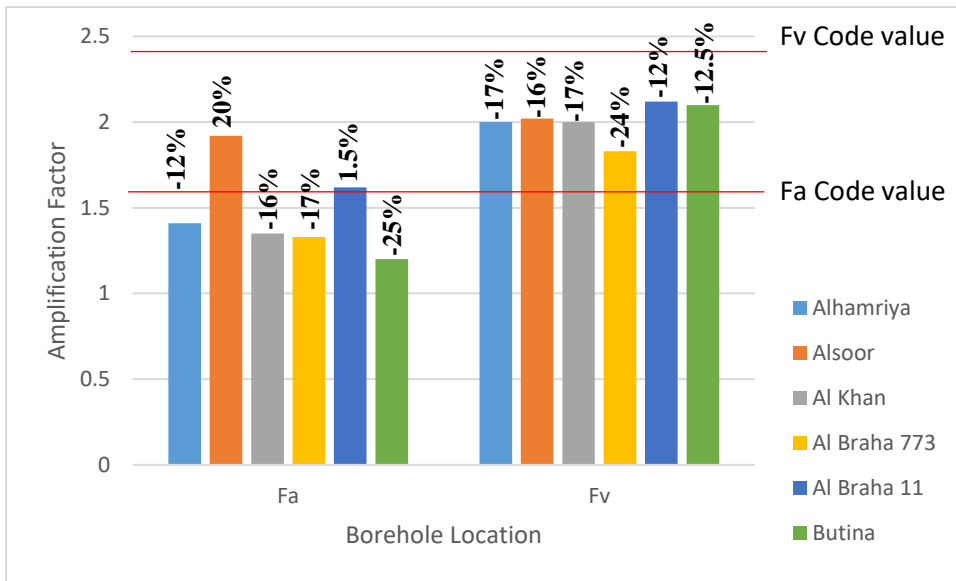


Figure 61: Amplification factors (Fa & Fv) obtained using the built-in degradation models and Khalil's velocity correlation.

Table 8: Amplification factors (Fa & Fv) obtained using the built-in degradation models and Irfan's velocity correlation.

Borehole/ Site Class D	Fa (at 0.2 s)		Fv (at 1.0 s)	
	Current Study	Code	Current Study	Code
Al Hemriyah	1.32	1.6	1.7	2.4
Al Soor	1.87	1.6	2.2	2.4
Al Khan	1.32	1.6	1.73	2.4
Al Braha-773	1.16	1.6	1.88	2.4
Al Braha-11	1.46	1.6	2.3	2.4
Al Butina	1.12	1.6	2.29	2.4

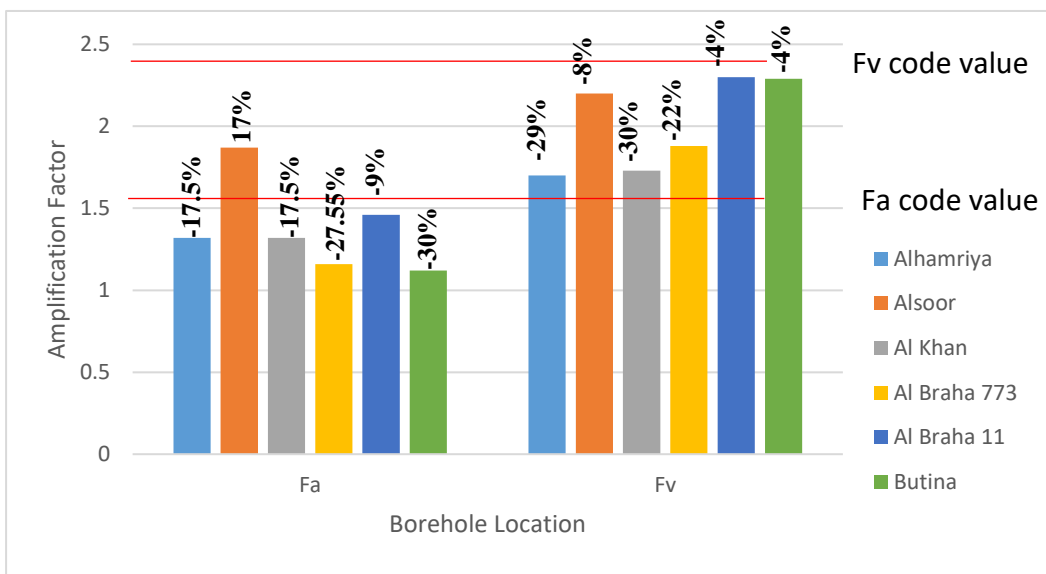


Figure 62: Amplification factors (Fa & Fv) obtained using the built-in degradation models and Irfan's velocity correlation.

Table 9: Amplification factors (Fa & Fv) obtained using the built-in degradation models and Niamatullah's velocity correlation

Borehole/ Site Class D	Fa (at 0.2 s)		Fv (at 1.0 s)	
	Current Study	Code	Current Study	Code
Al Hemriyah	1.31	1.6	1.97	2.4
Al Soor	1.84	1.6	2.34	2.4
Al Khan	1.3	1.6	1.88	2.4
Al Braha-773	1.14	1.6	1.88	2.4
Al Braha-11	1.39	1.6	1.96	2.4
Al Butina	1.14	1.6	2.22	2.4

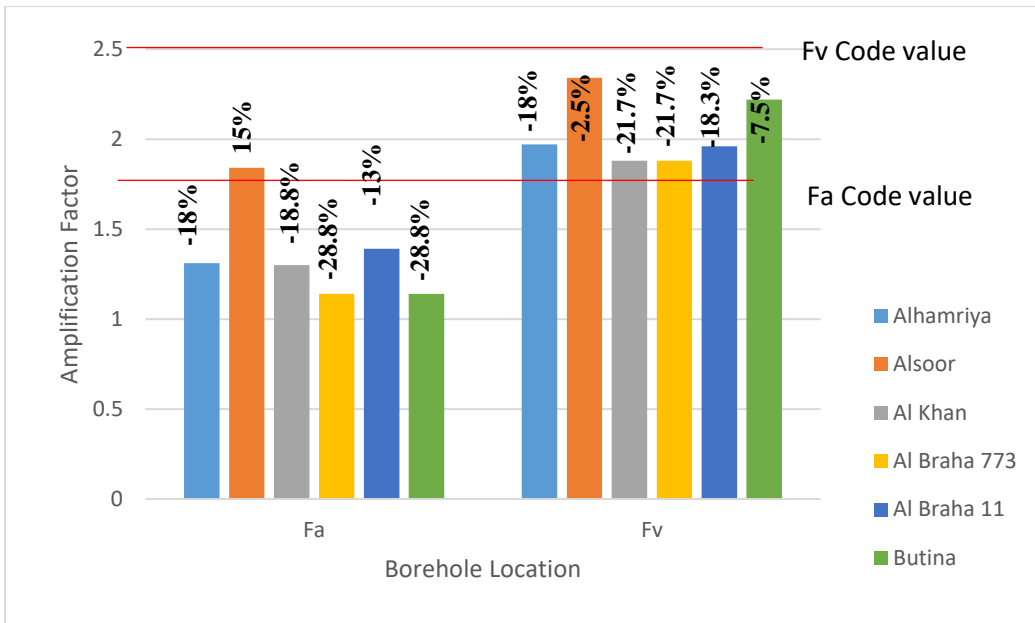


Figure 63: Amplification factors (Fa & Fv) obtained using the built-in degradation models and Niamatullah's velocity correlation.

Chapter 5. Conclusion and Future Work

In this study, the impact of shear wave velocity correlation and site-specific degradation model on the seismic site response analysis were investigated. To perform this study, bender element and cyclic triaxial tests were conducted to acquire the dynamic properties of the regional soils which are the shear wave velocity and the damping ratio at the corresponding shear strain values. Afterwards, the initial velocity correlation, shear modulus degradation model, and the damping reduction models were generated for the regional soils by A.M. Khalil [45]. Boreholes from all over the U.A.E. were gathered. Almost 38 boreholes were collected and used for the analysis. The collected boreholes were classified based on their calculated V_{30} . The results of the average V_{30} depicted that all boreholes were of class D [$180 \text{ (m/s)} \leq V_{30} \leq 360 \text{ (m/s)}$]. To study the effect of the shear velocity on the site response more precisely, the different boreholes were grouped into three categories based on the obtained values of the V_{30} ; lowest V_{30} which describe the boreholes that have an average $V_{30} \cong 250 \text{ (m/s)}$, mean V_{30} which describe the boreholes that have an average $V_{30} \cong 300 \text{ (m/s)}$, or highest V_{30} which describe the boreholes that have an average $V_{30} \cong 350 \text{ (m/s)}$. Two boreholes from each category were selected to be presented in this thesis. To study the effect of the shear velocity correlation, three different velocity correlations were used, which reflect the adaptation of general correlations developed by previous researchers, the site-specific developed velocity correlations using field methods, and the site-specific velocity correlations developed by laboratory methods, respectively. Each of the selected boreholes were modeled under all three velocity correlations while keeping the other parameters constant. The impact of the degradation models was analysed by adopting two different degradation setups in this study which are Seed et al. [33] models and A.M. Khalil's model [45]. The two sets represent the built-in degradation models reserved in the library of the computer programs which are commonly used by researchers and the site-specific developed degradation models, respectively. All boreholes were modelled using both sets of the degradation models while keeping the other parameters constant. Moreover, Uniform Hazard Spectra was developed and fitted for all the cases that was modelled during the research. The main conclusions of the research are listed below.

1. The results showed that as the depth increases the site amplification factor decreases. The reason behind this trend is related to the distance travelled by the wave because as the waves travel more, they tend to lose energy and thus less amplification will occur
2. As the initial velocity decreases the site amplification factor increases and vice-versa. This outcome is logical since less velocity reflects less shear modulus and hence less rigidity which leads to higher amplification.
3. The results showed that the use of the laboratory generated damping curve results in the highest amplification factors. This is because the variation in the lab damping reduction curve values was higher in terms of percentage and range than the shear modulus degradation curve values when compared to the built-in damping and shear modulus degradation curves which made it the dominant factor, and as the lab damping curve falls under the built-in damping curves this denotes less energy loss and thus higher amplification ratio is expected.
4. Adopting site-specific initial wave velocity instead of the correlations developed by literature or field can result normally in a lower initial velocity distribution. The difference observed is generally due the different soil composition of the tested soil which is the most significant factor to acquire different correlations. Additionally, the difference observed with the literature can also reflect the difference in the frequency used in the testing since literature recommendation could be underestimated [55]. Moreover, the difference observed with the field can also be considered due to the imperfect recreation of stress state and density of the material.
5. Applying laboratory generated degradation curves instead of the built-in degradation models led to obtain higher values of amplification factors with respect to the results obtained from modelling boreholes with built-in degradation models. The difference in the obtain amplification factors ranged from 6% up to 40%. This difference is particularly due to the different soil composition of the tested soil which resulted in the huge variation in the both the lab shear modulus degradation curve and the lab damping ratio degradation curves while compared with the built-in degradation curves.

6. Site amplification factors that were obtained from the study are noticed to have lower values from the NEHRP 2009 amplification factors. In some cases, having an SPT-values which are considered very low (3-11) can result in Fa value which is higher than the suggest value by the code. Adopting the lab degradation models and the lab velocity correlation resulted in a reduction of 14.5% up to 40% and from 4% up to 18% for Fa and Fv values respectively. Adopting the combination of lab degradation models and the lab velocity correlation in addition to the combination of built-in degradation models with the lab generated velocity correlation resulted in a similar trend. Both combinations have undergone a reduction of 9.4% up to 14% and 12% up to 25% regarding Fa values respectively, in addition to a reduction of 4% up to 13.3% and 12% up to 24% regarding Fv values respectively. However, in both combinations AlSoor and AlBaraha-11 boreholes have resulted in 40%, 20% and 6.3%, 1.5% Fa value increase respectively. Adopting the combination of built-in degradation models with the velocity correlation obtained from literature resulted in a reduction of 9% up to 30% and from 4% up to 30% for Fa and Fv values respectively. However, the results revealed that only AlSoor borehole resulted in an increase in the Fa value estimated by 17% when compared to the code.

As a future work, it would be recommended to further improve the laboratory developed degradation models. This could be done by executing resonant column test and integrate the obtained results with the outcomes of Khalil's study since the current degradation models are considered the results of dynamic triaxial machine which produce reliable results at high shear strain values only (10^{-6} to 10^{-3}) yet, the shear modulus and damping ratio values are considered unreliable outside that range and therefor bender element test is important to generate reliable degradation curves.

Also, this study has only discussed the 1-D site response analysis implications. Yet, the effect of lateral heterogeneities leading to reflections and the possible focusing of waves cannot be considered in such a study due to the nature of the one-dimensional approximations and the integrated assumptions in the analysis. Additionally, the impact of non-vertically incoming waves cannot be incorporated into the analysis. As a result, it would be recommended to perform two- and three-dimensional site response analysis.

References

- [1] H. D. Dewell, "Earthquake Resistant Construction 1-Data of Design," *Engineering News Record*, vol. 100, no. 17, pp. 650-655, 1929.
- [2] H. D. Dewell, "Earthquake Construction 2-Principles of Design," *Engineering News Record*, vol. 100, no. 18, pp. 699-702, 1929.
- [3] N. H. Heck and F. Neumann, "Destructive Earthquake Motions Measured for the First Time.," *Engineering News Record*, vol. 112, no. 19, pp. 804-807, 1993.
- [4] M. P. Romo and H. B. Seed, "Analytical Modeling of Dynamic Soil Response in the Mexico Earthquake," in *Proceedings of the International Conference, The Mexico Earthquakes.*, Mexico City, pp. 1-10, 1985.
- [5] E. E. Rinne, "Development of New Site Coefficients for Building Codes," in *Fifth US National Conference on Earthquake Engineering.*, Chicago, pp. 1-6, 1994.
- [6] M. H. T. Rayhani, M. H. E. Naggari and S. H. Tabatabaei, "Nonlinear Analysis of Local Site Effects on Seismic Ground Response in the Bam Earthquake," *Geotechnical and Geological Engineering*, vol. 26, no. 1, pp. 91-100, 2007.
- [7] H. B. Seed, R. C. Chaney and S. Pamukcu, "Foundation Engineering Handbook," in *Earthquake Effects on Soil-Foundation Systems*, Boston, Springer, 1991, pp. 594-672.
- [8] S. S. Kumar, A. M. Krishna and A. Dey, "Evaluation of dynamic properties of sandy soil at high cyclic strains," *Soil Dynamics and Earthquake Engineering*, vol. 99, pp. 157-167, 2017.
- [9] Z. Khan, "Dynamics properties (lecture slides a)," in *Dynamic of Machine foundations*, Sharjah, American university of Sharjah, 2020, p. 79.
- [10] Z. Khan, M. El-Emam, M. Irfan and J. Abdalla, "Probabilistic seismic hazard analysis and spectral accelerations for United Arab Emirates," *Natural Hazards*, vol. 67, no. 1, pp. 569-589, 2013.

- [11] Z. Wang, "Seismic Hazard Assessment: Issues and Alternatives," *Pure and Applied Geophysics*, vol. 168, no. 1, pp. 11-25, 2011.
- [12] H. Shah, M. Manoutchehr and T. Zsutty, "Seismic risk analysis for California State Water Project Reach C.," Blume Earthquake Engineering Center, Department of Civil Engineering, Stanford University, Stanford, California., 1976.
- [13] R. McGuire and D. Mayer-Rosa., *The Practice of Earthquake Hazard Assessment*, Collingdale, PA: DIANE Publishing Company, 1993.
- [14] H. Shah and W. Dong, "A re-evaluation of the current seismic hazard assessment methodologies," in *Eight World Conference on Earthquake Engineering*, San Francisco, pp. 1-7, 1989.
- [15] B. Gutenberg and C. F. Richter, "Frequency of earthquakes in California," *Bulletin of Seismological Society of America*, vol. 34, no. 4, pp. 185-188, 1944.
- [16] M. Al-Haddad, G. H. Siddiqi, R. Al-Zaid, A. Arafah, A. Necioglu and N. Turkelli, "A Basis for Evaluation of Seismic Hazard and Design Criteria for Saudi Arabia," *Earthquake Spectra*, vol. 10, no. 1, pp. 231-235, 1994.
- [17] L. Esteva, "Geology and probability in the assessment of seismic risk," in *Proceedings of the second International Congress of the International Association of Engineering Geologists*, Sao Paolo, 1974.
- [18] J. C. Stepp, W. J. Silva, R. K. McGuire and R. W. Sewell, "Determination of Earthquake Design Loads for a High Level Nuclear Waste Repository Facility," in *Proceedings of the Natural Phenomena Hazards Mitigation Conference*, Atlanta, GA, pp. 1-9, 1993.
- [19] M. C. Chapman, "A Probabilistic approach to ground motion selection for engineering design," *Bulletin of Seismological Society of America*, vol. 85, no. 3, pp. 937-942, 1995.

- [20] P. Bazzurro and C. A. Cornell, "Disaggregation of Seismic Hazard," *Bulletin of Seismological Society of America*, vol. 89, no. 2, pp. 501-520, 1999.
- [21] S. Harmsen, D. Perkins and A. Frankel, "Disaggregation of Probabilistic Ground Motions in the Central and Eastern United States," *Bulletin of Seismological Society of America*, vol. 89, no. 1, pp. 1-13, 1999.
- [22] K. KANAI, "Relation Between the Earthquake Damage of Non-Wooden Buildings and the Nature of the Ground," *Bulletin of the Earthquake Research Institute*, vol. 27, no. 1, p. 97, 1949.
- [23] Y. M. A. Hashash, C. Phillips and D. R. Groholski, "Recent Advances in Non-Linear Site Response Analysis," in *International Conferences on Recent Advances in Geotechnical Earthquake Engineering and Soil Dynamics*, San Diego, California, pp. 1-11, 2010.
- [24] R. Abbasnia, R. Ahmadi and H. Ziaadiny, "Effect of confinement level, aspect ratio and concrete strength on the cyclic stress–strain behavior of FRP-confined concrete prisms," *Composites Part B: Engineering*, vol. 43, no. 1, pp. 825-831, 2012.
- [25] B. Indraratna, J. Lackenby and D. Christie, "Effect of confining pressure on the degradation of ballast under cyclic loading," *Géotechnique*, vol. 55, no. 4, pp. 325-328, 2005.
- [26] S. S. Kumar, A. Dey and A. M. Krishna, "Importance of Site-Specific Dynamic Soil Properties for Seismic Ground Response Studies: Ground Response Analysis," *International Journal of Geotechnical Earthquake Engineering*, vol. 9, no. 1, pp. 78-98, 2018.
- [27] M. Omar, A. Shanableh, M. Balwan, M. Fattah and K. Hamad, "Influence of local soil conditions on ground response: site amplification in Sharjah, United Arab Emirates," *International Journal of Modern Engineering*, vol. 13, no. 2, pp. 34-40, 2013.

- [28] M. El-Emam, Z. Khan, J. Abdalla and M. Irfan, "Local site effects on seismic ground response of major cities in UAE," *Journal of the International Society for the Prevention and Mitigation of Natural Hazards*, vol. 79, no. 2, pp. 791-814, 2015.
- [29] Y. Hashash, M. Musgrove, J. Harmon, O. Ilhan, G. Xing, O. Numanoglu, D. Groholski, C. Phillips and D. Park, "DEEPSOIL 7, User Manual," Board of Trustees of University of Illinois at Urbana-Champaign, Urbana, IL, 2020.
- [30] G. Ordonez, "SHAKE2000- A computer program for the 1D analysis of geotechnical earthquake engineering problems," GeoMotions, LLC, Lacey, Washington, USA, 2000.
- [31] S. Kumar and A. Krishna, "Seismic ground response analysis of some typical sites of Guwahati city," *International Journal Geotechnical Earthquake Engineering*, vol. 4, no. 1, pp. 83-101, 2013.
- [32] D. Basu, A. Dey and S. S. Kumar, "One-dimensional effective stress non-masing nonlinear ground response analysis of IITGuwahati," *International Journal Geotechnical Earthquake Engineering*, vol. 8, no. 1, pp. 1-14, 2017.
- [33] H. B. Seed and I. M. Idriss, Soil moduli and dmaping factors for dynamic response analysis, California: University of California at Berkeley: Earthquake Engineering Research Centre, 1970.
- [34] E. H. Field and K. H. Jacob, "Monte Carlo simulation of the theoretical site response variability at Turkey Flat, California, given the uncertainty in the geotechnically derived input parameters," *Earthquake Spectra*, vol. 9, no. 4, pp. 669-701, 1993.
- [35] E. M. Rathje, A. R. Kottke and W. L. Trent, "Influence of Input Motion and Site Property Variabilities on Seismic Site Response Analysis," *Journal of Geotechnical and Geoenvironmental Engineering*, vol. 136, no. 4, pp. 607-619, 2010.

- [36] K. Kanai, "The Effect of Solid Viscosity of the Surface Layer on the Earthquake Movements," *Earthquake Research Institute*, vol. 28, no. 1, pp. 31-35, 1950.
- [37] K. Kanai, "Relation between the nature of surface layer and the amplitude of earthquake motions," *Bulletin Earthquake Research Institute*, vol. 30, no. 1, pp. 31-32, 1952.
- [38] I. M. Idriss and H. B. Seed, "Seismic Response of Horizontal Soil Layers," *Journal of the Soil Mechanics and Foundations Division*, vol. 94, no. 4, pp. 1003-1031, 1968.
- [39] P. B. Schnabel, J. Lysmer and H. B. Seed, "SHAKE - A computer program for earthquake analysis of horizontally layered sites," Earthquake Engineering Research Center, University of California, Berkeley, California, 1972.
- [40] P. W. Taylor and T. J. Larkin, "Seismic Site Response of Nonlinear Soil Media," *Journal of the Geotechnical Engineering Division*, vol. 4, no. 3, pp. 369-383, 1978.
- [41] U. S. T. D. o. Interior, "Earthquake Hazards Program," The National Earthquake Information Center (NEIC), Colorado, 1966.
- [42] I. I. S. Center, "Definitive record of the Earth's seismicity," International Association of Seismology and Physics of the Earth's Interior, 1964.
- [43] J. Bommer and A. B. Acevedo, "The use of real accelerograms as input to dynamic analysis," *Journal of Earthquake Engineering*, vol. 8, no. 1, pp. 43-91, 2004.
- [44] M. Irfan, "Seismic site response, analysis and characterization of major cities in U.A.E.," American University of Sharjah, College of Engineering, Sharjah, 2011.
- [45] A. M. Khalil, "Dynamic Properties of Soil in UAE from Field and Laboratory Tests," American University of Sharjah, Sharjah, 2020.
- [46] P. B. Schnabel, "Effects of local geology and distance from source on earthquake ground motions," University of California, Berkeley, California, 1973.

- [47] H. B. Seed, R. T. Wong, I. M. Idriss and K. Tokimatsu, "Moduli and damping factors for dynamic analyses of cohesionless soils," *Journal of Geotechnical Engineering*, vol. 112, no. 11, pp. 1016-1032, 1986.
- [48] J. I. Sun, R. Golesorkhi and H. B. Seed, "Dynamic Moduli and Damping Ratios for Cohesive soils," Berkeley: University of California, Earthquake Engineering Research Center, California, 1988.
- [49] N. H. Bismillah, "VARIATION OF SHEAR WAVE VELOCITY WITH SPT-N VALUES IN THE CITY OF SHARJAH," American University of Sharjah , Sharjah, 2014.
- [50] N. Hasancebi and R. Ulusay, "Empirical correlations between shear wave velocity and penetration resistance for ground shaking assessments," *Bulletin of Engineering Geology and the Environment*, vol. 66, no. 2, pp. 203-213, 2007.
- [51] T. Shibata, "Analysis of liquefaction of saturated sand during cyclic loading," in *Disaster Prevention Research Institute Bulletin*, vol. 13, no. 1, pp. 563-570, 1970.
- [52] H. Seed and I. Idriss, "Evaluation of liquefaction potential sand deposits based on observation of performance in previous earthquakes," in *ASCE National Convention (MO)*, St. Louis, Missouri, 1981.
- [53] G. Athanasopoulos, "Empirical correlations V_s – NSPT for soils of Greece: a comparative study of reliability," in *7th International Conference on Soil Dynamics and Earthquake Engineering*, Chania, Greece, pp. 1-14, 1995.
- [54] T. B. S. S. Council, "Recommended Provisions for Seismic Regulations for New Buildings and Other Structures," FEMA Earthquake Publications and Resources (FEMA P-750), Washington , 2009.
- [55] T. GODLEWSKI and T. SZCZEPAŃSKI, "Measurement of soil shear wave velocity using in situ and laboratory seismic methods - some methodological aspects," *Geological Quarterly* , vol. 59, no. 2, p. 358–366, 2015.

Appendix A

SAMPLES DEGRADATION MODELS

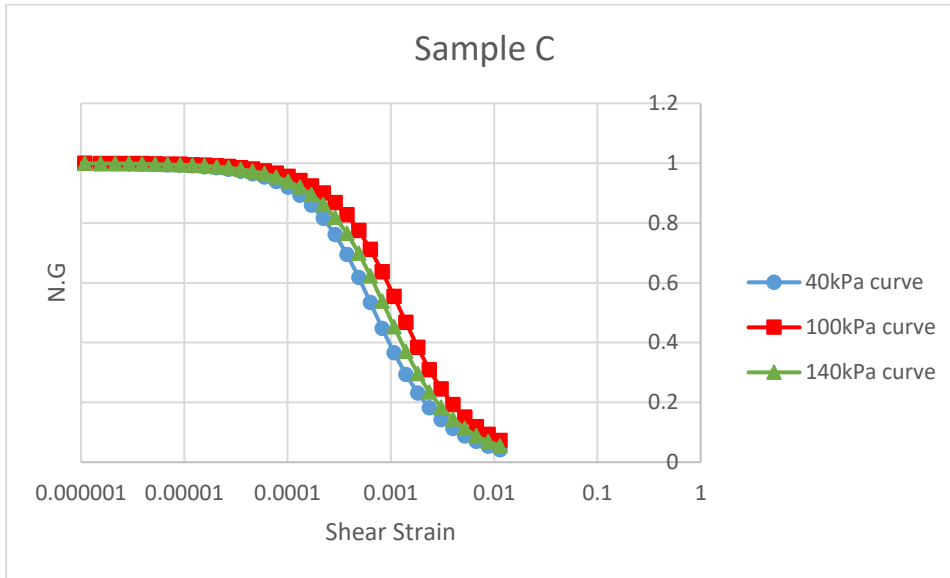


Figure A1

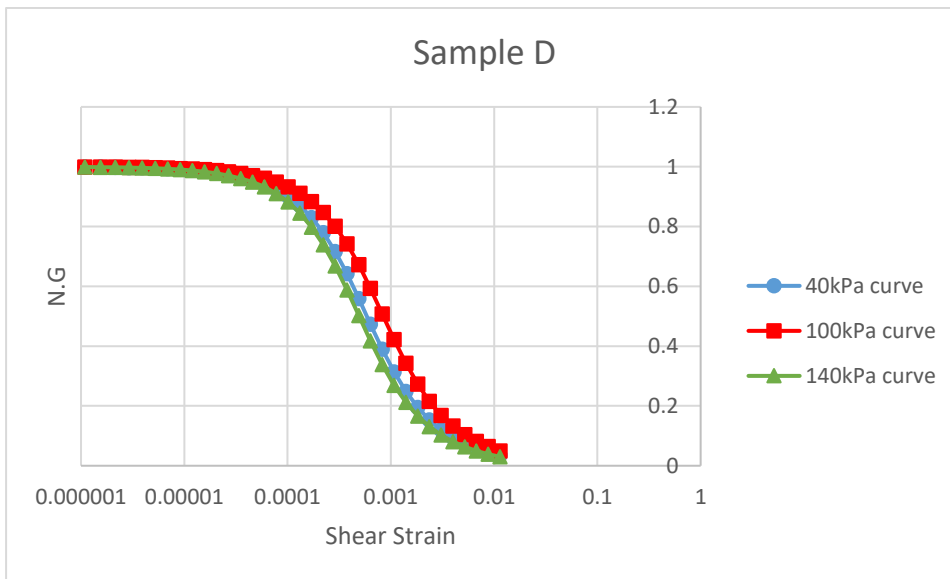


Figure A2

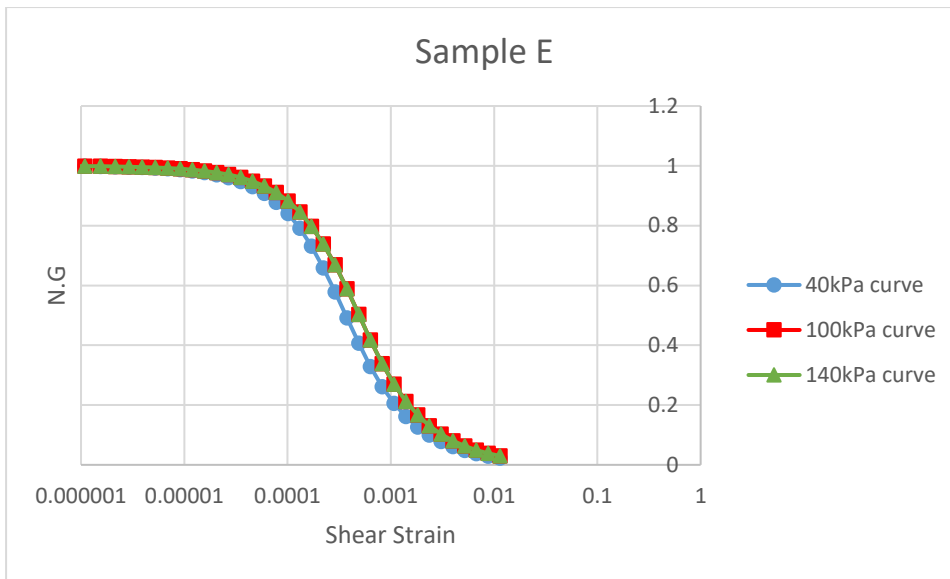


Figure A3

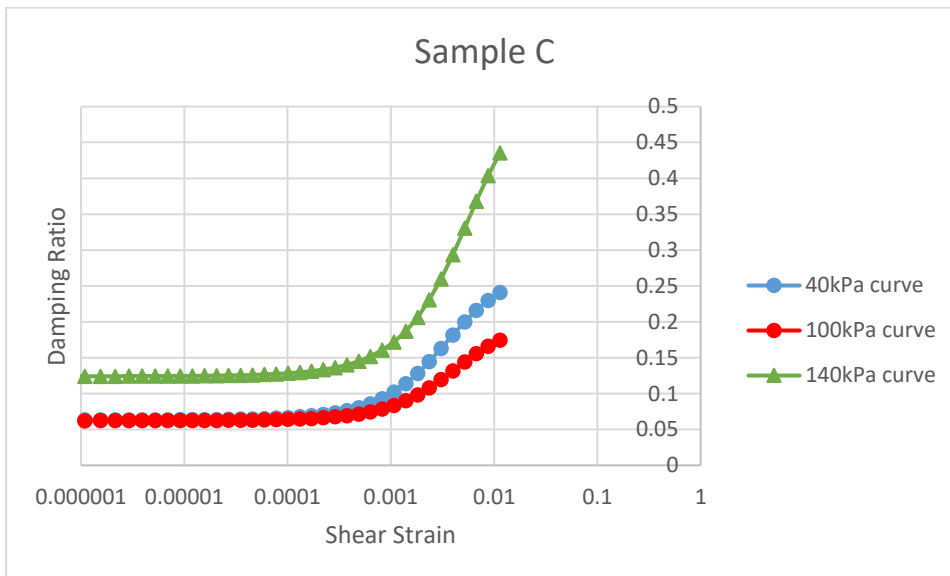


Figure A4

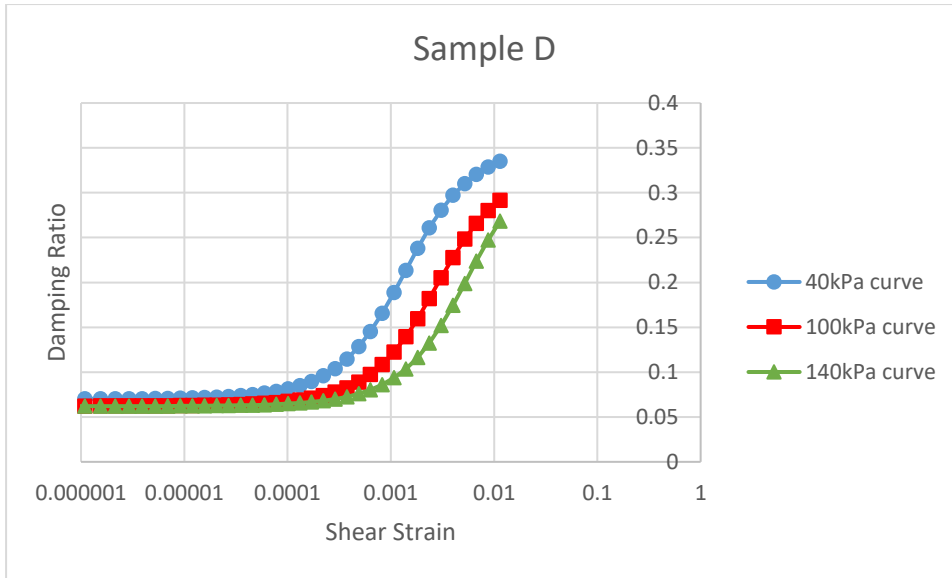


Figure A5

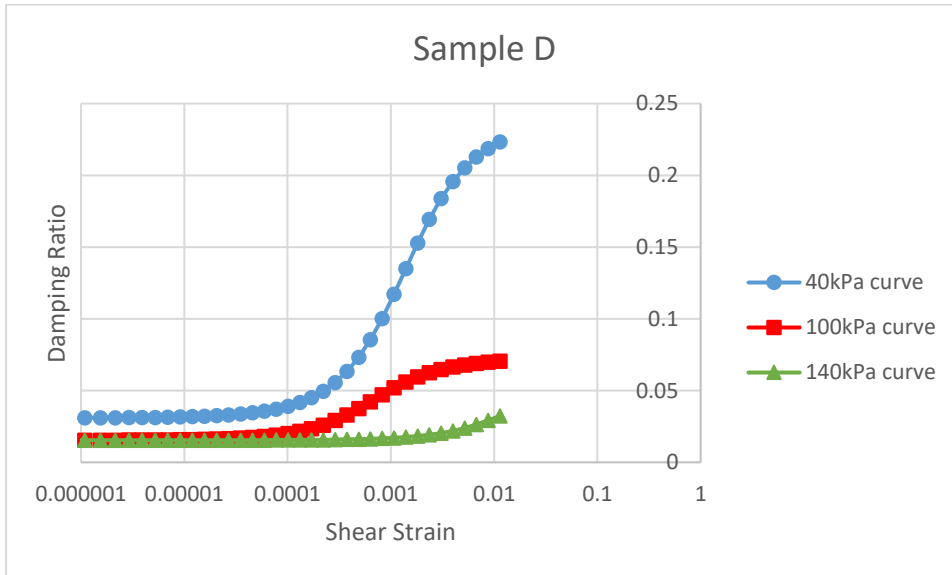


Figure A6

Appendix B
SOIL COLUMNS

Table B1

Name of Borehole	starting Depth (m)	Ending Depth (m)	Depth (m)	SPT
Plot No : 11, Al Baraha, Sharjah. BOREHOLE 1	0	0.5	0.5	5
	0.5	1	0.5	7
	1	1.5	0.5	1
	1.5	2	0.5	5
	2	2.5	0.5	8
	2.5	3	0.5	41
	3	3.5	0.5	24
	3.5	4	0.5	
	4	4.5	0.5	50
	4.5	5	0.5	
	5	5.5	0.5	50
	5.5	6	0.5	
	6	6.5	0.5	50
	6.5	7	0.5	
	7	7.5	0.5	50
	7.5	8	0.5	
	8	8.5	0.5	50
	8.5	9	0.5	
	9	9.5	0.5	50
	9.5	10	0.5	
	10	10.5	0.5	50
	10.5	11	0.5	
	11	11.5	0.5	50
	11.5	12	0.5	
	12	12.5	0.5	50
	12.5	13	0.5	
	13	13.5	0.5	50
	13.5	14	0.5	
	14	14.5	0.5	50
	14.5	15	0.5	
15	15.5	0.5	50	
15.5	16	0.5		
16	16.5	0.5	50	
16.5	17	0.5		
17	17.5	0.5	50	
17.5	18	0.5		
18	18.5	0.5	50	

18.5	19	0.5	
19	19.5	0.5	50
19.5	20	0.5	
20	20.5	0.5	50
20.5	21	0.5	
21	21.5	0.5	50
21.5	22	0.5	
22	22.5	0.5	50
22.5	23	0.5	
23	23.5	0.5	50
23.5	24	0.5	
24	24.5	0.5	50
24.5	25	0.5	
25	25.5	0.5	42
25.5	26	0.5	
26	26.5	0.5	50
26.5	27	0.5	
27	27.5	0.5	50
27.5	28	0.5	
28	28.5	0.5	50
28.5	29	0.5	
29	29.5	0.5	50
29.5	30	0.5	
30	30.5	0.5	50
30.5	31	0.5	
31	31.5	0.5	50
31.5	32	0.5	
32	32.5	0.5	50
32.5	33	0.5	
33	33.5	0.5	50
33.5	34	0.5	
34	34.5	0.5	50
34.5	35	0.5	
35	35.5	0.5	50
35.5	36	0.5	
36	36.5	0.5	50
36.5	37	0.5	
37	37.5	0.5	50
37.5	38	0.5	
38	38.5	0.5	50
38.5	39	0.5	
39	39.5	0.5	50
39.5	40	0.5	
40	40.5	0.5	50

	40.5	41	0.5	
	41	41.5	0.5	50
	41.5	42	0.5	
	42	42.5	0.5	50
	42.5	43	0.5	
	43	43.5	0.5	50
	43.5	44	0.5	
	44	44.5	0.5	50
	44.5	45	0.5	
	45	45.5	0.5	50

Table B2

Name of Borehole	starting Depth (m)	Ending Depth (m)	Depth (m)	SPT
Plot No - 24 / A, Al Soor. BOREHOLE 2	0.5	1	0.5	5
	1	1.5	0.5	3
	1.5	2	0.5	9
	2	2.5	0.5	6
	2.5	3	0.5	3
	3	3.5	0.5	1
	3.5	4	0.5	
	4	4.5	0.5	2
	4.5	5	0.5	
	5	5.5	0.5	7
	5.5	6	0.5	
	6	6.5	0.5	10
	6.5	7	0.5	
	7	7.5	0.5	20
	7.5	8	0.5	
	8	8.5	0.5	11
	8.5	9	0.5	
	9	9.5	0.5	17
	9.5	10	0.5	
	10	10.5	0.5	30
10.5	11	0.5		
11	11.5	0.5	37	
11.5	12	0.5		
12	12.5	0.5	27	
12.5	13	0.5		
13	13.5	0.5	29	
13.5	14	0.5		
14	14.5	0.5	8	

14.5	15	0.5	
15	15.5	0.5	16
15.5	16	0.5	
16	16.5	0.5	30
16.5	17	0.5	
17	17.5	0.5	30
17.5	18	0.5	
18	18.5	0.5	35
18.5	19	0.5	
19	19.5	0.5	32
19.5	20	0.5	
20	20.5	0.5	33
20.5	21	0.5	
21	21.5	0.5	33
21.5	22	0.5	
22	22.5	0.5	33
22.5	23	0.5	
23	23.5	0.5	33
23.5	24	0.5	
24	24.5	0.5	30
24.5	25	0.5	
25	25.5	0.5	25
25.5	26	0.5	
26	26.5	0.5	30
26.5	27	0.5	
27	27.5	0.5	50
27.5	28	0.5	
28	28.5	0.5	50
28.5	29	0.5	
29	29.5	0.5	50
29.5	30	0.5	
30	30.5	0.5	50

Table B3

Name of Borehole	starting Depth (m)	Ending Depth (m)	Depth (m)	SPT
Plot No :773/A , AL Baraha, Kalba, Sharjah. BOREHOLE 5	0	0.5	0.5	15
	0.5	1	0.5	19
	1	1.5	0.5	11
	1.5	2	0.5	10
	2	2.5	0.5	38
	2.5	3	0.5	44

3	3.5	0.5	41
3.5	4	0.5	
4	4.5	0.5	2
4.5	5	0.5	
5	5.5	0.5	4
5.5	6	0.5	
6	6.5	0.5	31
6.5	7	0.5	
7	7.5	0.5	50
7.5	8	0.5	
8	8.5	0.5	50
8.5	9	0.5	
9	9.5	0.5	50
9.5	10	0.5	
10	10.5	0.5	50
10.5	11	0.5	
11	11.5	0.5	34
11.5	12	0.5	
12	12.5	0.5	41
12.5	13	0.5	
13	13.5	0.5	22
13.5	14	0.5	
14	14.5	0.5	50
14.5	15	0.5	
15	15.5	0.5	50
15.5	16	0.5	
16	16.5	0.5	50
16.5	17	0.5	
17	17.5	0.5	50
17.5	18	0.5	
18	18.5	0.5	50
18.5	19	0.5	
19	19.5	0.5	50
19.5	20	0.5	
20	20.5	0.5	
20.5	21	0.5	
21	21.5	0.5	1
21.5	22	0.5	11
22	22.5	0.5	10
22.5	23	0.5	38
23	23.5	0.5	44
23.5	24	0.5	41
24	24.5	0.5	0
24.5	25	0.5	2

	25	25.5	0.5	0
	25.5	26	0.5	4
	26	26.5	0.5	0
	26.5	27	0.5	31
	27	27.5	0.5	0
	27.5	28	0.5	0
	28	28.5	0.5	50
	28.5	29	0.5	
	29	29.5	0.5	50
	29.5	30	0.5	
	30	30.5	0.5	50
	30.5	31	0.5	
	31	31.5	0.5	50
	31.5	32	0.5	
	32	32.5	0.5	50
	32.5	33	0.5	
	33	33.5	0.5	50
	33.5	34	0.5	
	34	34.5	0.5	50
	34.5	35	0.5	
	35	35.5	0.5	50
	35.5	36	0.5	
	36	36.5	0.5	50

Table B4

Name of Borehole	starting Depth (m)	Ending Depth (m)	Depth (m)	SPT
Plot No. 590,590/A & 619, Buttina , Sharjah. BOREHOLE 6	0	0.5	0.5	
	0.5	1	0.5	20
	1	1.5	0.5	47
	1.5	2	0.5	25
	2	2.5	0.5	19
	2.5	3	0.5	24
	3	3.5	0.5	39
	3.5	4	0.5	
	4	4.5	0.5	35
	4.5	5	0.5	
	5	5.5	0.5	50
	5.5	6	0.5	
	6	6.5	0.5	50
	6.5	7	0.5	
	7	7.5	0.5	50

	7.5	8	0.5	
	8	8.5	0.5	50
	8.5	9	0.5	
	9	9.5	0.5	50
	9.5	10	0.5	
	10	10.5	0.5	50
	10.5	11	0.5	
	11	11.5	0.5	22
	11.5	12	0.5	
	12	12.5	0.5	23
	12.5	13	0.5	
	13	13.5	0.5	29
	13.5	14	0.5	
	14	14.5	0.5	24
	14.5	15	0.5	
	15	15.5	0.5	50
	15.5	16	0.5	
	16	16.5	0.5	50
	16.5	17	0.5	
	17	17.5	0.5	50
	17.5	18	0.5	
	18	18.5	0.5	50
	18.5	19	0.5	
	19	19.5	0.5	50
	19.5	20	0.5	
	20	20.5	0.5	50
	20.5	21	0.5	
	21	21.5	0.5	50
	21.5	22	0.5	
	22	22.5	0.5	50
	22.5	23	0.5	
	23	23.5	0.5	
	23.5	24	0.5	
	24	24.5	0.5	
	24.5	25	0.5	
	25	25.5	0.5	
	25.5	26	0.5	
	26	26.5	0.5	
	26.5	27	0.5	
	27	27.5	0.5	
	27.5	28	0.5	
	28	28.5	0.5	50
	28.5	29	0.5	
	29	29.5	0.5	50

	29.5	30	0.5	
	30	30.5	0.5	50
	30.5	31	0.5	
	31	31.5	0.5	50
	31.5	32	0.5	
	32	32.5	0.5	50
	32.5	33	0.5	
	33	33.5	0.5	50
	33.5	34	0.5	
	34	34.5	0.5	50
	34.5	35	0.5	
	35	35.5	0.5	50

Table B5

Name of Borehole	starting Depth (m)	Ending Depth (m)	Depth (m)	SPT
Plot No :684-685 Hamriya (Sharq) Sharjah. BOREHOLE 5	0	0.5	0.5	
	0.5	1	0.5	10
	1	1.5	0.5	13
	1.5	2	0.5	17
	2	2.5	0.5	18
	2.5	3	0.5	20
	3	3.5	0.5	26
	3.5	4	0.5	
	4	4.5	0.5	50
	4.5	5	0.5	
	5	5.5	0.5	50
	5.5	6	0.5	
	6	6.5	0.5	50
	6.5	7	0.5	
	7	7.5	0.5	10
	7.5	8	0.5	13
	8	8.5	0.5	17
	8.5	9	0.5	18
	9	9.5	0.5	20
	9.5	10	0.5	26
10	10.5	0.5		
10.5	11	0.5		
11	11.5	0.5		
11.5	12	0.5		
12	12.5	0.5		
12.5	13	0.5		

13	13.5	0.5	
13.5	14	0.5	
14	14.5	0.5	10
14.5	15	0.5	13
15	15.5	0.5	17
15.5	16	0.5	18
16	16.5	0.5	20
16.5	17	0.5	26
17	17.5	0.5	
17.5	18	0.5	
18	18.5	0.5	
18.5	19	0.5	
19	19.5	0.5	
19.5	20	0.5	
20	20.5	0.5	
20.5	21	0.5	
21	21.5	0.5	10
21.5	22	0.5	13
22	22.5	0.5	17
22.5	23	0.5	18
23	23.5	0.5	20
23.5	24	0.5	26
24	24.5	0.5	
24.5	25	0.5	
25	25.5	0.5	
25.5	26	0.5	
26	26.5	0.5	
26.5	27	0.5	
27	27.5	0.5	
27.5	28	0.5	
28	28.5	0.5	50
28.5	29	0.5	
29	29.5	0.5	50
29.5	30	0.5	
30	30.5	0.5	50
30.5	31	0.5	
31	31.5	0.5	50
31.5	32	0.5	
32	32.5	0.5	50
32.5	33	0.5	
33	33.5	0.5	50
33.5	34	0.5	
34	34.5	0.5	50
34.5	35	0.5	

	35	35.5	0.5	50
--	----	------	-----	----

Table B6

Name of Borehole	starting Depth (m)	Ending Depth (m)	Depth (m)	SPT
Plot No :817 Mulk, Al Khan, Sharjah. BOREHOLE 9	0.5	1	0.5	21
	1	1.5	0.5	15
	1.5	2	0.5	11
	2	2.5	0.5	9
	2.5	3	0.5	6
	3	3.5	0.5	6
	3.5	4	0.5	
	4	4.5	0.5	8
	4.5	5	0.5	
	5	5.5	0.5	11
	5.5	6	0.5	
	6	6.5	0.5	22
	6.5	7	0.5	
	7	7.5	0.5	7
	7.5	8	0.5	
	8	8.5	0.5	11
	8.5	9	0.5	
	9	9.5	0.5	22
	9.5	10	0.5	
	10	10.5	0.5	31
	10.5	11	0.5	
	11	11.5	0.5	28
	11.5	12	0.5	
	12	12.5	0.5	36
	12.5	13	0.5	
	13	13.5	0.5	50
	13.5	14	0.5	
	14	14.5	0.5	50
14.5	15	0.5		
15	15.5	0.5	50	
15.5	16	0.5		
16	16.5	0.5	50	
16.5	17	0.5		
17	17.5	0.5	50	
17.5	18	0.5		
18	18.5	0.5	50	
18.5	19	0.5		

	19	19.5	0.5	50
	19.5	20	0.5	
	20	20.5	0.5	50
	20.5	21	0.5	
	21	21.5	0.5	50
	21.5	22	0.5	
	22	22.5	0.5	50
	22.5	23	0.5	
	23	23.5	0.5	50
	23.5	24	0.5	
	24	24.5	0.5	50
	24.5	25	0.5	
	25	25.5	0.5	50
	25.5	26	0.5	
	26	26.5	0.5	50
	26.5	27	0.5	
	27	27.5	0.5	50
	27.5	28	0.5	
	28	28.5	0.5	50
	28.5	29	0.5	
	29	29.5	0.5	50
	29.5	30	0.5	
	30	30.5	0.5	50

Vita

Ahmed Mohamed Zaroug Eltayeb was born in 1996, in Dubai, United Arab Emirates. He received his primary and secondary education in Sharjah, UAE. He received his B.Sc. degree in Civil and Environmental Engineering from the University of Sharjah in 2018. Ms. Ahmed Eltayeb was awarded highest level of honour for his exceptional performance during the four years of study.

In September 2018, he joined the Civil Engineering master's program in the American University of Sharjah as a graduate teaching assistant for four semesters which took place immediately after graduation. During his master's study, he co-authored two papers which were presented in international conferences. His research interests are in dynamics of soil, seismic response of soils, and soil stabilization.